

Design and Integration of a Form-Fitting General Purpose Robotic Hand Exoskeleton

by Eric M. Refour

Thesis submitted to the faculty of the Virginia Polytechnic Institute and State University
in partial fulfillment of the requirements for the degree of

Master of Science
In
Computer Engineering

Pinhas Ben-Tzvi, Chair
Daniel J. Stilwell
Alfred L. Wicks

September 29, 2017
Blacksburg, Virginia

Keywords: Exoskeleton, Robotic Systems, Mechatronics, Assistive Glove, Rehabilitation

Copyright © 2017

Design and Integration of a Form-Fitting General Purpose Robotic Hand Exoskeleton

by Eric M. Refour

ABSTRACT

This thesis explores the field of robotic hand exoskeletons and their applications. These systems have emerged in popularity over the years, due to their potentials to advance the medical field as assistive and rehabilitation devices, and the field of virtual reality as haptic gloves. Although much progress has been made, hand exoskeletons are faced with several design challenges that are hard to overcome without having some tradeoffs. These challenges include: (1) the size and weight of the system, which can affect both the comfort of wearing it and its portability, (2) the ability to impose natural joint angle relationships among the user's fingers and thumb during grasping motions, (3) safety in terms of limiting the range of motions produce by the system to that of a normal human hand and ensuring that the mechanical design does not cause harm or injury to the user, (4) designing a device that is user friendly, and (5) the ability to effectively perform grasping motions and provide sensory feedback for the system to be applicable in various application fields.

In order to address these common issues of today's state-of-the-art hand exoskeleton systems, this thesis proposes a mechanism design for a novel hand exoskeleton. The proposed hand exoskeleton is designed to assist users with grasping motions while maintaining natural coupling relationships among the fingers and thumb joints to resemble that of a normal human hand. The mechanism offers the advantages of being small-sized and lightweight, which makes it ideal for prolong use. In addition to presenting the proposed mechanism in detail with kinematic and dynamic analysis, the thesis provides the integration and development of several prototypes. These hand exoskeleton prototypes are

validated through simulations and experimental testing. In closing, several applications for these prototypes are discussed to highlight the potentials of the proposed hand exoskeleton design. The on-going future work for the proposed design is also explained to conclude this thesis.

Design and Integration of a Form-Fitting General Purpose Robotic Hand Exoskeleton

by Eric M. Refour

GENERAL AUDIENCE ABSTRACT

Hand exoskeletons are wearable devices that are designed to augment, reinforce, and/or restore hand performances and movements among the fingers and thumb. These hand exoskeleton systems have emerged in popularity within the medical field, where they serve as rehabilitation devices or assistive gloves, and within the field of virtual reality as haptic devices. Throughout the years, many hand exoskeleton designs have been proposed and even developed further into commercial products. Unfortunately, there still exist many design challenges for making an efficient and feasible hand exoskeleton without experiencing major tradeoffs. Some of the common challenges include designing a hand exoskeleton that is small in size, lightweight, and able to achieving natural grasping motions efficiently.

As an attempt to overcome these design challenges, the work of this thesis presents a mechanism design for a novel hand exoskeleton that can serve as a general purpose glove across several applications. The design of the mechanism is described in detail with preliminary analysis. In addition, this thesis presents the design and development of several prototypes, which were made by extending the mechanism into fully integrated systems. The experimental validations of these prototypes are presented as well as their application potentials. To conclude the thesis, a discussion of the on-going future work is given.

ACKNOWLEDGEMENTS

Firstly, I would like to thank my family and friends, especially my mother Cynthia McNeil, grandmother Doris Refour, sister Kamilah Kassim, father Timothy Tabor, and brother Donte Tabor, for all their love and support throughout my academic studies. They helped me remain strong-minded throughout my time in college, despite the many challenges and hardships I faced along the way. I would also like thank Jihyeon Gong for all the support and encouragement she showed to me throughout my graduate studies.

This thesis will cover the work I accomplished for my Master's degree. My research would not have been successful without the help of many people. I would like to thank my advisor, Professor Pinhas Ben-Tzvi for giving me a chance to expand my knowledge by becoming a part of his Robotics and Mechatronics Lab at Virginia Tech. Besides being a supportive advisor, his encouraging words and enthusiastic attitude pushed me to perform at the highest quality. In addition to having an understanding advisor, I am grateful for having the opportunity to be surrounded by knowledgeable people in our lab. I am thankful for Bijo Sebastian, who served as my senior mentor in the lab. With his assistance throughout my research work, I was able to achieve great progress in completing my research goals.

TABLE OF CONTENTS

ABSTRACT	ii
GENERAL AUDIENCE ABSTRACT.....	iv
ACKNOWLEDGEMENTS	v
TABLE OF CONTENTS.....	vi
LIST OF FIGURES	x
LIST OF TABLES	xiv
CHAPTER 1	1
INTRODUCTION	1
1.1 Background	1
1.2 Contributions.....	3
1.3 Thesis Structure.....	5
1.4 Selected Publications.....	6
CHAPTER 2	7
LITERATURE REVIEW	7
2.1 Hand Anatomy and Function	7
2.1.1. Joints of the Finger and Thumb	7
2.1.2. Typical Functional Grasps	10
2.1.3. Natural Joint Relationship During Grasping.....	12

2.1.4.	Typical Force Output During Grasping	14
2.1.5.	Conclusion	16
2.2	Hand Exoskeleton Classifications	16
2.2.1.	Traditional Rigid Exoskeleton Gloves	17
2.2.2.	Soft Exoskeleton Gloves	22
2.3	Comparative Analysis	29
2.4	Conclusion.....	29
CHAPTER 3		30
PROBLEM STATEMENT AND PROPOSED SOLUTION		30
3.1	Motivations and Analysis of Related Research Problems	30
3.1.1.	Size and Portability Issues	31
3.1.2.	Natural Joint Angle Relationship Issues	32
3.1.3.	Sensory Feedback Issues.....	33
3.1.4.	Workspace Issues.....	35
3.2	Research Objectives and Hypothesis	36
3.3	Proposed Robotic Hand Exoskeleton.....	37
CHAPTER 4		39
ROBOTIC HAND EXOSKELETON DESIGN		39
4.1	Overview	39
4.2	Kinematics.....	40

4.3	Kinematic Modeling.....	42
4.4	Kinematic Design Optimization.....	47
4.4.1.	Optimization Objectives	47
4.4.2.	Optimization Results.....	52
4.5	Dynamics.....	65
CHAPTER 5		69
FORCE CONTROL.....		69
5.1	Background and Motivation.....	69
5.2	Series Elastic Actuation Literature Review	70
5.3	Proposed Design and Control Scheme	71
CHAPTER 6		76
PROTOTYPES DEVELOPMENT AND EXPERIMENTAL RESULTS		76
6.1	Two-Digit Prototype	76
6.1.1.	Prototype Integration	76
6.1.2.	Experiments	82
6.1.3.	Discussion.....	87
6.1.4.	Conclusion	89
6.2	Full Hand Prototype Design.....	90
6.2.1.	Motivation.....	90
6.2.2.	Mechanism Design Update.....	92

6.3	Children Two-Digit Prototype	94
6.3.1.	Motivation.....	94
6.3.2.	Robotic Exoskeleton Design.....	95
6.3.3.	Prototype Integration	97
6.3.4.	Experiments	103
6.3.5.	Conclusion	106
CHAPTER 7		107
APPLICATIONS OF THE PROPOSED HAND EXOSKELETON PROTOTYPES ...		107
7.1	Rehabilitation Application	107
7.1.1.	Overview.....	107
7.1.2.	Rehabilitation Software	108
7.1.3.	Demonstration.....	111
CHAPTER 8		113
CONCLUSION & FUTURE WORK.....		113
8.1	Summary	113
8.2	Future Work	115
REFERENCES		117

LIST OF FIGURES

Figure 2.1: Anatomy of the human hand	8
Figure 2.2: Motion terminology for the fingers ([12]).....	9
Figure 2.3: Motion terminology for the thumbs ([12]).....	9
Figure 2.4: Several commonly used hand grasps.....	12
Figure 2.5: CAD design and prototype of the direct drive two-digit hand exoskeleton being worn [28].....	18
Figure 2.6: Picture of the CyberGrasp hand exoskeleton [36].....	19
Figure 2.7: Prototypes of the SAFE Glove: Design II (top) and Design III (bottom) [35], [37].....	20
Figure 2.8: Prototype of the three-layered sliding spring hand exoskeleton [29].....	21
Figure 2.9: Mechanism design for the Exo-Glove [38]	23
Figure 2.10: Prototype of the BiomHED [39]	24
Figure 2.11: Prototype of the pneumatic hand exoskeleton (SNU)	26
Figure 2.12: Exploded and assembled view of the soft actuator mechanism [43]	27
Figure 2.13: Prototype of the proposed soft robotic glove and the waist belt pack [43] ..	28
Figure 3.1: Proposed design for a full hand exoskeleton system.....	37
Figure 4.1: (a) Design of the index finger mechanism, (b) Design of the thumb mechanism.	40
Figure 4.1: Index mechanism showing two configurations and the design parameters for kinematic modelling. The relaxed configuration is shown in gray, while the black & white schematic shows a flexion configuration	42

Figure 4.3: Simulation of the desired index finger trajectory starting at the origin of (0,0)	45
Figure 4.4: Simulation of the desired thumb trajectory starting at the origin of (0,0).....	45
Figure 4.5: Relationship of the joint angles from the finger mechanism during flexion and extension motions	46
Figure 4.6: Relationship of the joint angles from the thumb mechanism during flexion and extension motions.....	46
Figure 4.7: Optimization results for the index finger mechanism	54
Figure 4.8: Trajectory of the optimal solution for the index finger mechanism.....	54
Figure 4.9: Joint angle relationships of the optimal solution for the index finger mechanism	55
Figure 4.10: Optimization results for the middle finger mechanism	56
Figure 4.11: Trajectory of the optimal solution for the middle finger mechanism.....	57
Figure 4.12: Joint angle relationships of the optimal solution for the middle finger mechanism	57
Figure 4.13: Optimization results for the ring finger mechanism.....	58
Figure 4.14: Trajectory of the optimal solution for the ring finger mechanism	59
Figure 4.15: Joint angle relationships of the optimal solution for the ring finger mechanism	60
Figure 4.16: Optimization results for the pinky finger mechanism	61
Figure 4.17: Trajectory of the optimal solution for the pinky finger mechanism.....	62
Figure 4.18: Joint angle relationships of the optimal solution for the pinky finger mechanism	62

Figure 4.19: Optimization results for the thumb mechanism	63
Figure 4.20: Trajectory of the optimal solution for the thumb mechanism	64
Figure 4.21: Joint angle relationships of the optimal solution for the thumb mechanism	65
Figure 4.22: Dynamic diagram of the mechanism.....	66
Figure 5.1: Proposed SEA design	72
Figure 5.2: 3D printed prototype for the proposed SEA design	73
Figure 5.3: Proposed SEA design integrated on the two-digit hand exoskeleton.....	73
Figure 5.4: Block diagram for proposed force control	74
Figure 5.5: Preliminary results of the force control simulation	75
Figure 6.1: CAD model of the proposed two-digit prototype.....	76
Figure 6.2: Detailed design of the fingertip holder and its sensor housing	77
Figure 6.3: PCB design for the two-digit prototype	80
Figure 6.4: System architecture of the hand exoskeleton system	81
Figure 6.5: Experimental setup for the prototype: 1- Exoskeleton glove on mannequin, 2 - Embedded controller, 3 – Compressor, 4 - Air tank.	83
Figure 6.6: Experimental analysis at various stages of the bending motions for: (a) Index finger, (b) Thumb.....	84
Figure 6.7: Index finger joint angles in respect to execution time.....	85
Figure 6.8: Thumb joint angles in respect to execution time.....	87
Figure 6.9: Prototype on a human hand: 1- Absolute position sensor, 2 - FSR sensor, 3 - Vibration motor, 4 - Pneumatic actuator.....	88
Figure 6.10: CAD model of the proposed full hand exoskeleton system with the SEA units and redesigned mechanism	92

Figure 6.11: Close up view for the CAD model of the proposed full hand exoskeleton..	93
Figure 6.12: Index finger and thumb mechanisms for the proposed children hand exoskeleton	96
Figure 6.13: Detailed CAD design for the proposed children hand exoskeleton system .	99
Figure 6.14: Custom printed circuit board for the children hand exoskeleton system ...	102
Figure 6.15: Prototype of the children hand exoskeleton system (demonstrated by a child of age 5)	103
Figure 6.16: Experimental analysis for children hand exoskeleton prototype.....	104
Figure 6.17: Experimental results of the joint angle relationships for the index finger and thumb in respect to execution time for pincer grasp.....	105
Figure 7.1: (a) Software GUI initial screen layout	109
Figure 7.1: (b) Software GUI main screen layout.....	110
Figure 7.2: Volunteer demonstrating how to use the system.....	112

LIST OF TABLES

Table 2.1: Maximum Angular Displacement for the Fingers & Thumb [13], [14]	10
Table 2.2: Average natural joint angles of flexion/extension during cylinder grasp [19]	13
Table 2.3: Natural joint angles during tip-pinch grasp [20].....	13
Table 2.4: Strength of the cylindrical power grasp [25]	15
Table 4.2: Function variables for the mechanism optimization procedure.....	52
Table 4.3: Natural joint angles during tip-pinch grasp	52
Table 6.1: Experimental results and comparison for the index finger joints	85
Table 6.2: Experimental results and comparison for the thumb joints	86

CHAPTER 1

INTRODUCTION

1.1 Background

Exoskeletons have emerged in popularity within recent decades as a reflection of their great potentials for multiple applications. These application fields include interests from the military, industrial workplace, and medical field. An exoskeleton is defined as an orthotic robotic system consisting of links, joints, and/or artificial tendons/muscles, which correspond to that of a human body part. Using the corresponding joints and tendons, the exoskeleton system is able to transmit force/torque and motion through its links onto the joints of the desired body part. Generally, these robotic systems are worn to provide an enhancement in human strength or to restore movements in limbs that lack motor functionality.

One of the initial efforts to create an exoskeleton was attempted by General Electric in 1965 [1]. Their intentions were focused on creating a device in partnership with the US Army and Navy that would allow a user to lift a load of 1,500 lbs. (680kg). Since then, numerous exoskeletons have been developed, ranging across the three main categories of upper extremity, lower extremity, and full body exoskeleton systems. Upper extremity exoskeletons and full body exoskeletons [2] are popular in the fields of power-assistive devices [3], rehabilitation [4], [5], robot-teleoperation, and haptic interaction in virtual reality [4]. Lower extremity exoskeletons on the other hand, serve mainly as rehabilitation and power assistive devices for those with leg disabilities [6]–[8].

Although there are many categories of exoskeletons, the focus of this thesis will be on the field of hand exoskeletons, which is a subcategory of upper extremity exoskeletons. Approximately 19.9 million people in the U.S suffer from upper body dysfunctionalities that result in experiencing difficulties in lifting and grasping objects. In particular, over 6.7 million people have trouble grasping everyday objects such as a cup or a pencil [9]. Experiencing these disabilities can affect performing activities of daily living (ADLs), which include eating, toileting, and even bathing. These hand dysfunctionalities can result from injuries and diseases such as a broken bone, muscle sprain, stroke, spinal cord injury, and cerebral palsy. As an attempt to combat these disabilities, the proposal of using hand exoskeletons has held strong interests within the medical field. In some cases, several individuals who suffer hand impairments are fortunate enough to recover by undergoing rehabilitation. Generally, the rehabilitation process involves repeatedly performing different hand exercises and grasps to restore muscle memory, hand strength, and relearn natural hand motions. To assist these patients with their recovery, hand exoskeletons have been developed to serve as rehabilitation devices. For those who suffer more long-term or permanent hand impairments, hand exoskeletons have also been developed as assistive devices to help with grasping and performing tasks.

Other areas of interests for hand exoskeletons include the realms of virtual reality in which these systems are used to provide haptic feedback to create the realistic sensations of touch and force feedback. In addition, hand exoskeletons have been proposed for tele-operating purposes that can allow for the controlling of a robotic manipulator in a hazardous environment, for example.

Creating these wearable robotic systems can present multiple design challenges. Ideally, all exoskeletons should be designed light-weight, small sized in accordance with the desired body part(s), and comfortable for the user to wear. In addition, most exoskeletons require precise position and force control, advanced sensors and signals processing, and longer lasting power sources. Despite the great progress made since the initial exoskeleton prototypes of the 1960s, difficulties remain in achieving these design requirements. Limitations arise from finding lightweight actuators that still possess high torque and power to augment movements efficiently, mechanical design constraints that hinders making exoskeletons less unnatural in shape, size, and comfortable while maintaining effectiveness, and limited technology to interface the exoskeleton system with or at least reflect the nervous system to create an autonomously intelligent system.

The hand exoskeleton proposed in this thesis was design to address most of these common problems. The rest of this chapter will present the research contributions made by this thesis work. In addition, an outline for the following chapters of the thesis is given.

1.2 Contributions

In this thesis, we present the design and integration of a novel hand exoskeleton mechanism. Two prototypes were designed and initial experimental testing have been completed to evaluate the systems potentials to serve as both assistive devices and rehabilitation devices. A third prototype was also developed, experimentally tested, and evaluated. This third prototype was designed to serve as a child-size rehabilitation and diagnostic device, in collaboration with doctors at a Nationwide Children's Hospital. The

work of this thesis presents the following contributions to the research field of hand exoskeletons:

1. A novel exoskeleton glove that is capable of enforcing natural joint angles onto the fingers and thumb during bending motions
2. A hand exoskeleton that is designed with linkage mechanisms placed alongside the fingers and thumb, which allows for: (i) a simplified 1 degree of freedom (DOF) link mechanism for each finger and thumb that have corresponding links and joints to its appropriate finger/thumb and (ii) an overall lightweight and small sized frame for the exoskeleton glove.
3. Implementation of a compacted series elastic actuator (SEA) module that allows for: (i) bidirectional force control for each finger/thumb mechanism and (ii) adequate workspace.
4. A novel child sized hand exoskeleton system that was designed to be both a rehabilitation device and a diagnostic system.
5. A method to optimize design parameters like the constraint link lengths and angle positioning in order to minimize the height and size profiles of the linkage mechanisms. This allows the mechanisms to be placed alongside the fingers and thumb without causing great discomfort and affecting performance.
6. Implementation of a 3D Graphical User Interface (GUI) that: (i) can serve as a rehabilitation software that actuates the fingers/thumb to perform particular grasps for therapy purposes, (ii) displays a CAD model of the human hand to illustrate each finger and thumb trajectory and joint angles during extension/flexion motions, (iii) displays position and force sensor data, (iv) offers a record data feature that can

be used for the evaluation of therapy progress, and (v) a passive mode that allows the user to perform the grasps on their own.

1.3 Thesis Structure

The rest of the thesis is organized as follows:

Chapter 1: Presents the main contributions of this thesis

Chapter 2: Provides both a detailed analysis on the human hand anatomy and its functionalities, and a comprehensive literature review on robotic hand exoskeletons, which includes a comparative discussion for several of these state-of-the-art systems

Chapter 3: Identifies several factors that challenge many of the existing hand exoskeleton systems and presents the proposed hand exoskeleton as a well-rounded solution.

Chapter 4: Presents the conceptual design for the proposed mechanism of the primary hand exoskeleton system and its related kinematic and dynamic analysis.

Chapter 5: Provides a background on series elastic actuators and presents a proposed series elastic actuator design to achieve force control using the proposed hand exoskeleton, along with its experimental evaluation.

Chapter 6: Presents the design and integration of following prototypes: (i) a two-digit prototype using the original primary proposed hand exoskeleton mechanism, (ii) an extended prototype of a full hand exoskeleton using the original proposed mechanism, and (iii) a two-digit children hand exoskeleton prototype that uses an alternative proposed mechanism. Experimental analyses are provided for these prototypes, with discussions evaluating their performances.

Chapter 7: Explores several applications for the proposed hand exoskeleton as well as the secondary proposal of children hand exoskeleton system. These applications include assistive grasping and rehabilitation therapy.

Chapter 8: Concludes the thesis by providing a summary of the work and a discussion about potential future work.

1.4 Selected Publications

Disclosure: Content from these publications were used throughout this thesis.

Conference Papers

1. **E. Refour**, B. Sebastian, and P. Ben-Tzvi, “Design and Integration of a Two-Digit Exoskeleton Glove”, ASME International Design Engineering Technical Conferences and Information in Computers and Engineering Conference (IDETC/CIE), 2017. *Submitted and Accepted.*
2. **E. Refour**, B. Sebastian, and P. Ben-Tzvi, “Design and Implementation of a Child-Sized Robotic Hand Exoskeleton”, *Completed Draft, Pending Submission.*

Journal Papers

1. **E. Refour**, B. Sebastian, and P. Ben-Tzvi, “Design and Integration of a Two-Digit Exoskeleton Glove”, ASME Journal of Mechanisms and Robotics, *Submitted September 2017.*
2. **E. Refour**, B. Sebastian, and P. Ben-Tzvi, “A Form-Fitting General Purpose Exoskeleton Robotic Glove with Series Elastic Actuation and Force Control”, *In Preparation, Pending Submission, October 2017.*

CHAPTER 2

LITERATURE REVIEW

2.1 Hand Anatomy and Function

To design a hand exoskeleton system, a basic understanding of the anatomy of the human hand and its functionalities is needed. The hand is complex structure that performs various functions to accomplish daily tasks. The basic structure of the human hand is constructed of bones, joints, muscles, tendons, and skin. Normally, the human hand consists of five digits: the thumb and four fingers (index, middle, ring, and the little finger), and a central region of metacarpal bones (which are superficially surrounded by the palm) that connects the five digits to the wrist.

2.1.1. Joints of the Finger and Thumb

As shown in Figure 2.1, the fingers of the human hand mainly consist of three essential phalanges (distal, middle, and proximal phalanges) and three joints (distal-interphalangeal (DIP), proximal-interphalangeal (PIP), and metacarpal-phalangeal (MCP) joints) that connect the three phalanges and metacarpal together. On the contrary, the thumb of the human hand consists of two phalanges (distal and proximal) and two joints (interphalangeal (IP) and metacarpal-phalangeal (MCP) joints), which connect the two phalanges and metacarpal together.

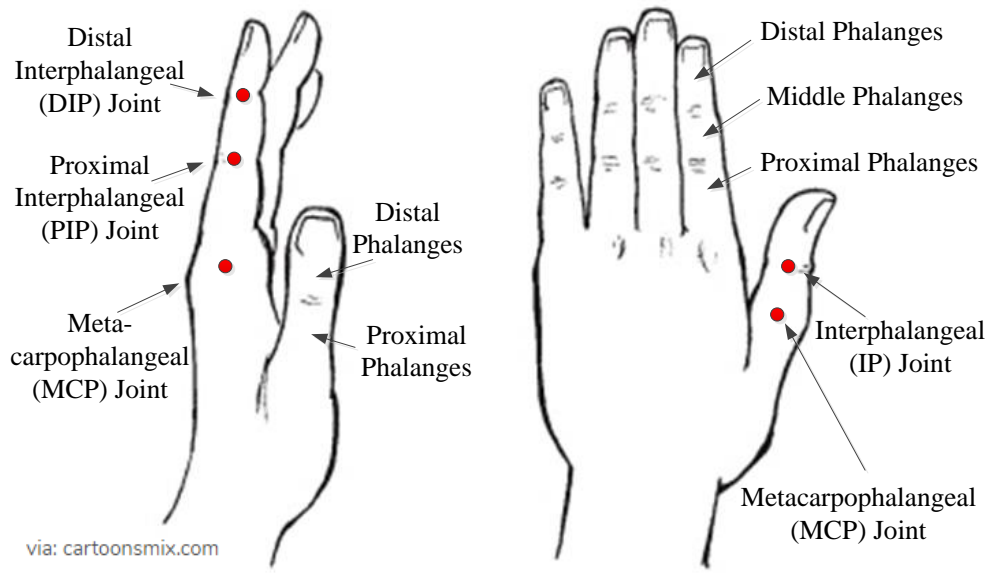


Figure 2.1: Anatomy of the human hand

The MCP joint of the fingers hosts three main DOFs, one for extension/flexion, abduction/adduction, and circumduction, while the other joints (PIP and DIP) mainly host one DOF for extension/flexion [10], [11], as illustrated in Figure 2.2. Like the MCP joint of the fingers, the carpometacarpal (CMC) joint in the wrist for the thumb, also known as the trapeziometacarpal (TMC) joint, hosts the three different DOFs for extension/flexion, abduction/adduction, and circumduction. In contrast, the MCP and IP joints of the thumb mainly host one DOF for extension/flexion, shown in Figure 2.3.

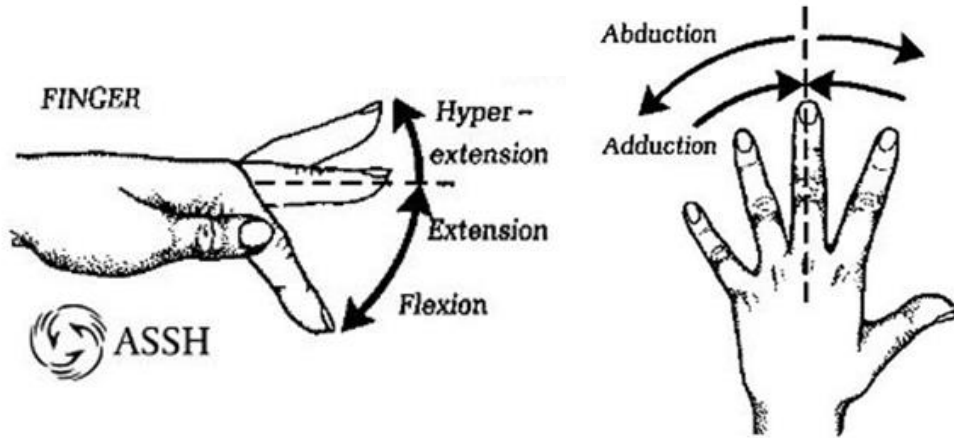


Figure 2.2: Motion terminology for the fingers ([12])

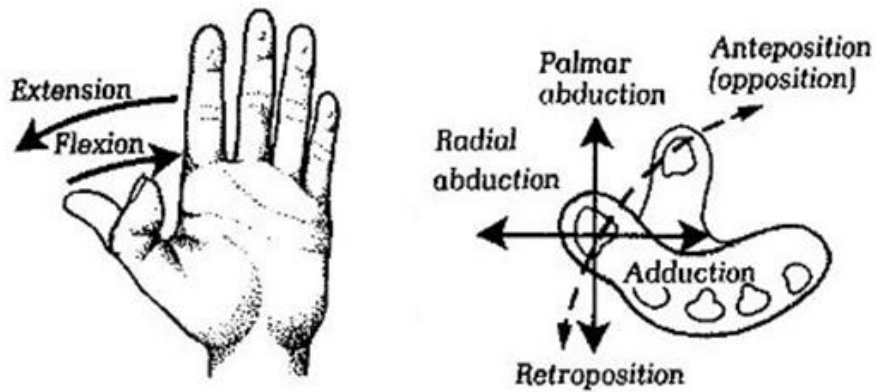


Figure 2.3: Motion terminology for the thumbs ([12])

Independently, each finger and thumb can generate a limited Range of Motion (RoM) across its joints for the different DOFs. Studies have been performed to record these RoM for healthy individuals to identify an average baseline across different age groups. In [13], [14], researchers presented the maximum angular displacements of the different joints of the finger and thumb. Their results are shown in Table 2.1. From studies such as these, an interesting observation has been made that shows that the joints of each finger and thumb are inherently coupled. The movement of the finger MCP joint and the thumb TMC joint,

which both serve as the primary joints for flexion and extension movements, can cause the other corresponding joints to move involuntarily [14], [15]. This observation can easily be verified by bending the index finger towards its maximum flexion angle and observing how the PIP and DIP joints also bend. This coupling is not limited to the MCP and TMC joints nor is it limited to flexion and extension movements. Other joints can generate some involuntary movement among their fellow joints through bending. In addition, the MCP and TMC joints can cause their fellow joints to move accordingly during abduction and adduction motions.

Table 2.1: Maximum Angular Displacement for the Fingers & Thumb [13], [14]

	MCP Joint	PIP Joint (IP for thumb)	DIP Joint
Thumb (Normal)	0° -56°	5° -73°	n/a
Thumb (Functional)	10° -32°	2° -43°	n/a
Fingers (Normal)	0° -100°	0° -105°	0° - 85°
Fingers (Functional)	33° -73°	36° -86°	20° - 61°

With the hand being such a complex structure, there exist many other kinematic and dynamic constraints as well as joint/muscle behaviors that have yet to be described mathematically. For the scope of this thesis, the coupling constraints and joint relationships mentioned earlier in this section will serve as the main focus of study.

2.1.2. Typical Functional Grasps

The human hand can perform numerous complex grasps and motions, ranging from over 48 characterized grasps [16], [17]. A grasp is defined as a hand posture that allows an

object to be held firmly, regardless of the hand orientation. Several of these grasps are commonly used in everyday activities and tasks, as shown in Figure 2.4. These commonly used grasps can be grouped into three categories: power, precision, and intermediate [18].

An overall power grasp is described as one in which a large contact area between the fingers and palm is used to secure an object, while limiting any motion evoked by the fingers and thumb. This means that the arm produces all movements on the object. There exists a variety of different power grasps such as the cylindrical, palmar, and spherical grasps. The cylindrical grasp is normally used to hold a cylindrical object between the thumb and fingers with the object resting against the surface of the palm of the hand. The palmar grasp is similar to the cylindrical grasp, except that it holds an object diagonally across the palm area with the thumb positioned to help stabilize the grasp (sometimes positioned along the length of the object). Examples of these two power grasps would include holding a bottle or opening a lid with the cylindrical grasp, while using the palmar grasp to hold a spoon or use a hammer. A spherical grasp is used with round objects where the fingers are held in a cupping manner at varying degrees of finger flexions, to secure the round shaped object.

The precision grip category includes grasps like the pincer and the tip pinch grasp, while the intermediate category contains grasps such as the dynamic tripod grasp, which is used to hold a pen or pencil. The tip-pinch grasp is when the tips of the thumb and index finger (or another finger) are opposed against one another to hold an object in between. These precision grasps are mainly used to hold small objects or objects with flat surfaces.

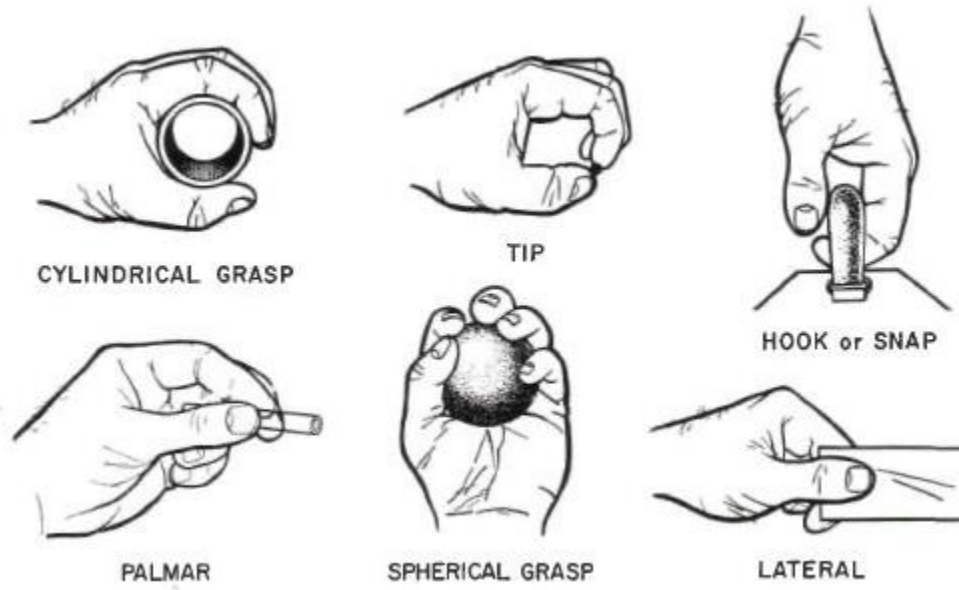


Figure 2.4: Several commonly used hand grasps

2.1.3. Natural Joint Relationship During Grasping

As the hand undertakes different postures and grasps to perform tasks and manipulate objects, the fingers and thumb undergoes different motion profiles. These profiles are influenced by factors such as the joint angle relationships, combinations of motion along the finger/thumb DOFs, and the ending positions for the fingers and thumb. Several of these commonly used grasps have been analyzed to evaluate these factors, specifically the joint angle relationships and motions from the fingers and thumb DOFs. The studies done by [19] measured the average joint angles of the hand after achieving precision and power grasps on a cylindrical object, while varying the combination of fingers and thumb used to secure the object. Table 2.2 shows the results of one of their experiments, which involved instructing a group of participants to perform a cylinder grasp with all four fingers and the thumb. Cylinder pillars of the various diameters (2 cm, 4 cm, 6 cm, and 8 cm) were used.

Table 2.2: Average natural joint angles of flexion/extension during cylinder grasp [19]

	MCP	PIP (IP for Thumb)	DIP
Index Finger	40.8° (SD 15.3°)	56.2° (SD 17.6°)	37.4° (SD 12.2°)
Middle Finger	53.0° (SD 20.0°)	59.9° (SD 17.2°)	35.9° (SD 15.1°)
Ring Finger	60.6° (SD 23.1°)	60.3° (SD 18.8°)	30.1° (SD 18.1°)
Pinky Finger	n/a	41.0° (SD 20.1°)	38.9° (SD 13.6°)
Thumb	n/a	30.6° (SD 15.0°)	n/a

In comparison to the natural joint angles achieved during a power grasp, the studies conducted by [20] provided natural joint angle relationships from a precision grasp. Table 2.3 presents the average results for participants performing the tip-pinch grasp using their index finger and thumb. The results specifically show the experimental data from patients performing a tip-pinch of 100g while maintaining a pulp distance of 1 cm.

Table 2.3: Natural joint angles during tip-pinch grasp [20]

	MCP	PIP (IP for Thumb)	DIP
Index Finger	49.1° (SD 9.5°)	41.0° (SD 10.7°)	38.5° (SD 6.8°)
Thumb	12.8° (SD 9.4°)	21.8° (SD 7.8°)	n/a

From observing the experimental results of performing both a power and precision grasp, it can be concluded that the average joint angles relationships of both grasps match each other when the standard deviations are considered.

2.1.4. Typical Force Output During Grasping

To grip different objects and maintain security while varying the positions and orientations of the arm and hand, the strength of the grip must be adjusted accordingly. Grip (and pinch) strength differs across each characterized hand grasp and can be impacted by factors such as age and illnesses. Medical instruments have been developed to help record the strength of the human hand. Among them, the Jamar dynamometer is one of the commonly used instrument to measure grip strength due to its reputation of being highly accurate [21]. Developed in 1954, the Jamar Dynamometer uses a sealed hydraulic system with adjustable hand spacing to measure the strength of the human handgrip up to a maximum 90 kg (200 lbs) [21], [22]. In terms of measuring the strength of a pinch, one of the most popular instruments used is the pinch gauge. The B&L Engineering pinch gauge is considered the industry's top brand as a result of it being highly cited in research literature and having a high accuracy rating [23]. Their top model can measure up to 27.2 kg (60 lbs) with an accuracy of 0.27 kg (0.6 lbs).

In [24], researchers used the Jamar dynamometer and B&L pinch gauge to measure the average grip strength of commonly used grasps such as the power, tip-pinch, key pinch, and palmer pinch grasps. Their experimental procedures involved using 628 volunteers, 318 women and 310 men of the age 20 -94 years old. Subjects within the age range of 20 -59 years old were healthy individuals, free of any diseases and injuries that could affect their strength results. During the strength recording of each grip, subjects were seated in the following conditions: (1) shoulders adducted and neutrally rotated, (2) elbow flexed at 90°, (3) forearm neutrally positioned, and (4) wrist oriented between 0° to 30° dorsiflexion and 0° to 15° ulnar deviation. The average grip strengths for the overall power grasps were

463.9 N (104.3 lbs) and 279.3 N (62.8 lbs) for the right hand of the men and women respectively, and 414.1 N (93.1 lbs) and 239.8 N (53.9 lbs) for their left hand in the same respect. For the tip-pinch grasps, the averages were 75.6 N (17.0 lbs) and 73 N (16.4 lbs) for right and left hand of men respectively, and 50.3 N (11.3 lbs) and 48 N (10.8 lbs) for the right and left hand of women respectively.

To measure the grip strength of the individual phalanges of the fingers while performing a cylindrical power grasp, researchers in [25] developed a force-measuring glove that contained about 20 miniature pressure sensors at the various phalangeal segments of each finger. Using this glove, 24 patients performed a cylindrical power grip using their maximum strength. Table 2.2 presents the resulting force measurements from this study.

Table 2.4: Strength of the cylindrical power grasp [25]

Phalangeal Segment	Index	Middle	Ring	Little
Meta-head	17.3 N	24.2 N	18.4 N	9.6 N
Proximal	21.0 N	29.3 N	22.3 N	11.6 N
Middle	26.1 N	36.5 N	27.8 N	14.5 N
Distal	45.9 N	64.1 N	48.8 N	25.4 N

By adding all of these individual forces together, the total grip strength from this experiment closely matches the power grip result of men right hand from [24], which was 463.9 N.

2.1.5. Conclusion

The fundamental knowledge of the human hand and its basic functionalities that were discussed within this section can be utilized to develop an adequate hand exoskeleton system. This ideal hand exoskeleton would be one that: (1) mimics the coupling relationship among the joints of the fingers and thumb to guarantee natural bending motions enforced by the system and (2) performs commonly used grasps of sufficient output forces that resemble the natural grip strength of a human hand.

2.2 Hand Exoskeleton Classifications

Great progress has been made within the field of hand exoskeletons, as discussed in Chapter 1. This progress ranges across both commercial and academic research prototypes. These exoskeleton systems are designed for various applications, which includes serving as rehabilitation devices, assistive devices, and/or haptic gloves. Usually, these hand exoskeletons are tailored and designed accordingly to meet their proposed application(s) requirements. These design parameters include the number DOFs to actuate, which digits to target, the weight of the system, suitable actuators to use (size, power, etc), and the controllability of the digits motion. In this section, a literature review is given on several state-of-the-art hand exoskeleton systems. The presented hand exoskeletons are divided into two major categories of design approaches, traditional rigid exoskeletons and soft exoskeleton gloves. Both design approaches have paved the way for advancing the field of hand exoskeletons and are designed to overcome each other's' disadvantages.

2.2.1. Traditional Rigid Exoskeleton Gloves

Traditional rigid hand exoskeletons are designed using rigid links and joints to apply forces to the corresponding joints of the human hand. This allows for the links to impose movements onto the fingers and thumb [26]–[37]. These rigid gloves are designed with the links placed on top of the fingers and thumb to resemble an external shell worn by the hand. This placement is primarily chosen as a result of the linkage mechanisms sizes exceeding the available spaces between fingers and thumb. In addition, choosing to place the links on top of the fingers and thumb allows for the joints of the exoskeleton glove to coincide with the joints of the fingers and thumb for alignment. This therefore ensures that the glove closely mimics the natural motions of human fingers and thumb. An overview of these previously proposed and developed rigid hand exoskeletons are summarized below, with a focusing on their design characteristics, actuation methods, sensors, and overall functionality.

Direct driven two-digit hand exoskeleton

This proposed design uses rigid linkage mechanisms directly driven by the actuators to exert forces onto the middle phalange of the finger and proximal phalange of the thumb to achieve desired bending [28]. Each linkage mechanism is an under-actuated revolute-revolute-revolute (RRR) design that consists of three serial planar links, which are actuated by a DC motor. A control scheme was implemented for this device to minimize any jerk disturbances created during actuation. Position and force sensors were incorporated within the design to provide basic sensory information. Overall, the system allows for a maximum bi-directional force output of 45 N and weighs 1 kg.

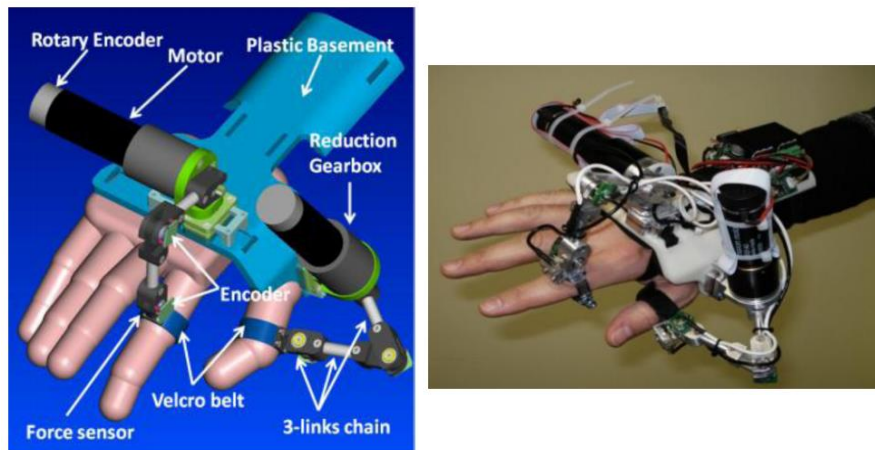


Figure 2.5: CAD design and prototype of the direct drive two-digit hand exoskeleton being worn [28]

Unfortunately, this prototype resulted in a large and heavy-weighted design. These drawbacks can affect the performance of the glove and the user's comfort when using it. In addition, the proposed prototype is only controlled using position feedback.

CyberGrasp

The CyberGrasp system is a popular commercial product that primarily serves as a haptic device that provides force feedback for virtual reality or tele-operating purposes [36]. The rigid exoskeleton design uses wires to create a pulley mechanism with five actuators, one for each finger/thumb. The design offers adjustability and a full RoM for the hand to prevent any obstruction of natural movements. The actuators allow a maximum output force of 12 N for each finger and thumb.



Figure 2.6: Picture of the CyberGrasp hand exoskeleton [36]

Despite being a successful commercial product, the CyberGrasp contains several drawbacks. This hand exoskeleton does not contain adequate sensors and thus requires an addition system to provide positions information for the user's hand. In addition, the actuators are located in a separate actuation module that can create issues for portability. Overall, the system is complex, bulky in size, and expensive in cost, having a market price of \$39,000.

SAFE Glove

The SAFE glove was developed as a lightweight, portable, self-contained assistive device [35], [37]. The design uses the rigid link approach with routed cables for each finger/thumb mechanism. The cable system is actuated using DC motors for all the finger/thumb mechanisms, which offer both active and passive force actuations with an output rate of 35 N passive and 10 N active at the tips of the fingers/thumb. Due to the linkage-cable mechanisms, the glove provides adjustability for various hand size. It contains sensors to measure positions and interactive forces and is able to perform force feedback control. The total weight of the system was approximately 430 g.

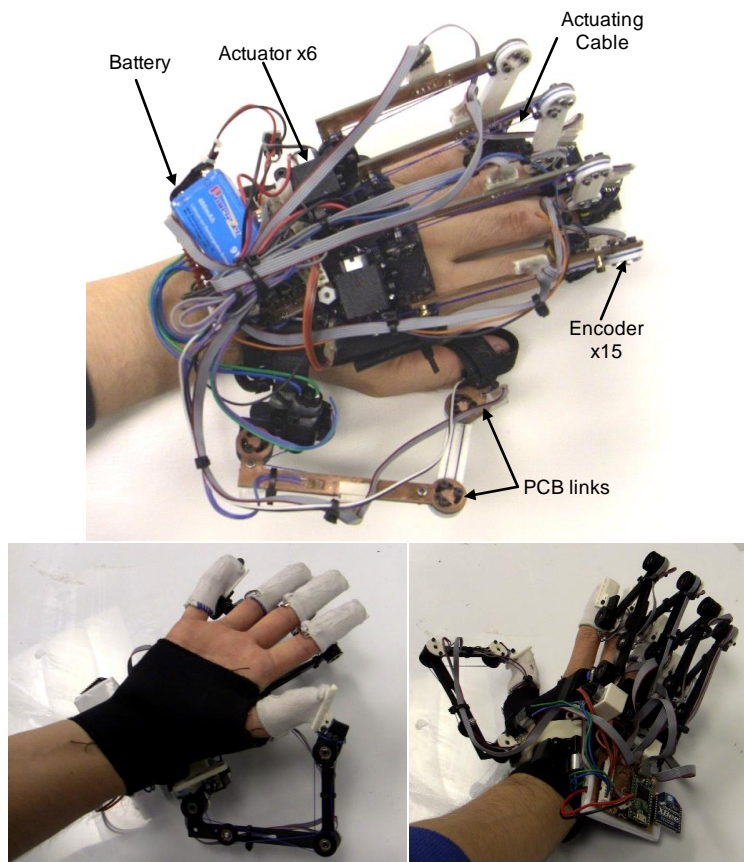


Figure 2.7: Prototypes of the SAFE Glove: Design II (top) and Design III (bottom) [35], [37]

One of the main drawbacks with this device is its bulky size, which measured to be approximately 50 mm above the dorsum of the hand. In addition, the natural coupling relationship of the finger/thumb joints were not taken into account and was instead designed only in respect to the total RoMs for the fingers and thumb.

Three-layered sliding spring glove

This hand exoskeleton glove was proposed as a novel alternative to the traditional rigid linkages, cable-drive, or pneumatic actuated systems [29]. The design uses a three-layered sliding spring mechanism to perform the flexion and extension motions for each finger and thumb. A single linear motor was used to push and pull against the sliding spring mechanisms to achieve the desired bending for all fingers and thumb. The overall system was compacted in size and lightweight, weighing 320 g on the arm and hand. The bending profiles enforced by the glove matched that of the natural flexion/extension joint angles of the human fingers and thumb.

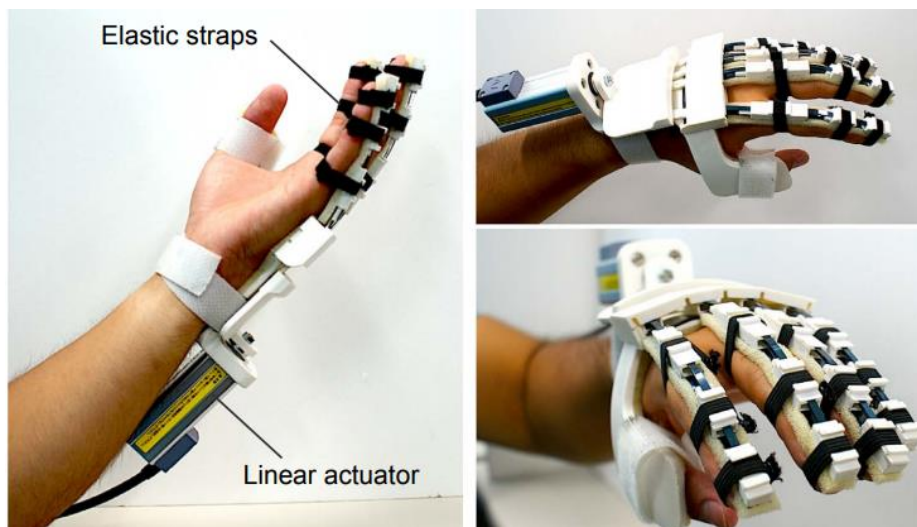


Figure 2.8: Prototype of the three-layered sliding spring hand exoskeleton [29]

Unfortunately the design lacks the ability to control the individual fingers separately and does not actuate the thumb at all since it is fixed. The glove also obstructs the natural RoM for the user's wrist. In addition, this hand exoskeleton does not incorporate force sensors or force feedback control into the design. As a result, the device may not be able to efficiently perform some of the commonly used grasps.

2.2.2. Soft Exoskeleton Gloves

As an alternative approach to the traditional rigid hand exoskeletons, researchers proposed the idea to replace rigid links and frames with softer components. Primarily, this alternative approach has been accomplished by either using (i) cables that are attached to the fingers and thumbs in a manner that would allow them to enforce bending motions when pulled [38]–[41], or (ii) elastic polymers that serve as inflatable membranes that bend when inflated and can thus actuate the fingers and thumb accordingly [42]–[45]. Several of these developed soft hand exoskeletons are reviewed below. The focus of this literature review is to explain the main characteristics of these exoskeleton systems, the types of actuations used, as well as the sensors, functionalities, and features of the systems.

Exo-Glove

The Exo-Glove is a wearable robotic hand exoskeleton that was designed using a soft tendon routing system [38]. The design goal was to present a soft wearable system that would be compact in size and lightweight. The system provides stable grasping while only incorporating the actuation of the index and middle fingers into the routing system. The design was bio-inspired, imitating the basic function of natural tendons in the fingers and thumb that transmit muscular forces to assist bending motions. The cable system consisted

of three components, as shown in Figure 2.9: (1) thimbles to insert and hold the tip of the finger/thumb, (2) pulleys made of fabric straps that are attached to the phalanges of the finger/thumb and Teflon tubes that were stitched to the fabric to allow for cable routing, and (3) Bowden cables that act as tendons in which one end is connected to the actuation unit and the other to the finger/thumb.

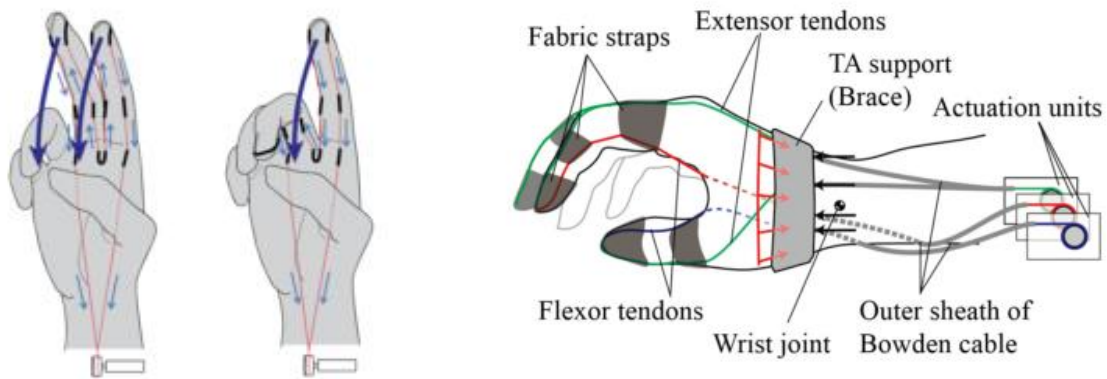


Figure 2.9: Mechanism design for the Exo-Glove [38]

Although this approach offers a stable grasp, it is unable to achieve other commonly used grasps that are used for ADL since it does not actuate the other fingers and thumb. In addition, the tendon routing system does not incorporate the natural coupling relationships among the joints of the fingers and thumb. The use of pulley cables also introduces the risks of friction and sheared force from the cables attached to the soft material of the glove being applied. These issues can drastically affect performance over time.

BiomHED

The BiomHED is an upper extremity exoskeleton system that was designed to provide assistance for users with hand impairments [39]. The design goal was to allow users to perform distal hand movements while concurrently performing proximal arm movements. The BiomHED uses exo-tendons that correspond to the anatomy and geometry of the major tendons in the hand, which assist in the actuation of the fingers and thumb movements. This mechanism is achieved using four cables for each finger and thumb to control the digit, mimicking the natural muscle-tendon units. Thermo plastic guides are used for the tendon routing. By routing the tendons to specific guides, some of the coupling relationships among the joints were achieved in the design. For the actuation method, seven DC geared motors are placed on a forearm based to transmit tension to the exo-tendon mechanisms. The system can produce a maximum force of 10 N from each actuator and weighs a total weight of 1 kg, which includes the motors and forearm bracket.



Figure 2.10: Prototype of the BiomHED [39]

Unfortunately, this design only allows for the independently control of the index finger and thumb. As a result, grasping and hand movements that require the additional control of the other four individual fingers cannot be achieved; only pinching grasps can be accomplished. In addition, the system does not offer encoders with the motors to measure the individual joint angles of the fingers and thumb. Thus, the system requires the use of a motion capture system to provide information for the joint angles.

Seoul National University (SNU) Pneumatic Hand Exoskeleton

The hand exoskeleton glove produced by the BioRobotics Laboratory at SNU was developed as a soft wearable, assistive device [42]. The goal was to overcome the drawbacks of rigid links and joints exoskeleton systems by developing a novel design that use pneumatic artificial muscles. By using these artificial pneumatic muscles as actuators, the mechanism could become simple, compacted in size, and lightweight. These artificial muscles were made using elastic polymer membranes that can cause flexion motions among the fingers and thumb when inflated with air. To achieve the bending motions, a linkage system was employed with the artificial muscles to serve as a guide for the muscles to bend in a desired manner. It allowed for the expansion of the artificial muscles to be constrained at the phalange regions of the fingers and thumb, therefore concentrating the enforced motions at the fingers and thumb joints. The total weight for the hand exoskeleton was less than 150 g, excluding the pneumatic actuators and air compressors. The total grip force outputted by the glove was 42.2 N when using air pressure of 2.8 bar.

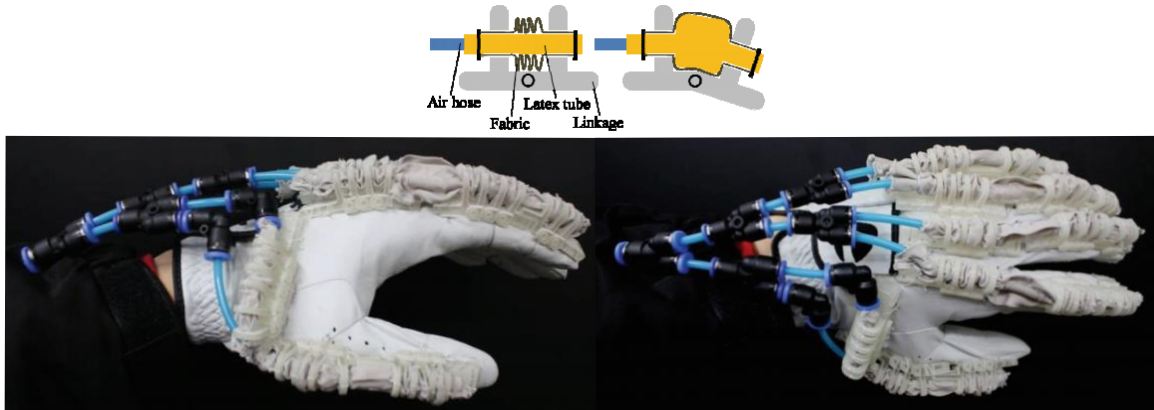


Figure 2.11: Prototype of the pneumatic hand exoskeleton (SNU) [42]

Like most pneumatic systems, this hand exoskeleton lacks feasible portability due to the complex system that is required for the pneumatic actuators (air tank, air compressor, solenoid valves, tubing, control boards, etc). In addition, the design does not adopt a coupling mechanism among the joints to mimic the joint angle relationships that allow for the natural bending profiles of the fingers and thumb. Another drawback of this device is the lack of controllability, specifically the ability to control the output forces or positions of each finger and thumb. The use of one pneumatic actuator for all fingers and thumb also hinders the ability to perform various grasps that requires controlling each finger/thumb individually.

Harvard Soft Robotic Glove

This soft hand exoskeleton was developed as an assistive device to help perform an overall power grasp to achieve many ADLs [43]. The goal was to design a soft wearable system that would provide comfort while wearing it. The mechanisms for the fingers and thumb was made of soft Kevlar fiber and silicone elastomers that serve as multi-segment actuators. When inflated with pressurized fluids, the soft actuators bend to enforce the flexion RoMs among the user's fingers and thumb. The fabrication of these soft actuators consist of: (1) a half-rounded rubber body that is supported by a 3D printed mold, (2) a strain limited layer that is applied to the flat face of the rubber body, and (3) a radial strain limited layer that is wrapped around the rubber body and flat strain layer either clockwise or counter-clockwise. Certain combinations of applying these radial strain limited layers can result in a twisting, expanding, or bending profile, as shown in Figure 2.12.

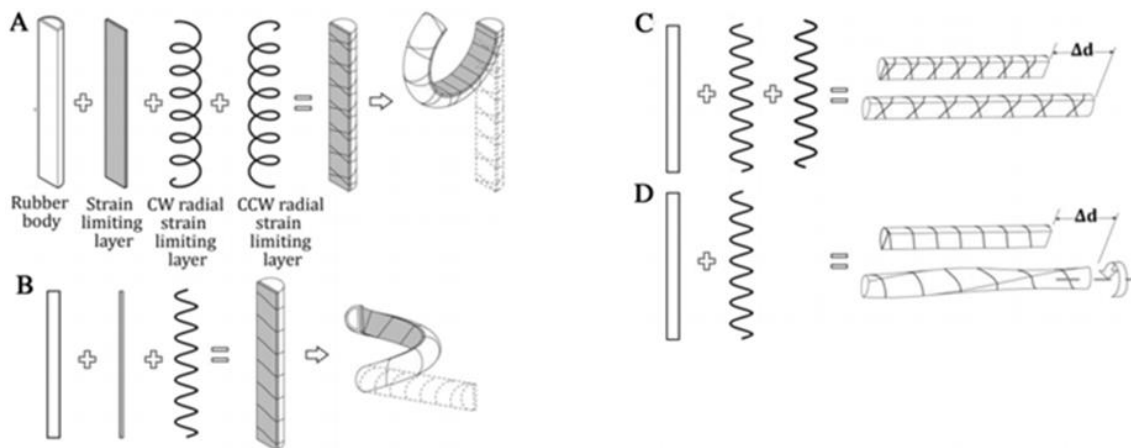


Figure 2.12: Exploded and assembled view of the soft actuator mechanism [43]

To integrate the design into a working system, the mechanisms were further developed into a full glove with a portable waist belt pack that houses the pneumatic system (water

pump reservoir, controller boards, batteries, valve switches, and tubes). In addition, a pressure controller was implemented to control the output forces of the glove.

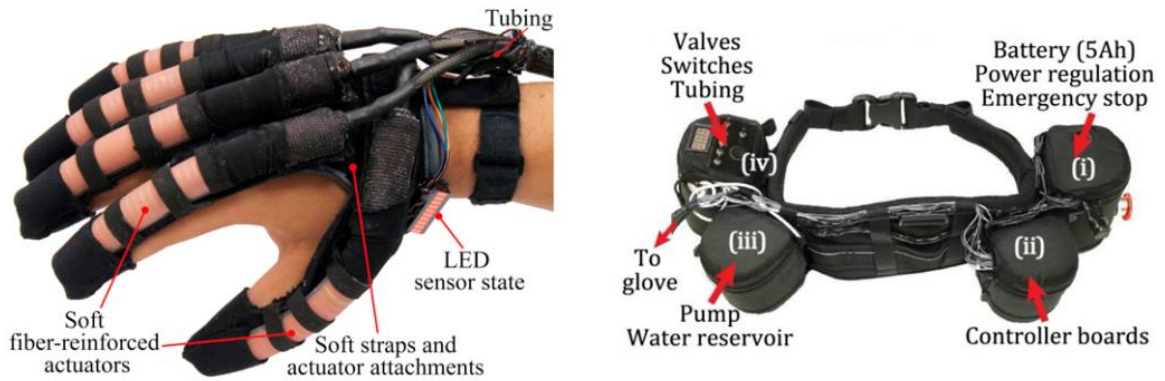


Figure 2.13: Prototype of the proposed soft robotic glove and the waist belt pack [43]

Unfortunately, the design does not focus on achieving the natural coupling relationships between the joints of the fingers and thumb. As a result, natural bending profiles during flexion and extension motions are not accounted for. Despite developing a waist belt pack to carry the pneumatic system, the portability of the system is still limiting factors that is only feasible for patients in a wheelchair or those healthy enough to carry the additional weight throughout their everyday routine.

2.3 Comparative Analysis

Unfortunately, both of these design approaches have their fair share of disadvantages. The major drawback of a traditional hard rigid exoskeleton is that it results in a bulky and heavy-weighted glove, which can cause user fatigue during prolonged usage. The soft gloves driven by tendon cables have the following drawbacks: discomfort produced by the pre-tensioning of the cables, loss in efficiency caused by friction along the tendon path, and the creation of shear forces applied onto the soft material by the tendons during flexion and extension motions. These factors together hinder effective force transmissions in these tendon driven systems, which thereby decrease the repeatability of the systems. On the other hand, the soft inflatable robotic gloves are challenged by their inability to provide natural flexions and extensions profiles for the human fingers and thumb. The use of pneumatic and hydraulic actuators for these soft hand exoskeleton systems can create additional issues for portability and the implementation of force and/or position feedback controls. Without controllability, these systems are limited to only achieving the two basic configurations of fully extended and flexed fingers/thumb (open or closed fist).

2.4 Conclusion

With the human hand being such a complex system, many of these state-of-the-art hand exoskeleton systems are unable to efficiently imitate all of the hand functionalities. As a result, hand exoskeletons are designed to prioritize certain features over the others in accordance to their intended application requirements. However, certain tradeoffs can drastically affect the performance of the system. These concerns are discussed in detail in the next chapter.

CHAPTER 3

PROBLEM STATEMENT AND PROPOSED SOLUTION

A literature review on hand exoskeletons was given in the previous chapter, describing the two approaches for designing hand exoskeleton systems and presenting several state-of-the-art examples. The analysis highlighted the advantages and disadvantages of both approaches, ultimately identifying common problems and tradeoffs in designing hand exoskeletons. This chapter further discuss these common design problems and presents the goals of the proposed mechanism for a new hand exoskeleton.

3.1 Motivations and Analysis of Related Research Problems

With the human hand being a complex structure, there exist many design concerns for developing an efficient hand exoskeleton. The design process must consider the various capabilities of the human hand such as sensory processing and motor skills, grasping strength, fingers and thumbs trajectories while bending, and the velocities and torques of the fingers and thumbs. It is difficult to achieve all the capabilities of the human hand without any tradeoffs. Not only is this due to the hand having complex motions that have yet to be mathematically characterized, but also it is primarily a result of technology limitations (actuators, sensors, etc) and application requirements. The following subsections will present some of the common design challenges for developing hand exoskeletons that can emulate the basic abilities of the human hand.

3.1.1. Size and Portability Issues

When it comes to designing exoskeletons in general, the weight of the system is one of main concern. This concern increases in importance when the desired exoskeleton systems is one that need to be portable, such as for assistive purposes or strength enhancing. In terms of hand exoskeletons, the ideal weight of the device should be light enough for the user to wear without experiencing discomfort or limiting the workspace of the arm, wrist, hand, fingers, and thumb. Sensors and actuation units can affect the portability of the system. Many exoskeleton systems require powerful motors that can produce high torque motions, which can unfortunately lead to using heavy weighted actuators. In addition to weight, some actuators require additional equipment setup that can make it difficult to achieve portability. For example, many of the presented soft hand exoskeletons use pneumatic and hydraulic actuators that require air/fluid tank reservoirs, compressors, pressure regulator valves, air/fluid tubes, and even solenoid valves to control the flow of air/fluids. One impulsive solution to make these systems portables would be to use compact air compressors/fluid pumps and small air/fluid reservoirs that could fit inside a backpack for the user to wear, along with any additional equipment. Although this approach may seem plausible, it creates greater concerns such as: (1) having less available air for the pneumatic and/or hydraulic actuators to use between refills of the reservoir tanks, and (2) the additional weight from the backpack that the user now has to carry, which can be a serious issue for the elderly, toddlers, and disabled bodies.

The size of the exoskeleton systems can also affect performance and user experience. Ideally, the design of an exoskeleton system should consider the proxemics of the user. For hand exoskeletons, an ideal size would be one that does not drastically affect the user's

perceived space for their hand. Instead, it should be small enough for the user to readjust their perception with ease to adopt the hand exoskeleton as part of their own personal space. This readjustment is commonly done for wristwatches once users become comfortable from wearing them. The bulky frame size of the rigid hand exoskeletons discussed in Chapter 2 creates great difficulties for their users to readjust their perceived hand space. The rigid links tends to extend outwards from the top of the fingers and thumb by a great amount. Other components of hand exoskeletons, such as sensors and actuators can also add an increase in size.

3.1.2. Natural Joint Angle Relationship Issues

It is important to design a hand exoskeleton that can emulate natural joint angles during grasping motions, especially for rehabilitation purposes. In general, an ideal hand exoskeleton system should improve the hand functionalities for the user without causing discomfort. If a hand exoskeleton is unable to produce natural bending profiles for the fingers and thumb during grasping motions, it can negatively affect performance and user experience. In particular, one can imagine the feeling of discomfort when having to grasp an object in an unfamiliar and unnatural manner. In the case of rehabilitation purposes, patients undergo a physical therapy process that requires them to practice different grasping motions in order to relearn muscle memory to regain certain functionalities in their hand. As one could conclude, it is important for the patients to practice correct and natural bending profiles during therapy so that they can relearn the correct way to grasp different objects. Not only could practicing unnatural bending profiles of grasping affect the patient's recovery process, but it could also create a huge safety concern if a hand

exoskeleton (designed for any application in general) bends the fingers and thumb beyond the physical constraints of each joint and its RoMs.

3.1.3. Sensory Feedback Issues

The natural functionality of sensory feedback within the human body is a task of the nervous system. Neurons, which are the basic units that make up the nervous system, are the cells responsible for transmitting information to other nerve cells, muscle, and gland cells. For the processing of sensory information, there exist special afferent neurons that receive sensory impulses for action potentials, which are eventually transmitted to the areas of the brain known for sensory perception. These sections of the brain along with the afferent neurons and neural pathways, come together to form sensory systems throughout the nervous system of the human body. Several of these commonly known sensory systems are the ones responsible for vision, hearing, smell, taste, and touch. When it comes to performing the sense of touch using the human hands, it is essential for the brain to receive sensory feedback for interaction forces and perceived sensations from skin contact such as temperature, vibrations, texture, and pain. These sensations are critical for the performance of the hand and its ability to react properly to sensory feedback. For instance, these reactions can prompt the hand to release its grip when touching an object of extreme temperature or strengthen its grip for readjustment when holding an object vibrating at a high frequency.

Designing a hand exoskeleton that can assist users with grasping motions while incorporating such high level sensory feedback can present several difficulties. Limitations in technology make it almost impossible to imitate the complex sensory nervous system of the human body. Although there exist sensors that can measure some of these sensations

such as temperature, the process of transmitting the information from these sensors back to the human brain has proven to be a complex task. Some of the approaches that have shown great potential towards achieve this goal are the disciplines of brain-computer interface (BCI) and neuroprosthetics [46]. Both fields focus on developing devices that can provide biological functionality whether it's an attempt to be a substitute for a damaged motor, sensory, or cognitive modality within the human body, or a device that connects to the brain for purposes like assisting, mapping, augmenting, or repairing either human cognitive functions or sensory-motor functions. To achieve these goals, both fields are engaging in research efforts to safely implant devices inside humans that will communicate with the nervous system of the body through the transmission of small electrical currents to the nerves. These electrical currents are used to imitate the natural impulses produced by neurons. These implants can thus be used to simulate the natural sensations of touching objects of different textures and temperature, or even the feeling of pain when using a prosthetic hand or hand exoskeleton. However, this approach faces serve obstacles such as health and safety concerns for the human body and issues in biocompatibility, size and weight, power consumption, data transmission, and how to safely implant the device.

Hand exoskeletons and other exoskeletons systems in general, have adopted an alternative BCI method that offers more feasibility without the risks and concerns of implanted devices. The method is to either translate the brain's activity into action commands that prompt the exoskeleton to execute specific functions, or allow each unique action performed by the exoskeleton to send a specific stimulus to the human body using haptic sensors like vibration motors. The monitoring of the electrical activities of the brain can be done using electroencephalography (EEG) sensors. Difficulties can occur in both

approaches such as: (1) successfully characterizing brain activities to find unique patterns for each desired function, (2) finding appropriate areas on the body to place haptic sensors, (3) the accuracy of the affordable sensors that are suitable for daily activities.

In addition to incorporating stimulus-based feedback, some state-of-the-art hand exoskeleton systems have integrated force sensors to achieve interactive force feedback. This allows the ability to grasp various objects while maintaining stability, without causing harm to the user or unwanted damages to the object. Achieving this ideal force control within a robotic system can present many challenges because of the limitations from the actuators and sensors used.

3.1.4. Workspace Issues

The overall purpose of a hand exoskeleton system is to provide the user with a great experience, whether it's being used to recover hand functionality or assist with a hand impairment. Ideally, the hand exoskeleton should accomplish its functionalities without restraining the natural RoMs for the user's hand, wrist, and overall arm. Without ensuring natural motions from the fingers, thumbs, and hand, there exist the risks of unnatural bending that can lead to serious injuries. Beside safety concerns, the possibility of affecting performance is also a risk when the hand exoskeleton is not designed to achieve natural RoMs. Thus, the preservation of the natural RoMs during the enforced movements by the hand exoskeleton helps to ensure the safety of the bending fingers and thumb as well as the ability to achieve comfortable grasping motions for everyday task.

3.2 Research Objectives and Hypothesis

Using the proposed mechanism for a novel hand exoskeleton, this thesis hypothesizes that the following objectives can be accomplished:

- **Size** –A small sized design that allows the glove to be worn without drastically affecting the user’s perceived space for their hand nor restricting normal movements for the hand, wrist, and arm.
- **Weight** –A lightweight design to prevent any constraints on performance and the ability to accomplish grasping for ADLs. In addition, the overall weight will allow the system to be portable.
- **Portability** –A portable design to allow the user to use the proposed hand exoskeleton as a general-purpose glove that includes being a rehabilitation device as well as an assistive glove and haptic device.
- **Safety** –A safe design that does not cause any harm or injuries to the user and contains protection protocols (whether through software or mechanical design) that ensure movements are within the natural RoMs of the hand.
- **User friendly** –An easy to wear design that is also simple to use.
- **Sensory processing** –A design that incorporates some of the basic sensory feedback of the natural human hand, such as position and force information for all fingers and thumbs.
- **Force control** –A design that accurately controls the applied forces by the hand exoskeleton when interacting with its environment, thus offering compliance when necessary.

3.3 Proposed Robotic Hand Exoskeleton

This thesis presents the mechanism design for a robotic hand exoskeleton that can overcome several of the common issues of both rigid and soft hand exoskeletons. A two-digit prototype of this proposed design is first presented as a proof of concept. The two-digit prototype is further developed into a full hand exoskeleton design. The proposed hand exoskeleton is designed to assist users with grasping motions, while maintaining a natural coupling relationship among the finger and thumb joints that reflect that of a normal human hand. The design employs single degree of freedom linkage mechanisms to achieve active flexion and extension of the fingers and thumb.

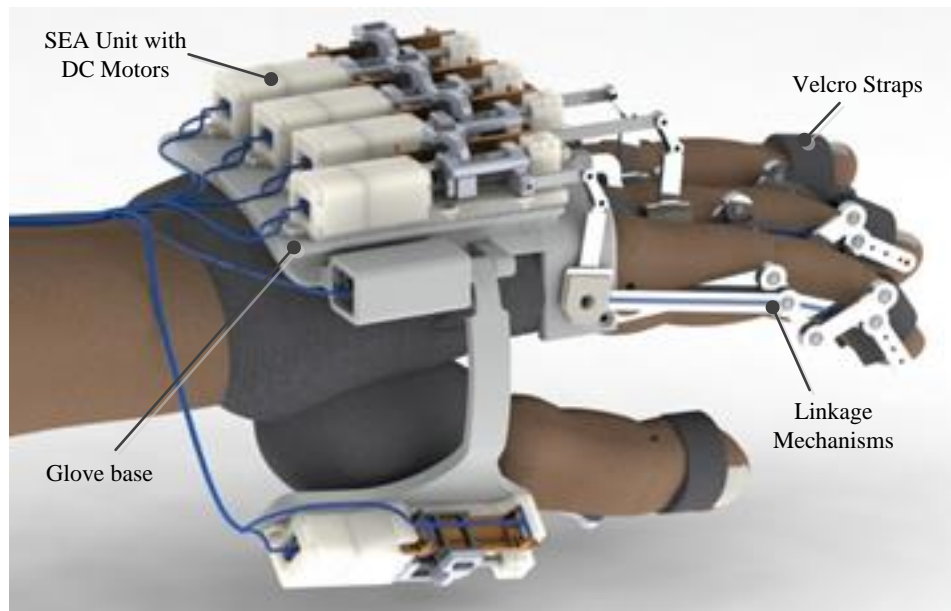


Figure 3.1: Proposed design for a full hand exoskeleton system

Each mechanism is designed to have a slim and compact profile that allows the links to be placed alongside the corresponding digit. This approach greatly reduces the overall weight and size of the system, which makes it ideal for prolonged usage. In addition, the

proposed system is capable of processing position information for the fingers and thumb movements, interaction forces exerted by the fingers/thumb, and is able to provide haptic feedback. To create intelligent sensory feedback, a force control scheme is presented using a proposed compacted design for a SEA unit. Figure 3.1 presents the proposed design of the full hand exoskeleton.

CHAPTER 4

ROBOTIC HAND EXOSKELETON DESIGN

4.1 Overview

As discussed in Chapter 2, the human fingers and thumbs contain joints that are inherently coupled. This essentially causes the fingers and thumbs to act as a single DOF system during flexion and extension motions. Using this knowledge, the hand exoskeleton mechanism for each finger and thumb was designed as a single DOF system. This approach allows for a reduction in the number of needed actuators, which in return reduces the overall weight and size of the hand exoskeleton.

In order to design an exoskeleton glove that satisfies the goals mentioned above, existing studies on human grasping motions, such as the common pinch, were reviewed [47]–[49]. As mentioned before, [20] performed experiments to measure the joint angles for the index finger and thumb during a tip-pinch motion. The data showed that with a tip-pinch force of 100g and a pulp distance of 1cm, the index finger yielded joint angles of 49.1° (SD 9.5°), 41.0° (SD 10.7°), and 38.5° (SD 6.8°) for the MCP, PIP, and DIP joints respectively while the thumb yielded 12.8° (SD 9.4°), and 21.8° (SD 7.8°) for the MCP and IP joints. As discussed in Section 2.1.3, these joint angles from a precision grasp closely resemble the joint angles produced from the power grasps of [19]. As a result, this data was used as a reference to achieve the natural coupling relationship among the joints of the fingers and thumb when designing the exoskeleton glove.

The conceptual design of the mechanism for the proposed hand exoskeleton was inspired by the USC/Belgrade Robotic Hand [50]. Since the coupling mechanism used in this robotic hand was proven successful, the design approach for the proposed hand exoskeleton was to adopt a similar coupling mechanism that can be modified and made suitable for an exoskeleton glove.

4.2 Kinematics

The basic design of the mechanism consists of planar links that are connected through revolute joints, as detailed in Figure 4.1. Together these links and joints form a four bar mechanism design.

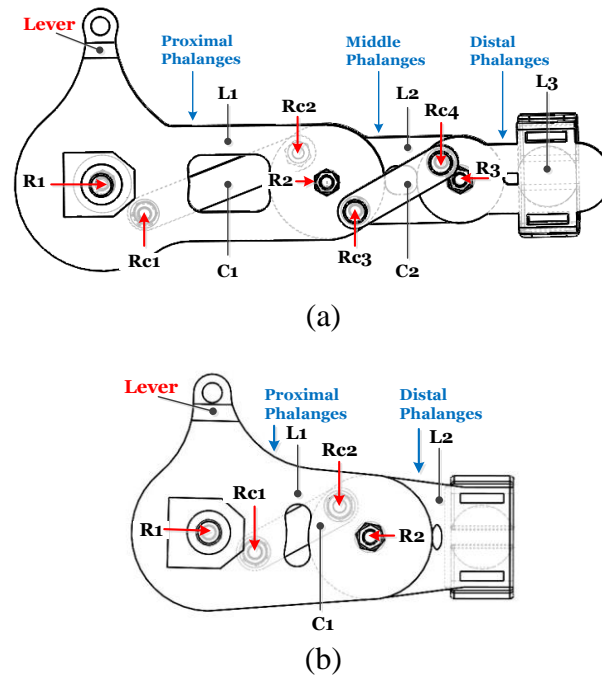


Figure 4.1: (a) Design of the index finger mechanism, (b) Design of the thumb mechanism.

The basic structure of the mechanism for the index finger is composed of links L_1 , L_2 , and L_3 , which correspond to the proximal, middle, and distal phalanges of the finger respectively, as shown in Figure 4.1. These three links are connected through three revolute joints, R_1 , R_2 , and, R_3 . Specifically, links L_i and L_{i+1} are connected through revolute joint R_{i+1} . The constraint links C_1 and C_2 are used to produce the coupling relationship between the L_i links. Constraint link C_1 connects link L_2 to a fixed base frame (ground) by revolute joints R_{c1} and R_{c2} , while constraint link C_2 connects links L_1 to L_3 through joints R_{c3} and R_{c4} . The thumb mechanism is similar, containing only links L_1 and L_2 , which are connected by revolute joint R_2 . The coupling action for the thumb mechanism is achieved by the constraint link C_1 , which connects link L_2 to the base frame through the revolute joints R_{c1} and R_{c2} . The assembly of the mechanisms shown in Figure 4.1, can be summarized in the following steps:

- Link L_1 is connected to the ground at joint R_1
- Link L_1 is connected to link L_2 at joint R_2
- Link L_2 is connected to link L_3 at joint R_3 *
- Constraint link C_1 connects to the ground at constraint joint R_{c1} and to link L_2 at constraint joint R_{c2}
- Constraint link C_2 connects to link L_1 at constraint joint R_{c3} and to link L_3 at constraint joint R_{c4} *

Note: * only applied for the finger mechanism and not for the thumb mechanism.

The flexion and extension motions are achieved when a rotary motion is applied at joint R_1 from pushing and pulling respectively on the lever of link L_1 . This causes link L_1 to bend and as it bends, the constraint links C_1 and C_2 translates the motion along to links L_2

and L_3 , as illustrated in Figure 4.2. The design procedure for the thumb mechanism follows the same steps, but with only two main links L_i and one constraint link C_i . This collectively provides the coupling motion that reflects the natural flexion and extension of a human finger.

4.3 Kinematic Modeling

Before a detailed mechanical design of the exoskeleton glove could be created, the lengths of various links and positioning of revolute joints had to be determined based on the general dimensions of a human hand and the joint angles desired to be achieved in reference to [20]. To this extent, a kinematic modeling of the mechanism was completed. The modelling was accomplished through the consideration of the following design parameters (illustrated in Figure 4.2.):

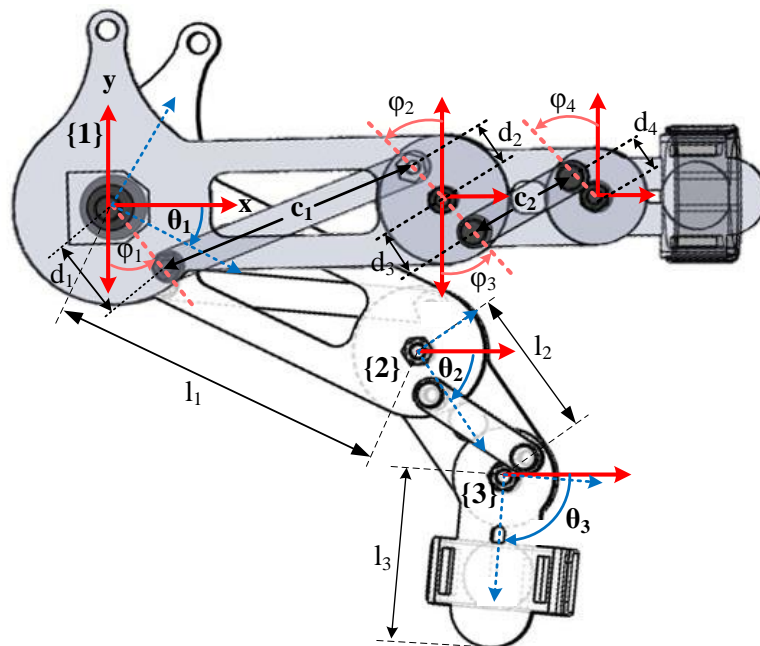


Figure 4.2: Index mechanism showing two configurations and the design parameters for kinematic modelling. The relaxed configuration is shown in gray, while the black & white schematic shows a flexion configuration

- l_i - length of link L_i , measured as the normal distance from R_i to R_{i+1} . For l_3 , the distance is measured from R_3 to the tip of the end-effector/ L_3
- c_i - length of constraint link C_i , measured as the normal distance from R_{c_i} to $R_{c_{i+1}}$
- θ_i - joint angle of link L_i , defined as the angle measured from the x-axis of the base coordinate frame to the x-axis of the body coordinate frame
- d_i - the radial distance of constraint joint R_{c_i} to the origin of the corresponding link body coordinate frame
- φ_i - the angle made by constraint joint R_{c_i} in respect to the vertical y-axis of the body coordinate frame for link L_i , measured in the counter-clockwise direction

The finger mechanism has three planar links with body coordinate frames attached to the joint, which are defined as $[(x_1, y_1, \theta_1), (x_2, y_2, \theta_2), (x_3, y_3, \theta_3)]$ respectively. The location of each link is represented by the x_i and y_i terms, while the θ_i terms reflect the joint angles produced by the flexion/extension motions. These joint angles are measured from the x-axes of the original base coordinate frames of the links to the x-axes of the new body coordinate frames, which result from the mechanism being in motion. The base coordinate frame is illustrated in Fig. 4 by red coordinate lines (x, y), while the body coordinate frames are shown by the blue dotted lines. All of the coordinate frames are right handed, with the z-axes pointing forward (out of the page).

The thumb mechanism on the other hand has two links, which are defined by the coordinates $[(x_1, y_1, \theta_1), (x_2, y_2, \theta_2)]$. For the single DOF mechanism for the fingers, establishing θ_1 as the input variable in the modeling yields the following eight constraint equations:

$$\begin{aligned}
x_1 &= 0 \\
y_1 &= 0 \\
x_2 &= x_1 + l_1 \cos \theta_1 \\
y_2 &= y_1 + l_1 \sin \theta_1 \\
x_3 &= x_2 + l_2 \cos \theta_2 \\
y_3 &= y_2 + l_2 \sin \theta_2 \\
c_1^2 &= [x_2 - (d_2 \sin \varphi_2 \cos \theta_2 + d_2 \cos \varphi_2 \sin \theta_2) - d_1 \sin \varphi_1]^2 \\
&\quad + [y_2 + (d_2 \cos \varphi_2 \cos \theta_2 - d_2 \sin \varphi_2 \sin \theta_2) + d_1 \cos \varphi_1]^2 \\
c_2^2 &= [(x_3 - (d_4 \sin \varphi_4 \cos \theta_3 + d_4 \cos \varphi_4 \sin \theta_3)) \\
&\quad - (x_1 + (l_1 + d_3 \sin \varphi_3) \cos \theta_1 + d_3 \cos \varphi_3 \sin \theta_1)]^2 \\
&\quad + [(y_3 + (d_4 \cos \varphi_4 \cos \theta_3 - d_4 \sin \varphi_4 \sin \theta_3)) \\
&\quad - (y_1 + (l_1 + d_3 \sin \varphi_3) \sin \theta_1 - d_3 \cos \varphi_3 \cos \theta_1)]^2
\end{aligned} \tag{1}$$

The endpoints for each L_i link are expressed by the x_i and y_i equations above. The C_i constraint links are considered as absolute distance constraints. Using these equations, the position of each finger and thumb can be determined and used as sensory feedback for the proposed hand exoskeleton in its applications.

For the kinematic model, the link lengths L_i were set to general dimensions of human fingers and thumb. The other design parameters were initially estimated using a MATLAB simulation and later determined using kinematic optimization. The design parameters that produced joint angles that closely resemble that of a natural finger and thumb, were selected as the best guess for the optimization procedure. Figure 4.3 and Figure 4.4 each present the kinematic simulation results using the estimated design parameters. For these simulations, the joint angles were measured using the following relationships: (i) MCP joint = θ_1 , (ii) PIP joint (IP for thumb) = $\theta_2 - \theta_1$, and (iii) DIP joint = $\theta_3 - \theta_2$.

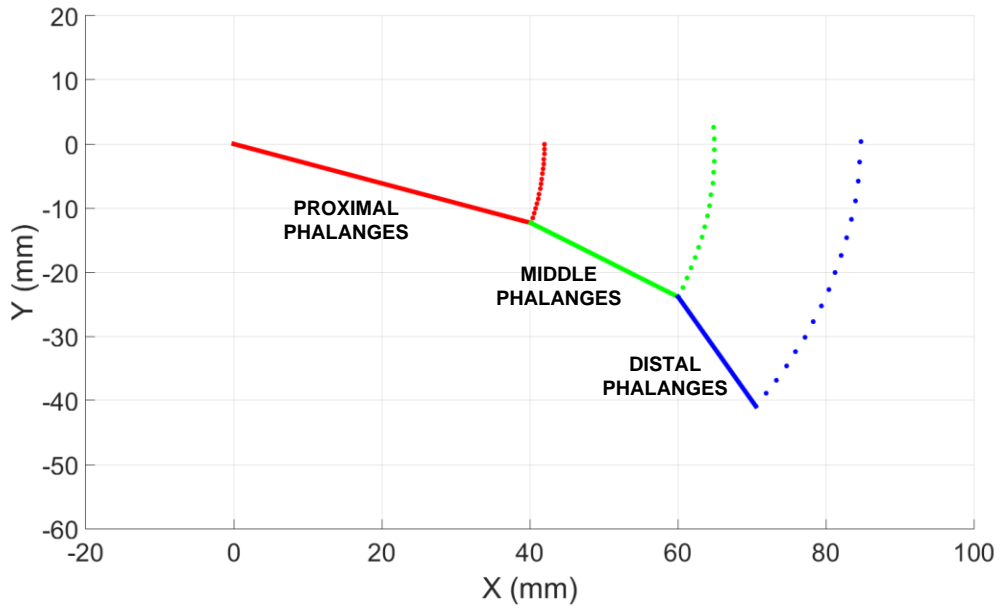


Figure 4.3: Simulation of the desired index finger trajectory starting at the origin of (0,0)

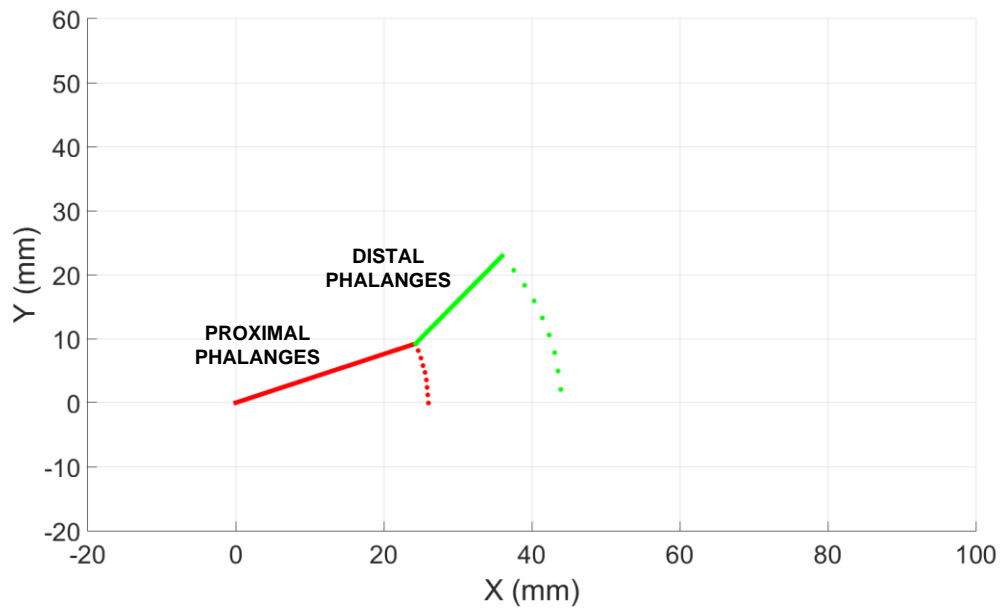


Figure 4.4: Simulation of the desired thumb trajectory starting at the origin of (0,0)

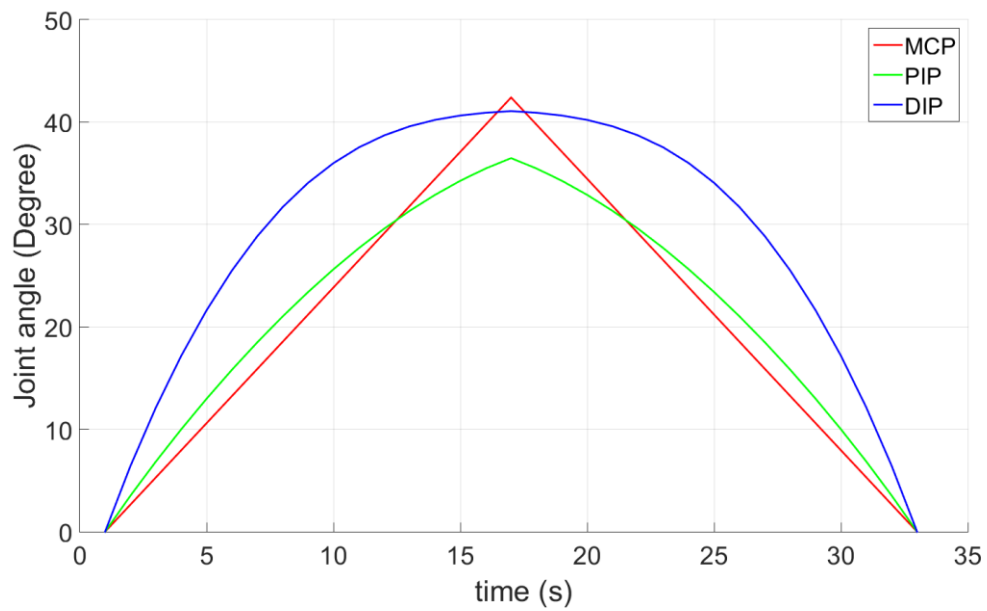


Figure 4.5: Relationship of the joint angles from the finger mechanism during flexion and extension motions

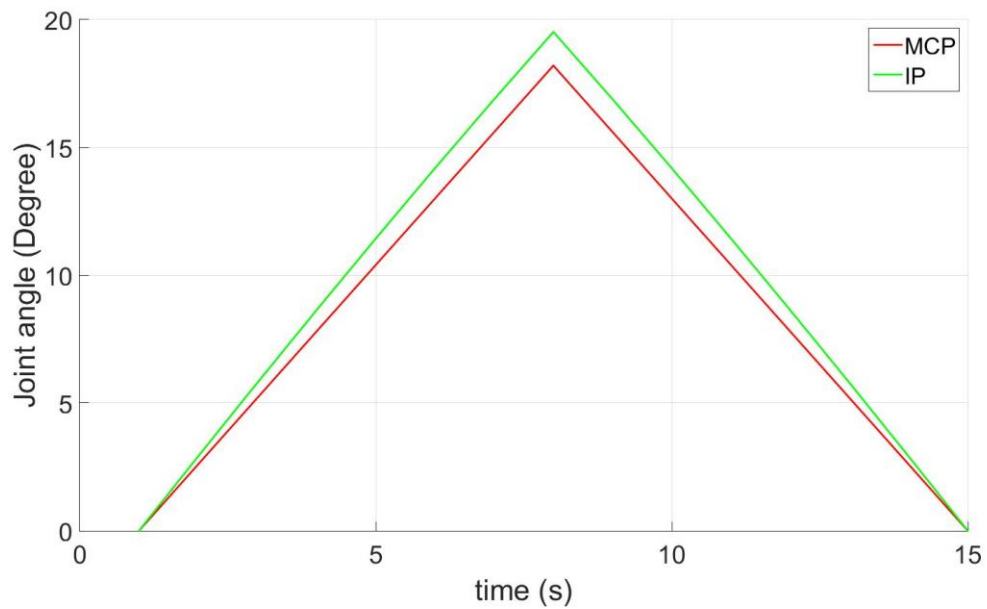


Figure 4.6: Relationship of the joint angles from the thumb mechanism during flexion and extension motions

These results show that the finger trajectory can provide maximum angles of 43° , 41° , and 37° for the MCP, PIP, and DIP joints respectively, while the thumb trajectory offers MCP and IP angles of 19° and 17° respectively. By comparing these joint angle relationships shown in Figure 4.5 and Figure 4.6 to the desired joint angles that were discussed in Section 4.1, it can be observed that the simulated trajectories resulted in the desired range. This therefore confirms that the proposed mechanisms can enforce joint angle relationships resemble the natural bending motions of the fingers and thumb during flexion and extension.

4.4 Kinematic Design Optimization

In order to determine the optimal combination of design parameter values that will produce natural joint angle relationships, an optimization procedure was employed.

4.4.1. Optimization Objectives

The optimization scheme was designed to accomplish two primary objectives: (1) minimize the differences between the relationships of the desired joint angles and the angles produced from the current design parameter values, and (2) minimize the height of the finger/thumb mechanisms by restricting how much the constraint links extend beyond the height of the corresponding finger/thumb. The referenced angles from Section 4.1 were again used as the desired angles for the optimizations. All four fingers used the joint angle relationship from the referenced index finger as their targeted joint angle relationships. The second objective was achieved as a linear inequality constraint.

This multi-objective optimization was implemented in MATLAB using the *fmincon* algorithm. The mathematic description for the algorithm is presented below:

Objective function:

$$\min_x F(x) = \{w_1 MCP_{Error} + w_2 PIP_{Error} + w_3 DIP_{Error}\} \quad (2)$$

Subject to:

$$Ax \leq b \text{ (Linear inequality)} \quad (3)$$

$$lb \leq x \leq ub \text{ (Lower and upper bounds)} \quad (4)$$

Where the variables:

- x - is a vector containing the design parameters variables:
 $\langle \varphi_1, \varphi_2, \varphi_3, \varphi_4, d_1, d_2, d_3, d_4 \rangle^T$, corresponding to Figure 4.1
- MCP_{Error} - is the difference in the desired MCP joint angular displacement and resulting MCP joint angle produced by the current optimization iteration trial
- PIP_{Error} - is the difference in the desired PIP joint angular displacement and resulting PIP joint angle produced by the current optimization iteration trial
- DIP_{Error} - is the difference in the desired DIP joint angular displacement and resulting DIP joint angle produced by the current optimization iteration trial
- w_i - the vector of weights that specify which joint errors have the higher priority for optimizing
- A - is a 2×2^n matrix of the constants $\begin{bmatrix} 0 & 0 & 0 & 0 & 1 & 1 & 0 & 0 \\ 0 & 0 & 0 & 0 & 0 & 0 & 1 & 1 \end{bmatrix}$, where n is the number of design parameters for the objective function

- b - is a $n \times 1$ matrix containing the variables $\begin{bmatrix} PP_H \\ IP_H \end{bmatrix}$, which represents the desired height for the intermediate and proximal phalanges of the corresponding finger/thumb. Again, n is the number of design parameters
- lb - is a vector containing the lower bound values for the design parameters variables of the vector x . The optimization procedure for each finger mechanism used the same lower bound values of: $\langle 20^\circ, 20^\circ, 20^\circ, 20^\circ, 7\text{mm}, 7\text{mm}, 7\text{mm}, 7\text{mm} \rangle$ and $\langle 20^\circ, 20^\circ, 7\text{mm}, 7\text{mm} \rangle$ for the thumb mechanism
- ub - is a vector containing the upper bound values for the design parameters variables of the vector x . The optimization procedure for each finger mechanism used the same upper bound values of: $\langle 70^\circ, 70^\circ, 70^\circ, 70^\circ, 12\text{mm}, 12\text{mm}, 12\text{mm}, 12\text{mm} \rangle$ and $\langle 75^\circ, 75^\circ, 12\text{mm}, 12\text{mm} \rangle$ for the thumb mechanism

These vector x variables are pass into the objective function to help calculate the current joint angle relationships, by using multibody dynamic principles. Other variables such as the link lengths (which are based off the phalanges lengths of the finger/thumb), are used in this calculation for joint angles in terms of Equation (1). The steps to calculate the joint angles are summarized below:

- 1) Initialize the generalized coordinates, which includes the coordinates for each body of the mechanism: $q = [(x_1, y_1, \theta_1), (x_2, y_2, \theta_2), \text{ and } (x_3, y_3, \theta_3)]$

- 2) Determine the constraint equations on position (θ_p). These are the same as the Equation (1) from Section 4.3, but re-written to be equal to zero. These equations will be solved simultaneously in order to obtain the valid configurations of the mechanism at each time step, which can be used to determine current position/joint angles.

$$\phi^K(q) = \theta_p \text{ (Equation (1) written in respect to equaling zero)} \quad (5)$$

- 3) Determine the driving constraint(s) of the mechanism that determines how much the system moves at each time step.

$$\phi^d(q, t) = [\theta_{StepSize} * t] \quad (6)$$

- 4) Compute the constraint matrix by combining the constraint equations and the driving constraint(s).

$$\phi(q, t) = \begin{bmatrix} \phi^K(q) \\ \phi^d(q, t) \end{bmatrix} \quad (7)$$

- 5) Obtain the velocity equations from the constraint equations using the Jacobian matrix-

$$v = \phi_q(q, t) * \dot{q}(t) - \phi_t \quad (8)$$

$$\theta_q = J\theta_p \text{ (simplified)} \quad (9)$$

- 6) **Obtain the acceleration** equations using the velocity equations.

$$\phi_q \ddot{q} = -(\phi_q \dot{q})_q * \dot{q} - 2\phi_{qt} - \phi_{tt} \quad (10)$$

- 7) Loop through each step size to:

- a. **Determine** the next position using the equation:

$$\theta_{q_{new}} = \theta_{q_{old}} + \dot{\theta}_q t + \frac{1}{2} \ddot{\theta}_q t^2 \quad (11)$$

- b. Solve the constraint equations for the corresponding joint angles using the new link positions
- c. Compute the next velocity and acceleration using the position results from 7b
- d. Determine the value of the driven joint at the next time step.
- e. Repeat loop until the last step is reached

The linear equality, nonlinear equality, and nonlinear inequality constraint equations were not needed since the objective function takes into account the Equation (1) to calculate the joint angles. For the thumb mechanism, the objective function only contain two joint parameters instead of the three shown above. As a result, the design parameter variables of x does not contain $\varphi_3, \varphi_4, d_3, d_4$ and the other variables as well as the lower/upper bounds are adjusted accordingly.

4.4.2. Optimization Results

The optimization was performed for each finger and thumb mechanism. In addition to the variable values discussed in the previous section above, the values for the other optimization variables are presented in Table 4.1. These values are based on the average fingers and thumb lengths for a selected group of individuals. The middle and ring fingers lengths were measured in respect to the “web area” of skin between the fingers.

Table 4.2: Function variables for the mechanism optimization procedure

	Index Finger	Middle Finger	Ring Finger	Pinky Finger	Thumb
L_1	45 mm	20 mm	17.5 mm	38 mm	26 mm
L_2	27 mm	28 mm	24 mm	19 mm	18 mm
L_3	18 mm	18 mm	15 mm	17 mm	---
PP_H	18 mm	18 mm	18 mm	18 mm	18 mm
IP_H	18 mm	18 mm	18 mm	18 mm	18 mm

Table 4.3: Natural joint angles during tip-pinch grasp

	MCP	PIP (IP for Thumb)	DIP
Index Finger	49.1° (SD 9.5°)	41.0° (SD 10.7°)	38.5° (SD 6.8°)
Thumb	12.8° (SD 9.4°)	21.8° (SD 7.8°)	n/a

The original guess for all optimization trials for each finger mechanism was $\langle 45^\circ, 45^\circ, 45^\circ, 45^\circ, 8\text{mm}, 8\text{mm}, 8\text{mm}, 8\text{mm} \rangle$ and $\langle 60^\circ, 45^\circ, 8\text{mm}, 7\text{mm} \rangle$ for the thumb procedure and later changed to the kinematic modeling results. The optimization procedure for each finger and thumb mechanism was performed 10 times in order to vary the w_i weights from a percentage $h=10\%–100\%$ in 10% increments, in which the weights relationship was defined as the following:

For all finger mechanisms:

- $w_1 = 1 - h$
- $w_2 = \frac{1}{3}h$
- $w_3 = \frac{2}{3}h$

Thumb mechanism:

- $w_{1,2} = \frac{1}{2}h$

The results from each optimization procedure are presented below.

Index Finger:

The resulting error values for the objective function during all the optimization executions are presented in Figure 4.7. As shown in the graph, Iteration #2 produced the smallest error of 1.89 for its the objective function result. This iteration corresponds to the weight combination of $[w_1, w_2, w_3] = [0.8, 0.067, 0.133]$ for the joints. From having the smallest error, the design parameters produced by this iteration were selected for the optimal solution of the objective function.

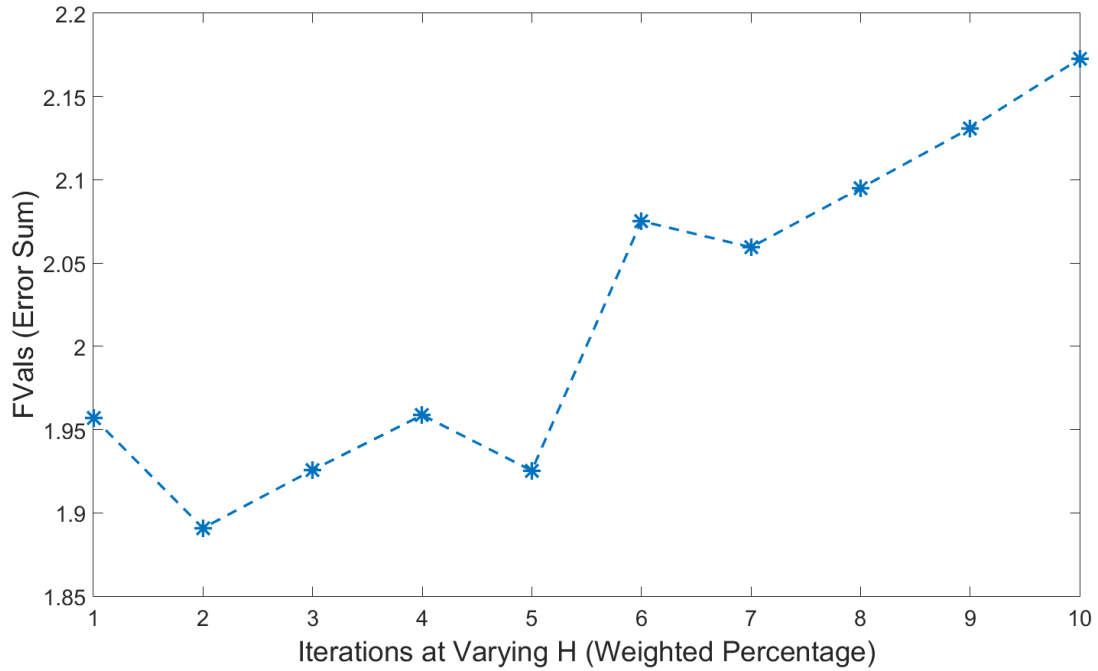


Figure 4.7: Optimization results for the index finger mechanism

The corresponding trajectory and joint angle relationships for this optimal solution are shown in Figure 4.8 and Figure 4.9 respectively.

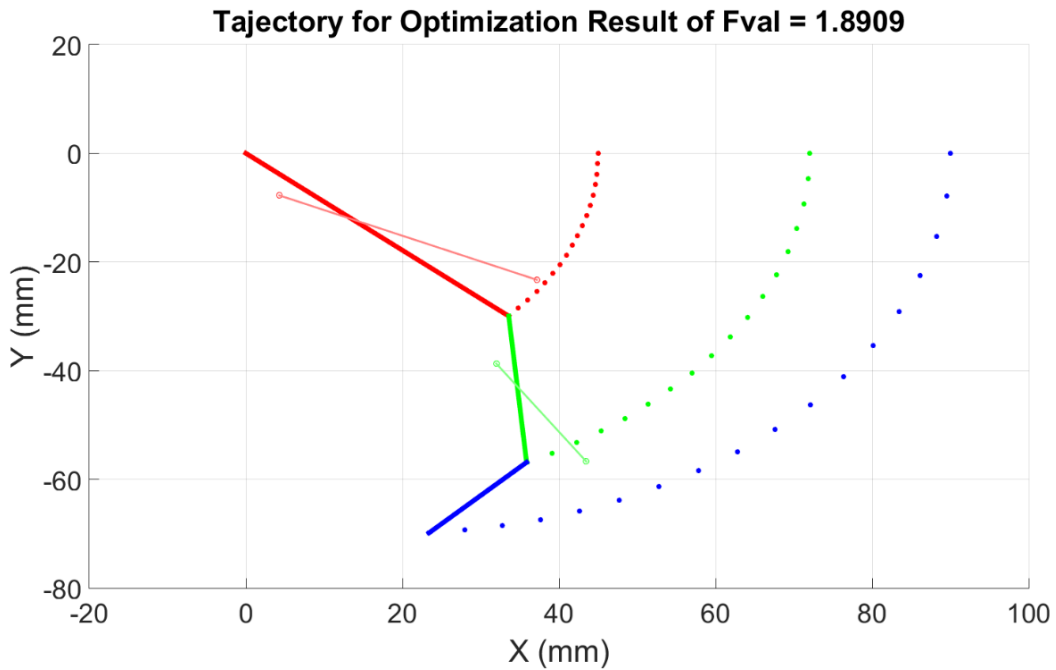


Figure 4.8: Trajectory of the optimal solution for the index finger mechanism

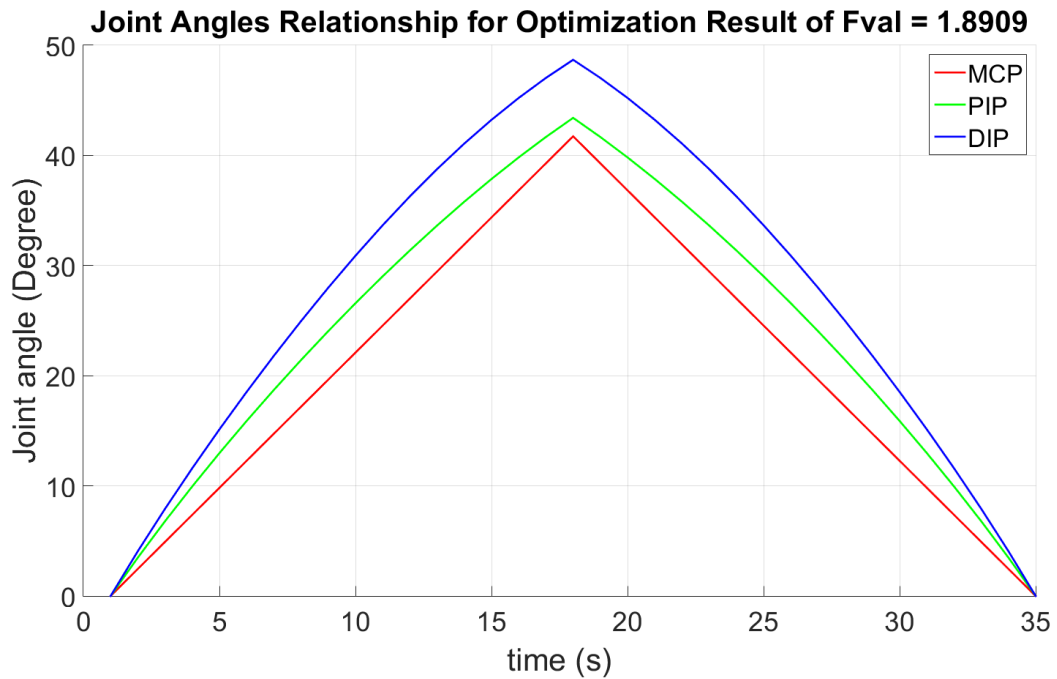


Figure 4.9: Joint angle relationships of the optimal solution for the index finger mechanism

The resulting angular displacements of 42° , 43° , and 48.68° for the MCP, PIP, and DIP joints respectively, were within the desired ranges for the MCP and PIP joint. The DIP joint angle was over the desired range by 3.38° , which is a feasible tradeoff for this optimal solution. The trajectory shows the constraint links as well to illustrate how much they extend. Overall, the results further proved that the corresponding design parameters for the optimal solution would be suitable for implementing the index finger mechanism.

Middle Finger:

Figure 4.10 presents the results of the optimization problem for the middle finger mechanism. As shown in the graph, Iteration #10 produced the optimal result for the

objective function by yielding the smallest error of 1.55. This iteration corresponds to the weight combination of $[w_1, w_2, w_3] = [0, 0.33, 0.66]$ for the joints.

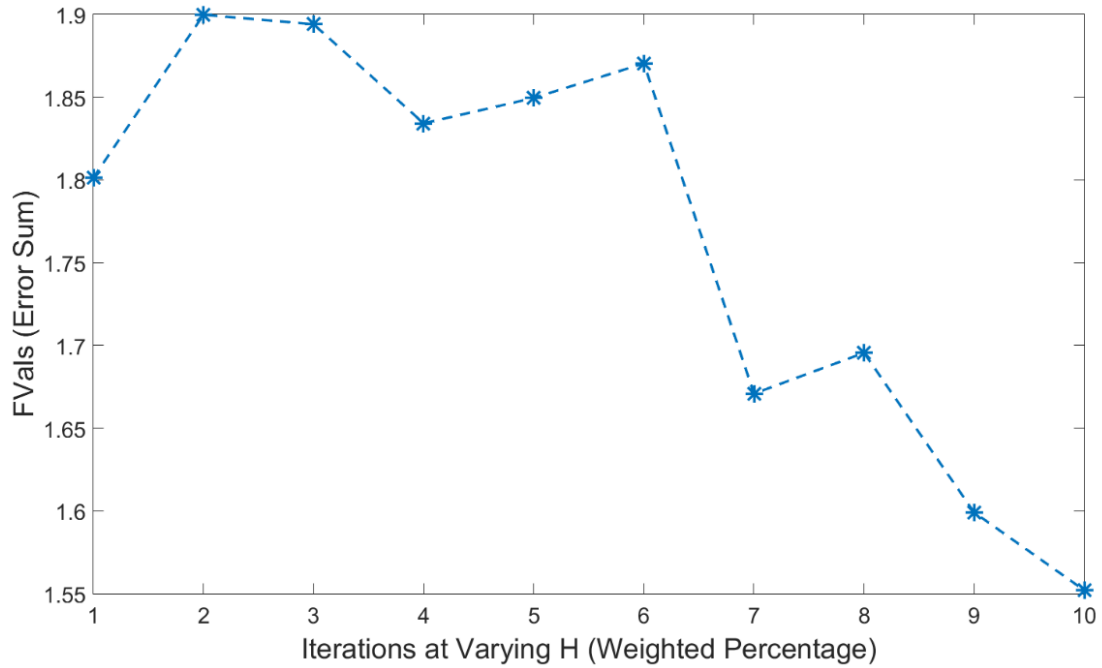


Figure 4.10: Optimization results for the middle finger mechanism

Figure 4.11 and Figure 4.12 each illustrates the corresponding trajectory and joint angle relationships for the optimal solution, respectively.

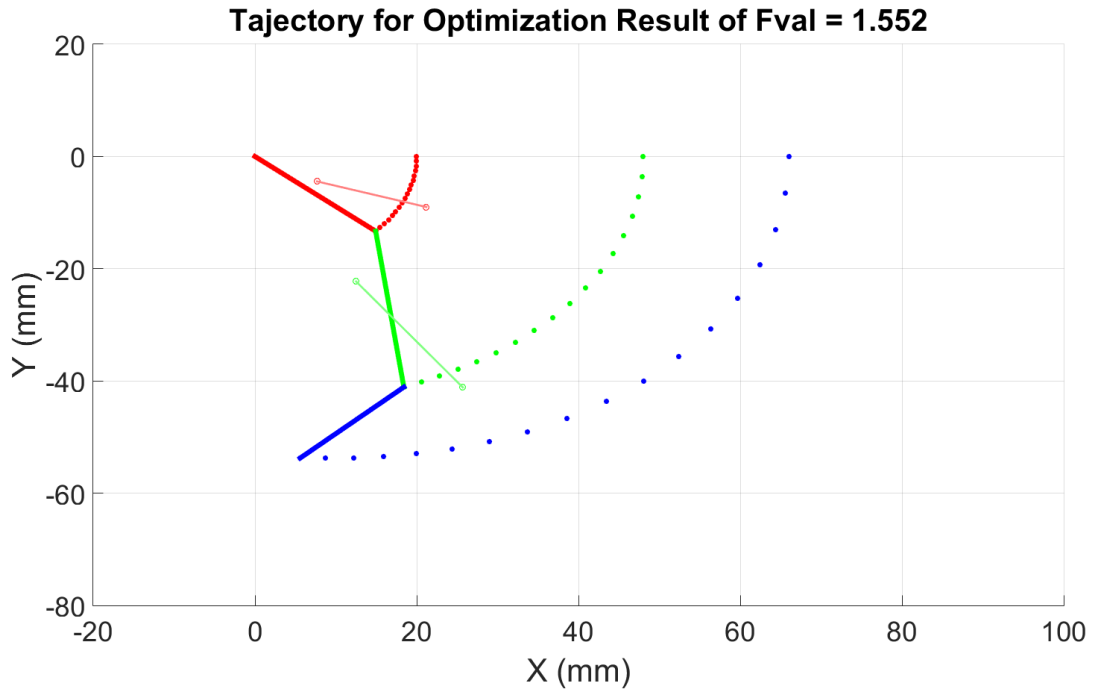


Figure 4.11: Trajectory of the optimal solution for the middle finger mechanism

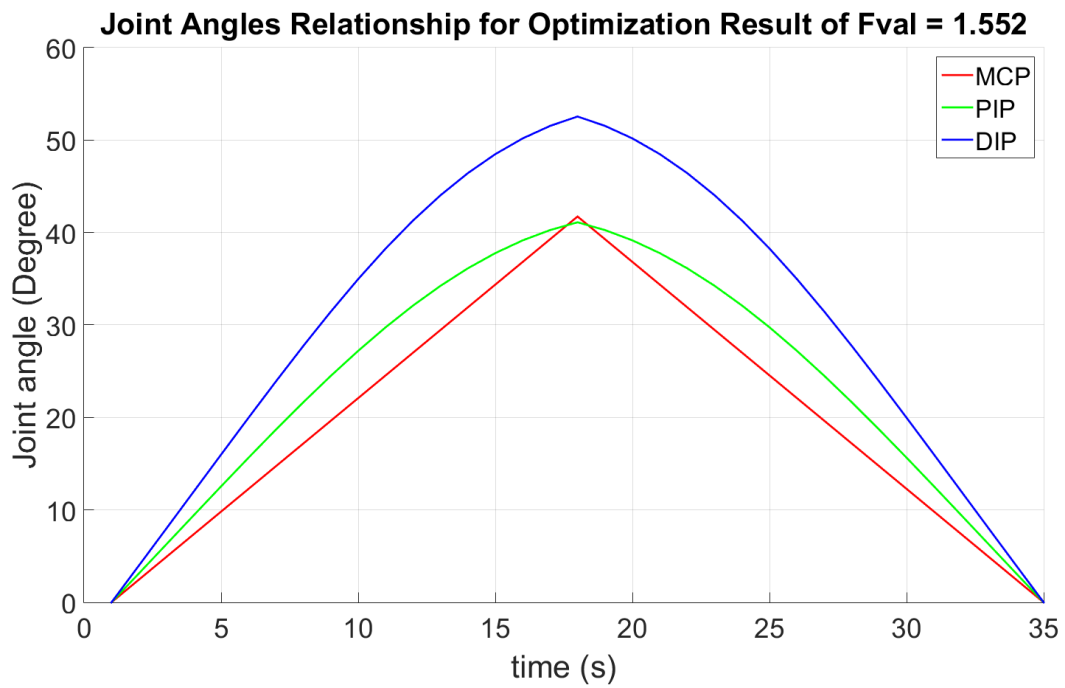


Figure 4.12: Joint angle relationships of the optimal solution for the middle finger mechanism

As predicted, the resulting angular displacements of 42° , 41° , and 52° for the MCP, PIP, and DIP joints respectively, were well within the desired ranges, but only for the MCP and PIP joints. There was a tradeoff with the DIP joint falling outside the desired range by 7.25° . Despite this tradeoff, the overall results proved that optimal solution would be suitable for implementing the middle finger mechanism.

Ring Finger:

The results of the optimization problem for the ring finger mechanism are presented in Figure 4.13. Iteration #9 produced the optimal result for the objective function, which had an error of 1.66. This iteration corresponds to the weight combination of $[w_1, w_2, w_3] = [0.1, 0.3, 0.6]$ for the joints.

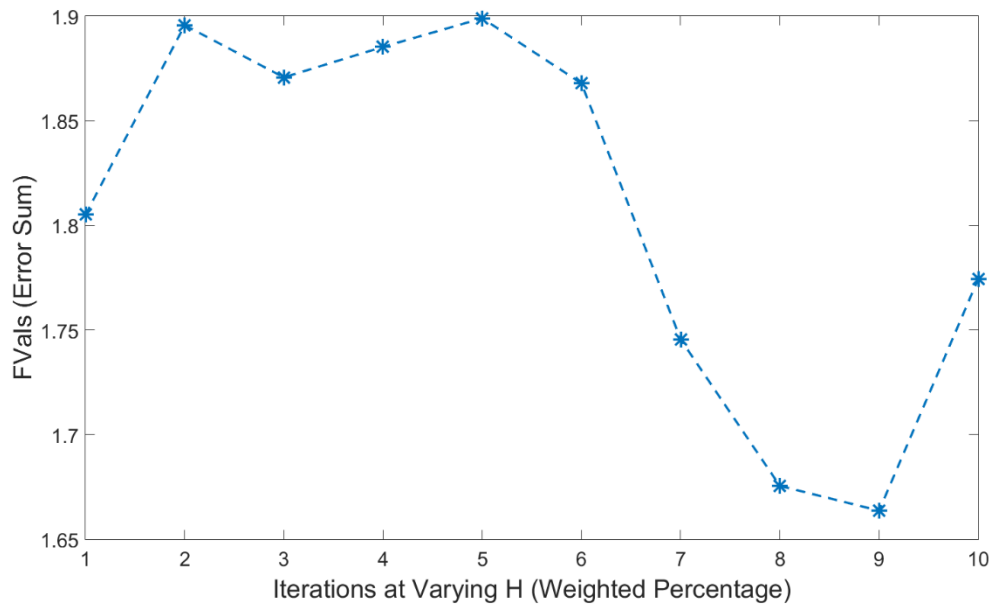


Figure 4.13: Optimization results for the ring finger mechanism

Figure 4.14 and Figure 4.15 each illustrates the corresponding trajectory and joint angle relationships for the optimal solution, respectively. The trajectory also shows the constraint links for the mechanism.

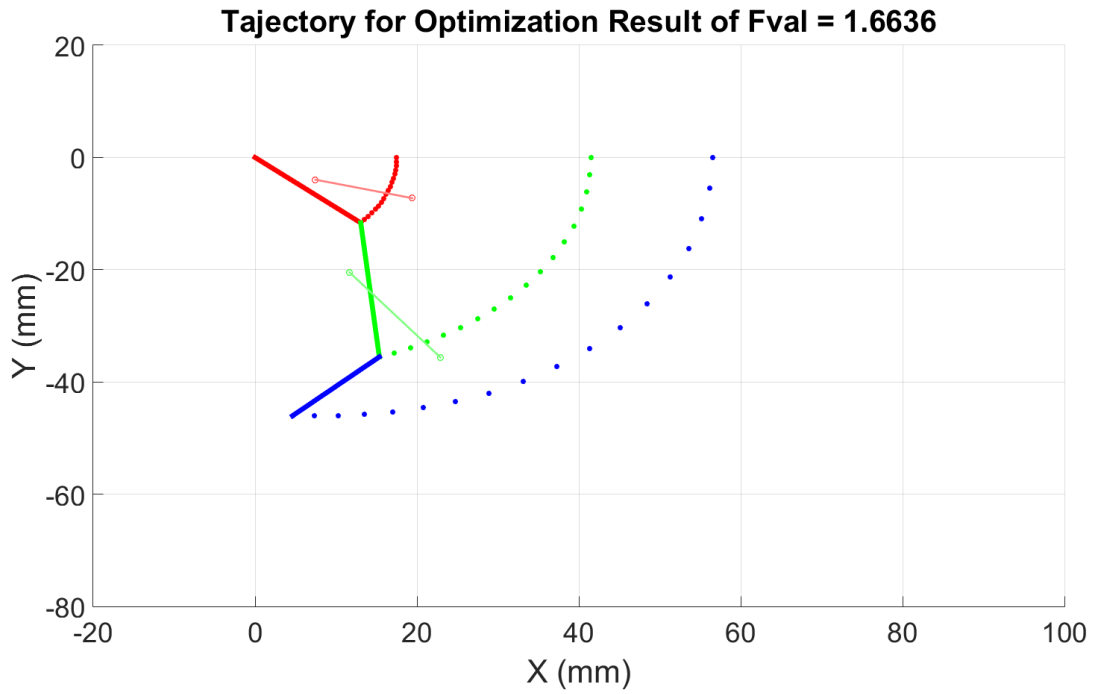


Figure 4.14: Trajectory of the optimal solution for the ring finger mechanism

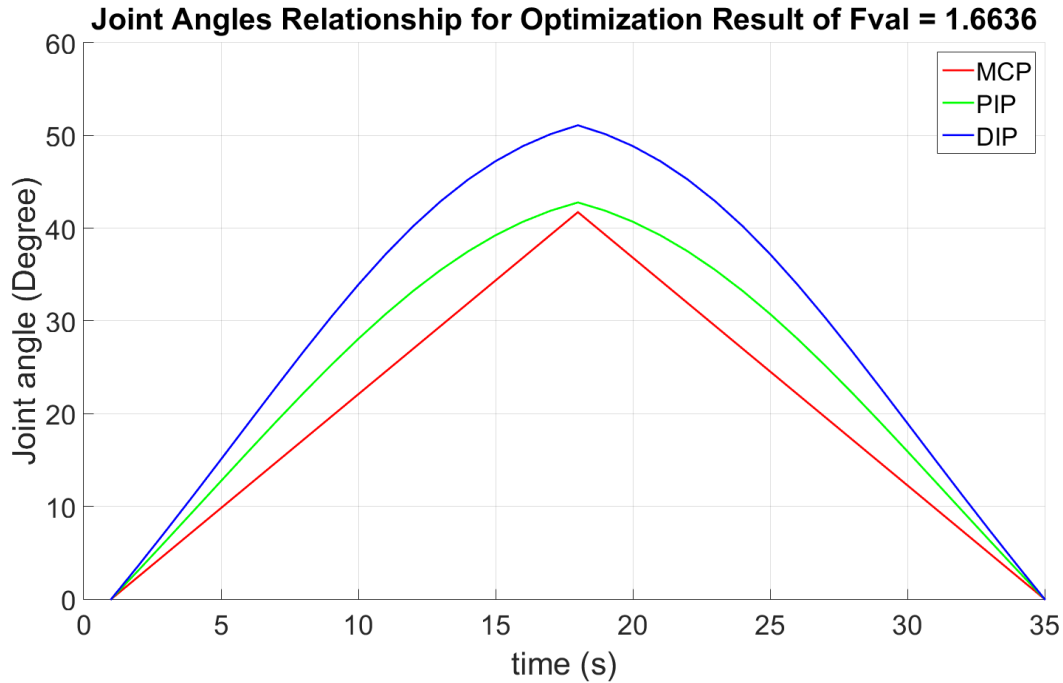


Figure 4.15: Joint angle relationships of the optimal solution for the ring finger mechanism

As shown by the graph, the optimal solution for the optimization of ring finger mechanism resulted in angular displacements of 42° , 43° , and 51° for the MCP, PIP, and DIP joints respectively. The MCP and PIP joints were within the desired ranges, while the DIP joint angle was over the desired range by 5.8° . Despite this minimum tradeoff, the results showed that the design parameters of the optimal solution are well suitable for the ring finger mechanism.

Pinky Finger:

Figure 4.16 presents the results of the optimization problem for the pinky finger mechanism. As shown in the graph, Iteration #2 produced the optimal result for the

objective function by yielding the smallest error of 1.87. This iteration corresponds to the weight combination of $[w_1, w_2, w_3] = [0.8, 0.067, 0.133]$ for the joints.

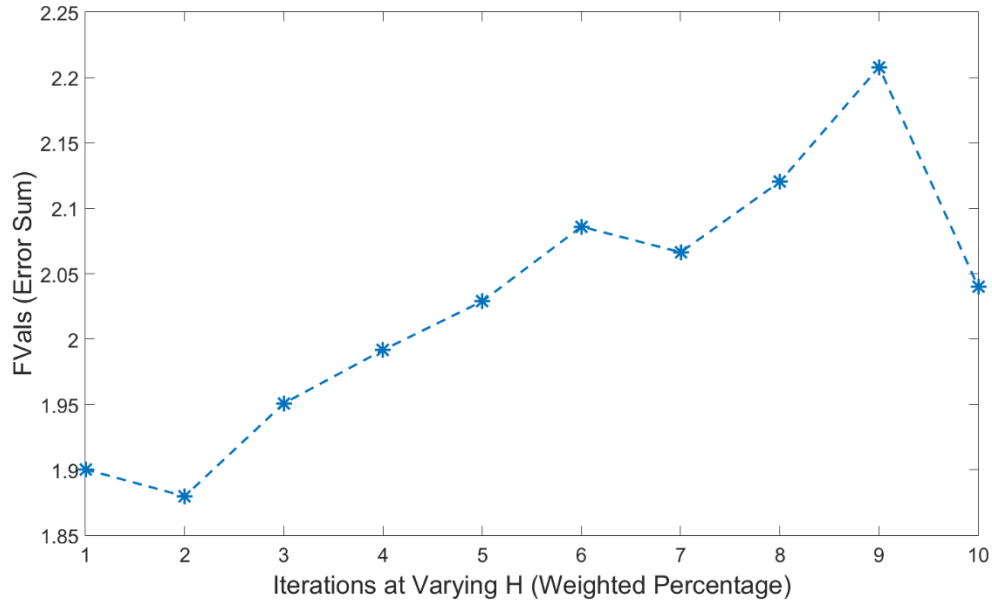


Figure 4.16: Optimization results for the pinky finger mechanism

Figure 4.17 and Figure 4.18 each illustrates the corresponding trajectory and joint angle relationships for the optimal solution, respectively.

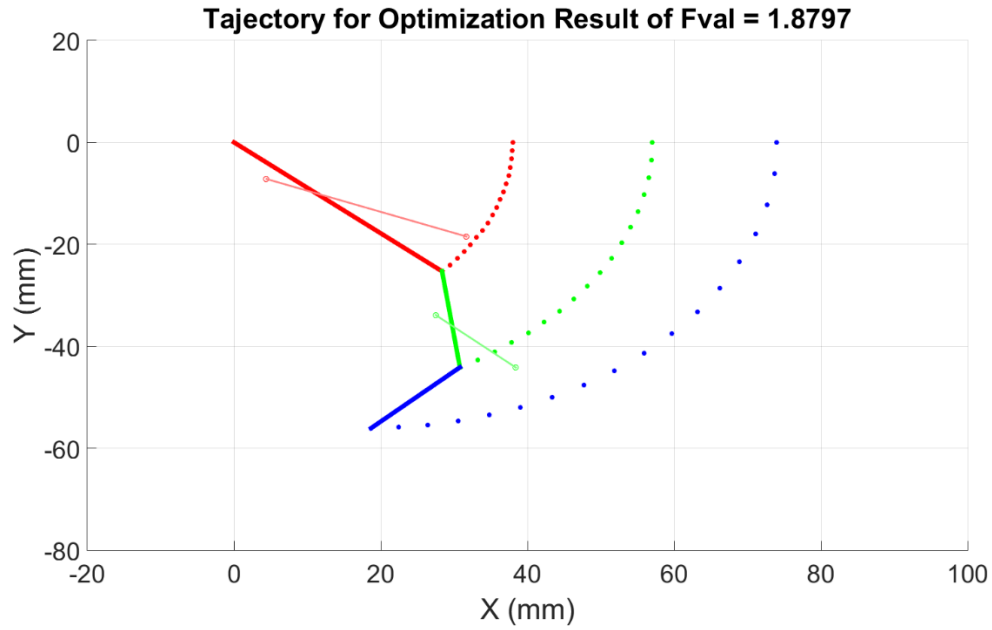


Figure 4.17: Trajectory of the optimal solution for the pinky finger mechanism

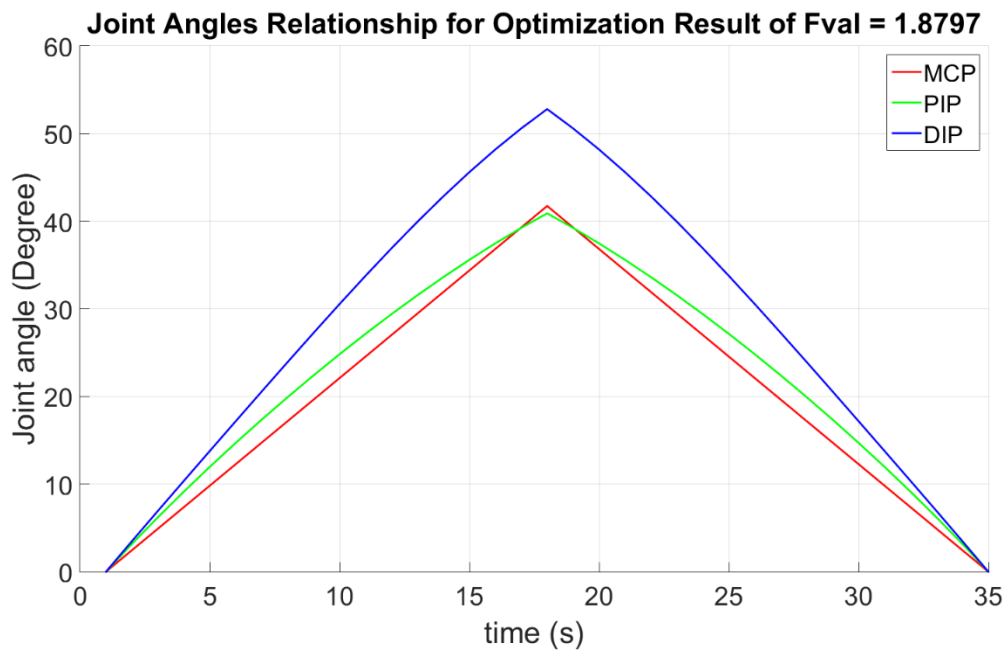


Figure 4.18: Joint angle relationships of the optimal solution for the pinky finger mechanism

As shown in the graph, the resulting angular displacements of 42° , 41° , and 53° for the MCP, PIP, and DIP joints respectively, were within the desired ranges for the MCP and PIP joint, while the DIP joint angle was over the desired range by 7.49° . Despite this tradeoff, the overall results proved that optimal solution would be suitable for implementing the pinky finger mechanism. In addition, the trajectory shows the constraint links as well to illustrate how much they extend.

Thumb:

The results of the optimization problem for the thumb mechanism are presented in Figure 4.19. Iteration #1 produced the optimal result for the objective function by yielding the smallest error of 8.05. This iteration corresponds to the weight combination of $[w_1, w_2, w_3] = [0.9, 0.033, 0.067]$ for the joints.

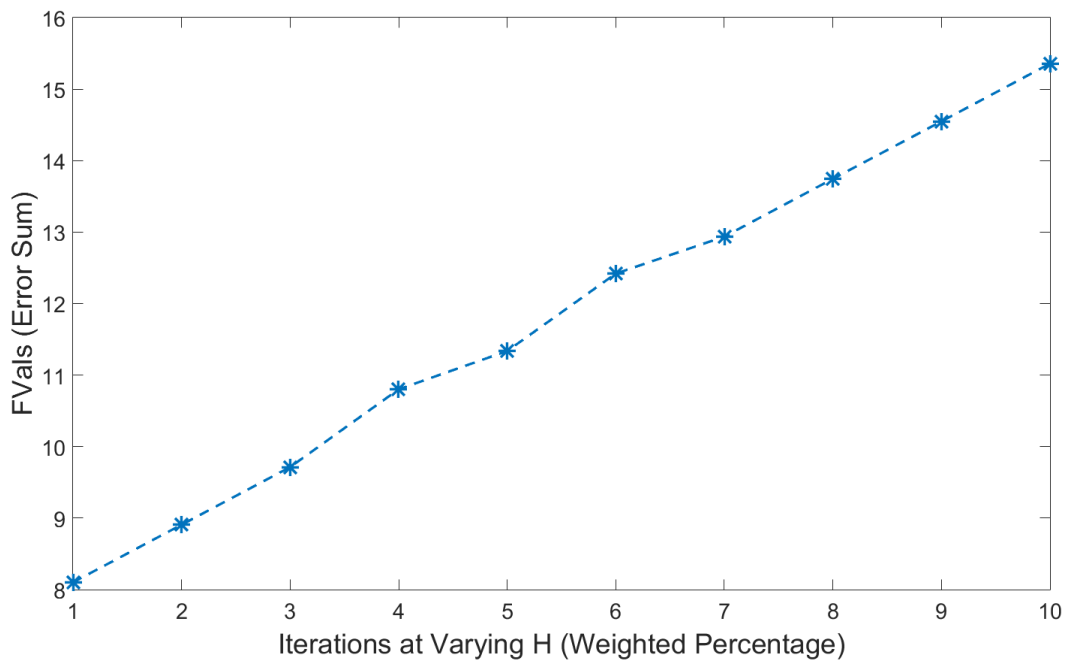


Figure 4.19: Optimization results for the thumb mechanism

Figure 4.20 and Figure 4.21 illustrates the corresponding trajectory and joint angle relationships for the optimal solution, respectively.

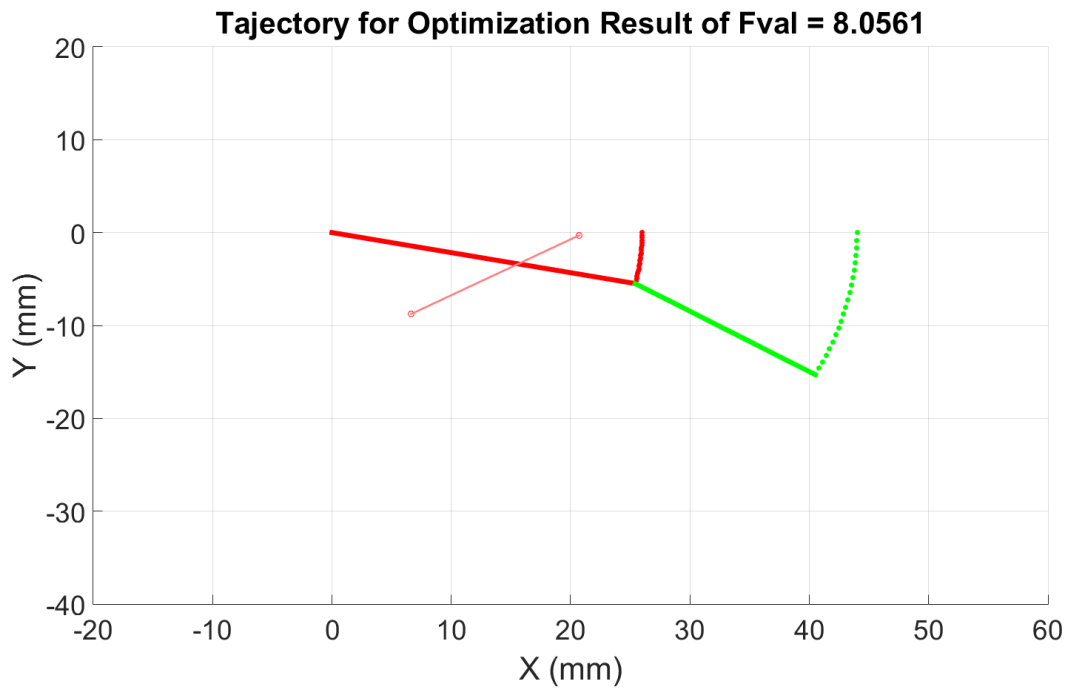


Figure 4.20: Trajectory of the optimal solution for the thumb mechanism

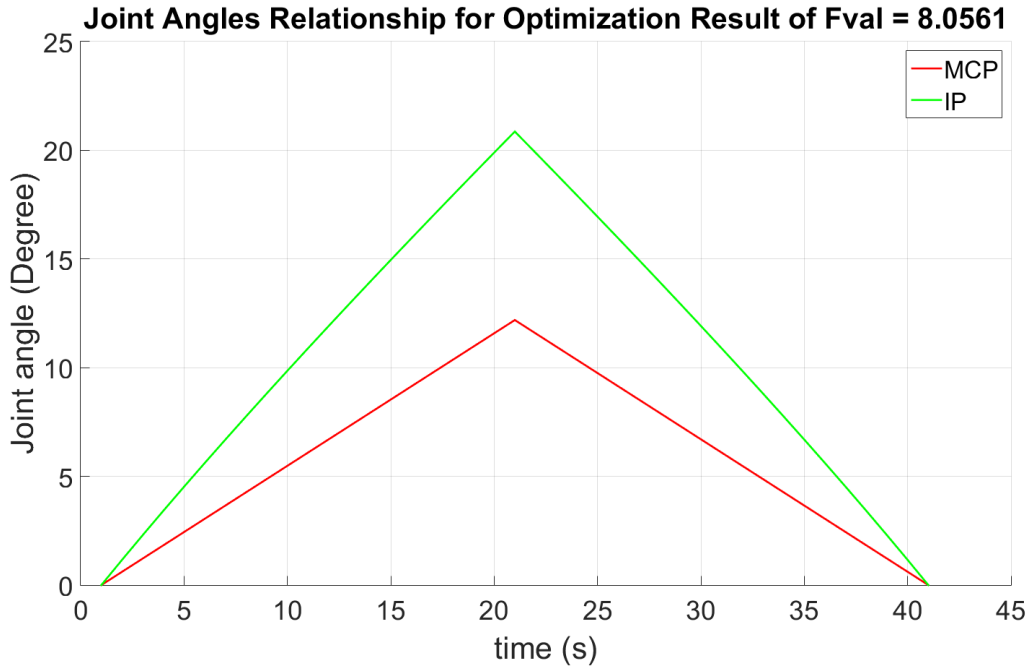


Figure 4.21: Joint angle relationships of the optimal solution for the thumb mechanism

As predicted, the resulting angular displacements of 12° and 21° for the MCP and IP joints respectively, were well within the desired ranges. The trajectory shows the constraint links as well to illustrate how much they extend. Overall, the results further proved that the corresponding design parameters for the optimal solution would be suitable for implementing the index finger mechanism.

4.5 Dynamics

The dynamic behavior of the proposed mechanism can be separated into two phases: (1) when the mechanism is in motion before contact and (2) when the mechanism makes contact with the environment. The second phrase offers more value than the first phrase due to the importance of studying the interaction forces that are applied on the tip of each

finger and thumb when the hand exoskeleton is interacting with an object. As a result, this phrase is discussed in detail in terms of a control aspect.

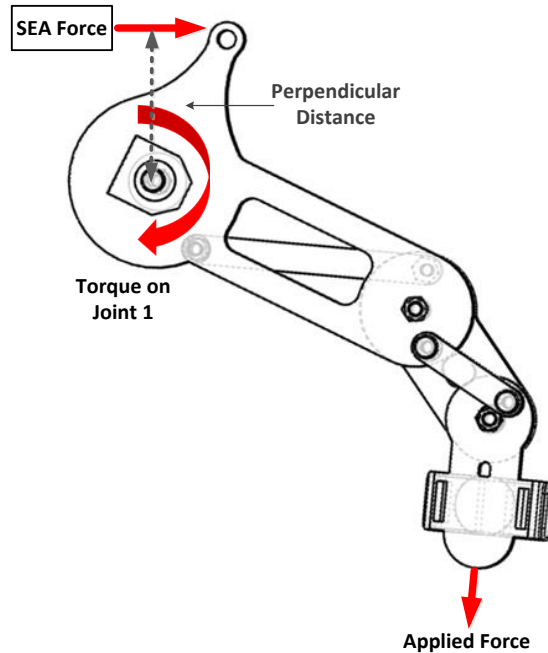


Figure 4.22: Dynamic diagram of the mechanism

Phase 1:

The mechanism comes into motion when the actuation unit pushes or pulls onto the lever of the mechanism, as shown in Figure 4.22. This pushing and pulling action on the lever creates a torque that causes the first link, L_1 to bend at its corresponding revolute joint R_1 . As a result of the coupling relationship designed into the mechanism, links L_2 and L_3 bend accordingly with link L_1 . As these links bend, the corresponding phalanges of the finger or thumb bend in respect, achieving the desired grasping motions.

Phase 2:

The idea for controlling the functionality of grasping an object with the hand exoskeleton is to command the mechanism to continue in motion (gripping) until it reaches

a desired force on each finger/thumb. Once the desired force is reached, the mechanism stops bending and the system becomes in a state of static equilibrium. During this state of static or quasi-static equilibrium, the relationship between the torques at the joints during bending and the forces/moments applied on the tip of the finger/thumb by the mechanism end-effectors can be analyzed. To achieve this, the Jacobian matrix is used to relate the torques being applied at each joint with the forces being applied at the mechanism end-effector. This is expressed below:

$$\tau = -{}^0J^T {}^0F \quad (12)$$

τ represents the generalized torque, ${}^0J^T$ represents the Jacobian matrix, and 0F represents the external generalized forces at the end-effector, which are reflected on the tips of the fingers and thumb. Using Figure 4.22, the above Equation (12) can be expressed in terms of the design parameters for the mechanism:

$$\begin{bmatrix} \tau_{\theta_1} \\ \tau_{\theta_2} \\ \tau_{\theta_3} \end{bmatrix} = -{}^0J^T \begin{bmatrix} F_{e_x} \\ F_{e_y} \\ \tau_{\theta_e^0} \end{bmatrix} \quad (13)$$

The Jacobian matrix can be determined using position of the end-effector, in this case the tip of the finger/thumb.

$$\begin{aligned} x_e &= L_1 \cos \theta_1 + L_2 \cos \theta_2 + L_3 \cos \theta_3 \\ y_e &= L_1 \sin \theta_1 + L_2 \sin \theta_2 + L_3 \sin \theta_3 \\ \vartheta_e &= \theta_1 + \theta_2 + \theta_3 \end{aligned} \quad (14)$$

By taking the derivative on the positions, the velocity equations can be obtained as:

$$\begin{aligned}
\dot{x}_e &= -\left(\frac{d\theta_1}{dt}\right)L_1 \sin \theta_1 - \left(\frac{d\theta_2}{dt}\right)L_2 \sin \theta_2 - \left(\frac{d\theta_3}{dt}\right)L_3 \sin \theta_3 \\
\dot{y}_e &= \left(\frac{d\theta_1}{dt}\right)L_1 \cos \theta_1 + \left(\frac{d\theta_2}{dt}\right)L_2 \cos \theta_2 + \left(\frac{d\theta_3}{dt}\right)L_3 \cos \theta_3 \\
\dot{\mathcal{G}}_e &= \frac{d\theta_1}{dt} + \frac{d\theta_2}{dt} + \frac{d\theta_3}{dt}
\end{aligned} \tag{15}$$

The transformation matrix that relates the joint velocities and the velocities of the mechanism end-effector (tip of the finger/thumb), both linear and angular velocities, can be written as below. This matrix is the Jacobian matrix.

$$\begin{bmatrix} \dot{x}_e \\ \dot{y}_e \\ \dot{\mathcal{G}}_e \end{bmatrix} = \begin{bmatrix} -L_1 \sin \theta_1 & -L_2 \sin \theta_2 & -L_3 \sin \theta_3 \\ L_1 \cos \theta_1 & L_2 \cos \theta_2 & L_3 \cos \theta_3 \\ 1 & 1 & 1 \end{bmatrix} \begin{bmatrix} \dot{\theta}_1 \\ \dot{\theta}_2 \\ \dot{\theta}_3 \end{bmatrix} \tag{16}$$

The equations for joint torques and end-effector forces can be expanded using the determined Jacobian matrix.

$$\begin{bmatrix} \tau_{\theta_1} \\ \tau_{\theta_2} \\ \tau_{\theta_3} \end{bmatrix} = - \begin{bmatrix} -L_1 \sin \theta_1 & -L_2 \sin \theta_2 & -L_3 \sin \theta_3 \\ L_1 \cos \theta_1 & L_2 \cos \theta_2 & L_3 \cos \theta_3 \\ 1 & 1 & 1 \end{bmatrix} \begin{bmatrix} F_{e_x} \\ F_{e_y} \\ \tau_{\theta_e^0} \end{bmatrix} \tag{17}$$

As a result, the torque being applied on the mechanism by the actuation unit can be calculated with the expanded equations below:

$$\begin{aligned}
\tau_{\theta_1} &= -L_1 \sin \theta_1 F_{e_x} - L_2 \sin \theta_2 F_{e_y} - L_3 \sin \theta_3 \tau_{\theta_e^0} \\
\tau_{\theta_2} &= L_1 \cos \theta_1 F_{e_x} + L_2 \cos \theta_2 F_{e_y} + L_3 \cos \theta_3 \tau_{\theta_e^0} \\
\tau_{\theta_3} &= \theta_1 F_{e_x} + \theta_2 F_{e_y} + \theta_3 \tau_{\theta_e^0}
\end{aligned} \tag{18}$$

CHAPTER 5

FORCE CONTROL

5.1 Background and Motivation

The human hand contains many sensory feedback functionalities that are essential for interacting with objects and performing tasks. When designing a hand exoskeleton, it is critical to incorporate features that can imitate some of the hand abilities to process sensory information, as mentioned in Chapter 3. Among the various types of sensory integration that are feasible with today's technology, force control is considered as a fundamentally necessity to ensure safe human and environment interactions using the robotic systems. Having a force controllable robotic system offers the ability to monitor applied forces and react accordingly to provide compliance when needed. It offers a milestone in achieving more intelligent responses and controls in robotic systems.

In the earlier years of robotics, the traditional method for implementing force control was to perform current control directly with the actuation unit, whether it is a direct drive servomotor or geared actuator, or even through a cable driven transmission. These actuator units however contain several limitations that overall affect the ability to precisely control force. These limitations include inefficient speed to torque ratios for servomotors, impedance known as the reflected inertia for geared actuators at the output of the gearbox, and the traditional concerns of friction, stiction, and bandwidth [51]. Stiction is known as the sticky friction caused by mechanical components sliding against each other, while bandwidth identifies the frequency range of which the actuator can output forces that can

be accurately controlled. The resistance force of stiction can be overcome with a higher breakaway force of the actuator, which in return limits the minimum force that the actuator can output. Using a cable drive system instead of the conventional gearbox can introduce lower stiction and backlash, which are difficult to model in a force controller. However, the large pulleys needed to match the desired transmission ratios of a gearbox can make these cable driven systems unfeasible for robotic systems with size constraints. Pressure actuators such as pneumatic and hydraulic systems can also require unfeasible complexity and factors (such as heavy weight, large size, etc.) to achieve force control. These systems suffer from low power density and high impedances as a result of friction and inertia.

These actuation units alone serve as poor candidates in achieving accurate force control. The ideal force controllable actuation unit is one that can perfectly output the desired force, regardless of any inertia produced from the movement of the payload [51]. This chapter presents the idea of using a series elastic actuator (SEAs) that can provide many benefits over these conventional actuators.

5.2 Series Elastic Actuation Literature Review

The basic design of a SEA consists of placing an elastic element, such as a torsional or compression spring in series between the drive train of the actuator and its payload. SEAs are used in many robotic systems to overcome the limitations of conventional actuation units. SEAs serve as good candidates to use for achieving ideal force control due to their elastic elements. These elastic elements allow for the storing of energy while introducing shock tolerance within the system. Not only does it help with making the system more compliant when interacting with the environment, the shock tolerance also allows the actuation unit to become more back drivable. As a result, this decreases the amount of

impedance in the system and the mechanical stiffness that negatively affect the force bandwidth. Most importantly, SEAs offer a way to achieve force control by means of primarily controlling position using Hooke's Law. In most cases, position is easier to control accurately in motors that use gear trains or have feedback encoders attached. Overall, SEAs utilize active sensing and closed loop controls to reduce the disturbances from friction and inertia to ultimately achieve the desired force output.

5.3 Proposed Design and Control Scheme

The design of the proposed SEA is detailed in Figure 5.1. The design uses a geared DC motor with a leadscrew shaft. The geared DC motor offers a high torque, at sufficiently low speed. The leadscrew shaft allows for the translation of rotary motion into linear movement. The designed was adapted from the traditional SEA design done by [52]. The overall actuation unit consists of three major components: a drive-train, output carriage, and compression springs. The drive-train component houses a nut that attaches to the leadscrew shaft, allowing the entire drive-train piece to move forward and backwards along the shaft as the motor rotates clockwise and counter-clockwise respectively. The drive-train component is coupled with the output carriage piece by the placement of compression springs between both components. Specifically, the drive-train component is placed between both ends of the output carriage piece. A compression spring is placed on each side of the drive-train, establishing springs between the drive-train and output carriage on both sides. Therefore as the drive-train component moves forwards and backwards along the leadscrew, the compression springs pushes and pulls against output carriage component, causing it to move in synchronization with the drive-train component. The

overall output force from the leadscrew motor and compression springs is reflected onto the output carriage piece. This force on the output carriage is used to push the level of the finger/thumb mechanism. To align all of the components together during motion, a guide rail is installed above the leadscrew shaft.

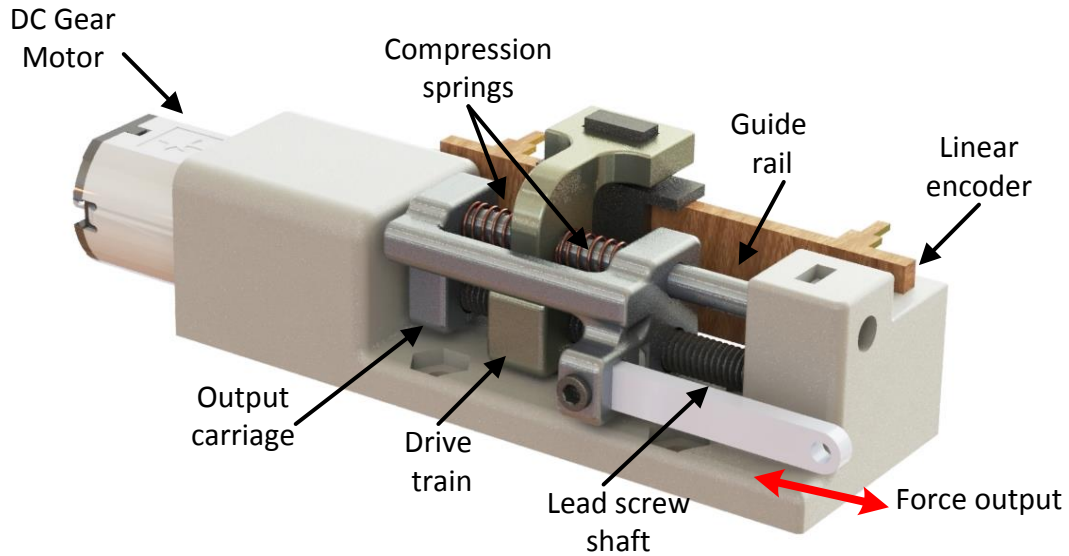


Figure 5.1: Proposed SEA design

During operation, the output forces can be measured through the deflection of the compression springs. To measure the spring deflection, a linear encoder is incorporated into the SEA design by attaching the scale of the encoder onto the drive-train component, as shown in Figure 5.1. This attachment allows the scale of the encoder to move in accordance with the drive-train for tracking its position. Using absolute rotary encoders placed onto the glove mechanisms at the MCP joint of the fingers and thumb, the position for the output carriage piece can also be tracked. As a result, the deflection of the springs can be calculated using the positioning information for both the drive-train and the output carriage components. By optimizing the stiffness of the springs, the desired force

bandwidth and sensitivity can be attained from the SEA unit. A prototype of the proposed SEA design was 3D printed and is shown in Figure 5.2 along with a size comparison.

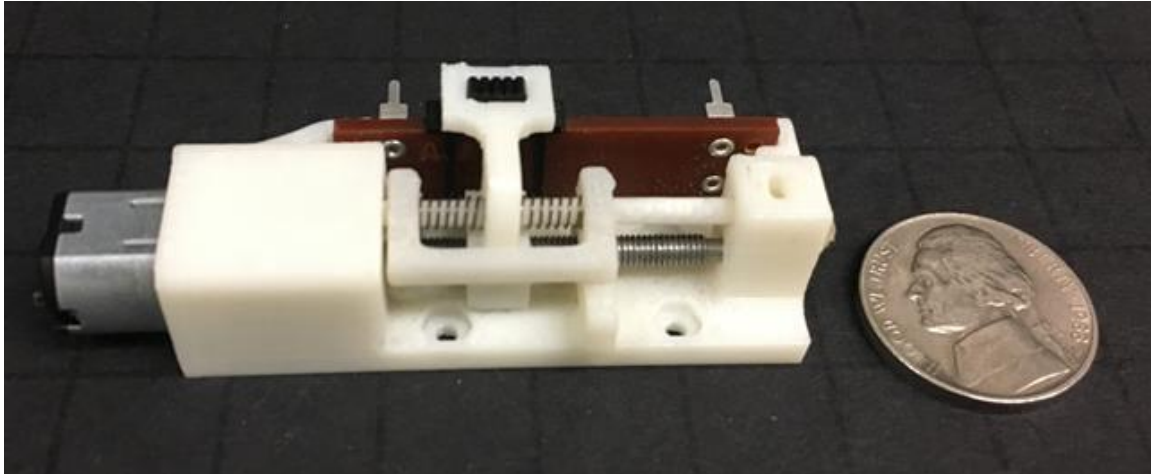


Figure 5.2: 3D printed prototype for the proposed SEA design

By equipping both the index finger and thumb mechanism of the proposed hand exoskeleton with the SEA actuation unit as shown in Figure 5.3, the exoskeleton glove will be able to grasp objects of various shapes and strengths while maintaining a stable grip through force control.

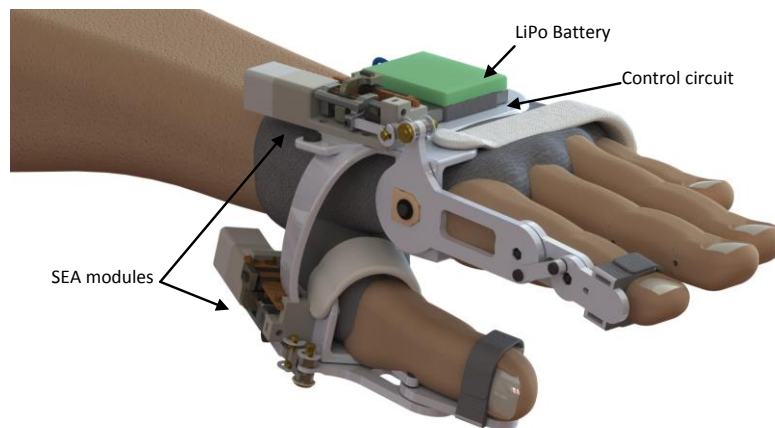


Figure 5.3: Proposed SEA design integrated on the two-digit hand exoskeleton

Using the dynamic modeling of the mechanism from Section 4.5, the force applied on the end-effector can be controlled using the following scheme shown in Figure 5.4.

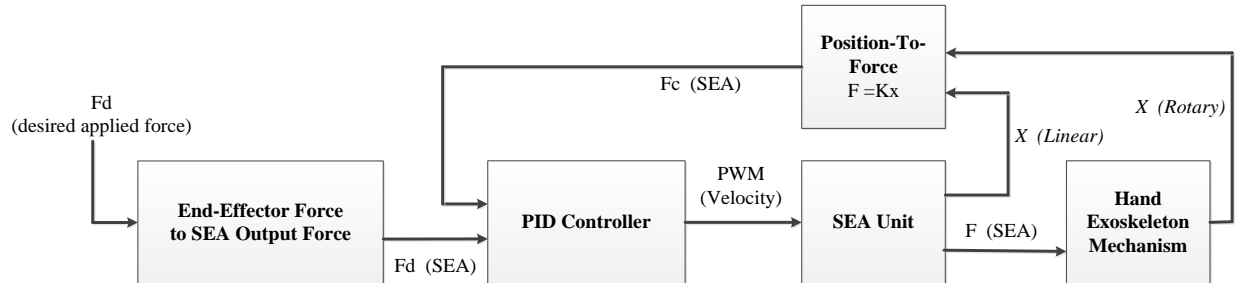


Figure 5.4: Block diagram for proposed force control

The user can specify a desired force to be applied by the end-effector of the mechanism. The end-effector force is used to obtain the corresponding desired force that the SEA unit should produce. This force is used as an input to a PID controller, which outputs a PWM signal to be applied to the DC motor of the SEA unit. As the motor of the SEA unit moves, the drive-train moves either forwards or backwards accordingly. Using the linear potentiometer, the position of the drive train is measured. As the SEA unit actuates the mechanism, the rotary position sensor is used to determine the position of the output carriage of the SEA unit. Using these two positions, the compression amount of the SEA springs can be calculated. As a result, the actual force being applied by the SEA unit can be determined and used as a feedback into the PID controller.

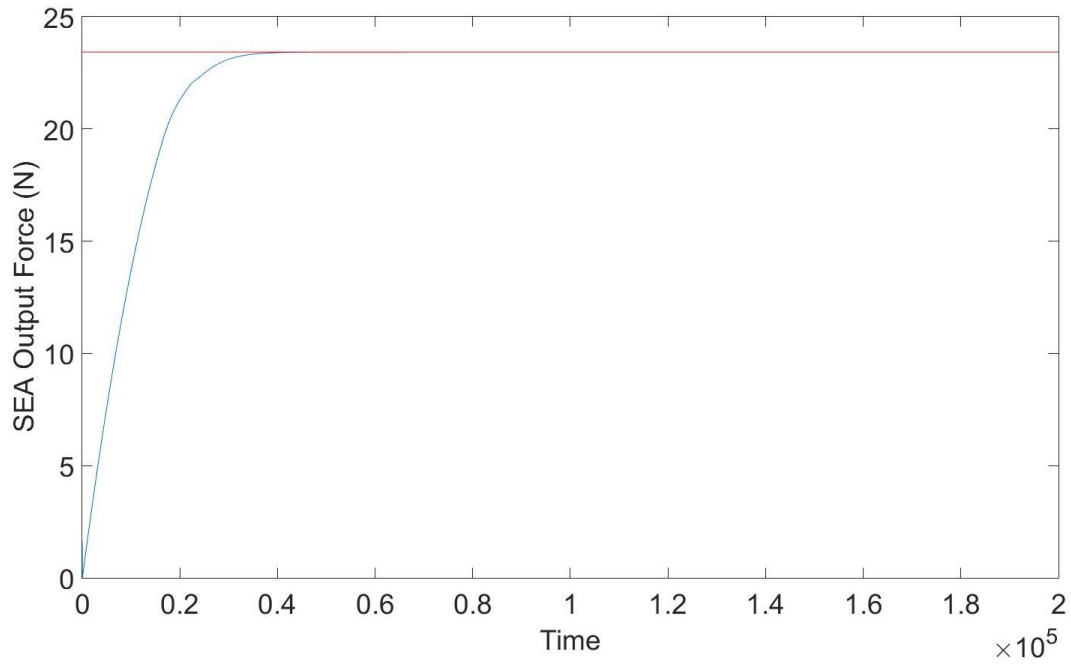


Figure 5.5: Preliminary results of the force control simulation

Figure 5.5 shows the preliminary results that were conducted using an estimated mass, damping, and stiffness values of a spring. The desired force was 23 N and the results show that the system was able to achieve this target.

CHAPTER 6

PROTOTYPES DEVELOPMENT AND EXPERIMENTAL RESULTS

6.1 Two-Digit Prototype

6.1.1. Prototype Integration

The basic mechanisms that were presented in Chapter 4, were used to fully developed a two-digit prototype. The prototype weighs 24g, making it lightweight as compared to the two finger exoskeleton of [53], which weighs 180g. To complete the prototype implementation, a circuit board and software interface were developed to control the glove and all integrated sensors. The circuit board and pneumatic system were kept separate so that they could be either incorporated into a backpack or kept on a table while the exoskeleton glove was being used.

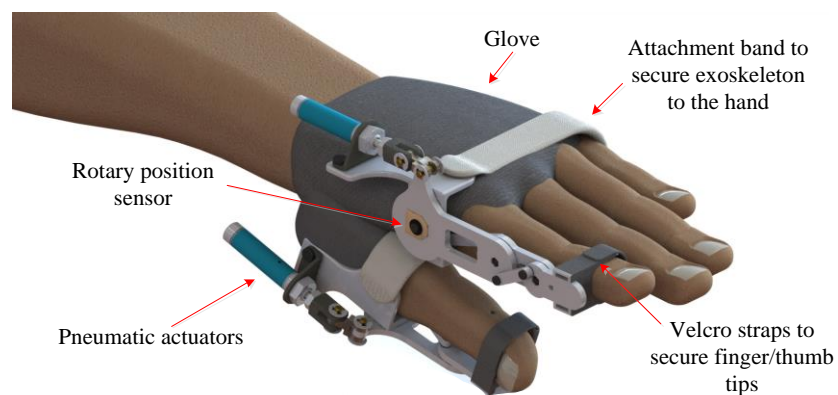


Figure 6.1: CAD model of the proposed two-digit prototype

6.1.1.1 Mechanical Design

The conceptual design of the mechanism was further developed as a prototype using Solid Works. The CAD model was incorporated to include details for housing necessary sensors and attachments for the user's fingers/thumb, as shown in Figure 6.1 and Figure 6.2. Once the CAD model was completed, the bending profiles were validated to ensure the correctness of the link lengths and joint positions. The mechanisms for the index finger and the thumb were then 3D printed separately using ABS plastic. As a way to connect both the finger and thumb mechanisms together for ensuring stability for attaching the user's hand, a connector plate was developed. This connector plate is composed of a base for each mechanism, in which they are fixed to using screws and nuts. Each of these base plates contain space for an actuator to be placed to interact with the mechanisms accordingly. The connector plate is fastened onto the back of the user's hand using elastic Velcro straps. This allows for the adjustment of the hand exoskeleton to suit various hand sizes.

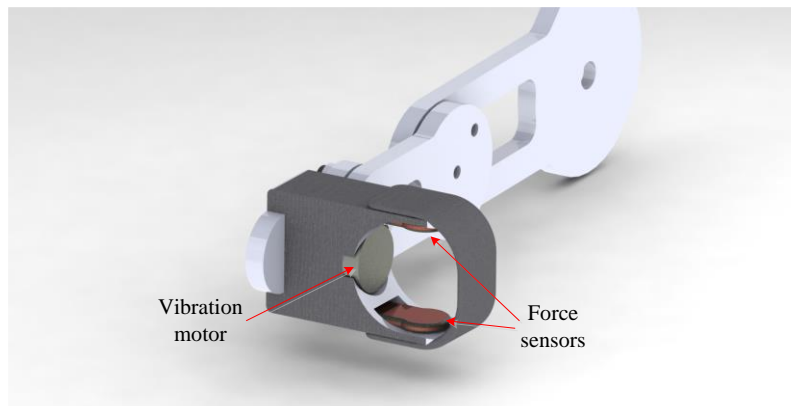


Figure 6.2: Detailed design of the fingertip holder and its sensor housing

6.1.1.2 Electrical Design

Actuation

To achieve flexion and extension motions with adequate speed and force, Bimba double acting pneumatic actuators were used for the index finger and thumb mechanisms of the exoskeleton glove. With these actuators, the glove can complete flexion and extension motions within 1s with a force of 10 N. The complete pneumatic system consists of an air compressor (150 PSI), a 0.5-gallon air reservoir, a pressure regulator, air tubing, and SMC solenoid valves, which control the air flow into the pneumatic actuators.

Sensors

Position Sensors:

For absolute position sensing, Bourns rotary encoders were placed on each of the finger and thumb mechanisms at the R_1 joints, which correspond to the MCP joints on the human hand. The readings from the electrical encoders corresponds to the angular position of the L_1 links of the finger and thumb mechanisms. A digital protractor was used to manually calibrate the encoder values into angle measurements. The remaining joint angles of the PIP and DIP joints of the index finger and the IP joint of the thumb are calculated using the kinematic model of the mechanism. Using the kinematic model, the position of the final link corresponding to the distal phalanges of the finger and thumb, can also be calculated.

Force Sensors:

Force sensitive resistors (FSR) by Interlink Electronics were used to measure the amount of force being applied on the index finger and thumb by the exoskeleton frames during grasping. These FSR sensors have a continuous analog resolution and a force

sensitivity range of 0.2 N – 20 N. Two force sensors are placed on each of the finger/thumb tip pieces, as shown in Figure 6.2. The force sensors were calibrated using known weights.

Vibration Sensors:

In addition to the sensors, vibration motors were added to the design in order to provide feedback to the user. This feedback can be used in several applications such as, providing haptic feedback for virtual reality applications, acting as a stimulus to prompt the user to perform certain tasks for rehabilitation, or as feedback for tele-navigation [54]. The motors used were Adafruit mini vibration motors, which are rated for 5 V max with a current draw of 100 mA. The motors have a weight of 0.9 g and can provide a vibration sensation that resembles that of a standard mobile phone vibrating unit.

Electrical Circuit:

A custom printed circuit board (PCB) was developed to connect the sensors and actuators with the microcontroller unit and other electrical components. The force sensors and encoders were connected to the microcontroller unit as inputs while the pneumatic actuators and vibration motors were the output connections. The pneumatic actuators were controlled using the solenoid valves to produce a linear actuation. The microcontroller itself powers these solenoid valves on/off via N-MOSFET switches. The vibration motors are directly connected to a motor driver since the current ratings of these motors exceed the tolerance of the microcontroller input/output (I/O) pins. The microcontroller connects to the motor driver with two enable pins for each vibration motors, one for the index finger and another for the thumb.

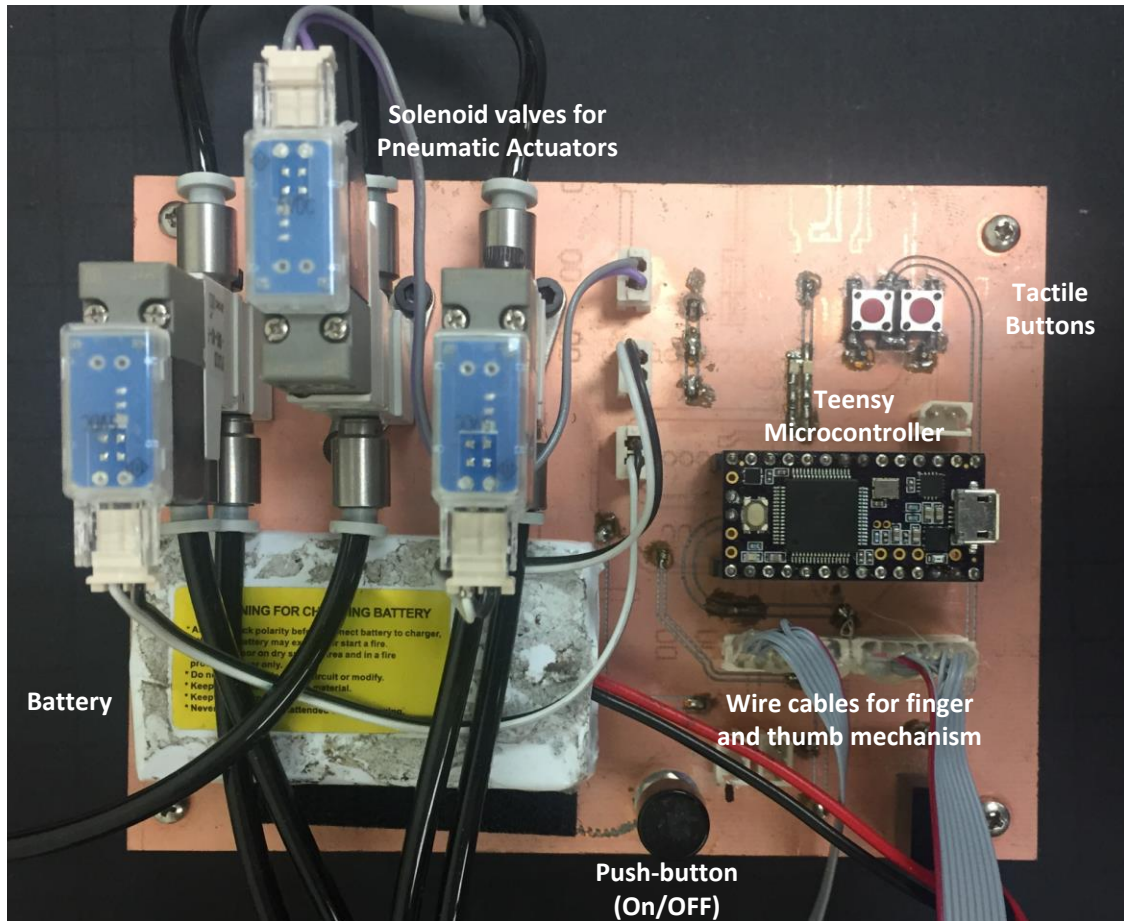


Figure 6.3: PCB design for the two-digit prototype

A Teensy 3.1 board serves as the microcontroller unit for the system. It is rated at a clock frequency of 72 MHz, which provides sufficient speed for acquiring sensor data from the encoders and force sensors while performing commands to control the vibration motors and the actuation for flexion or extension of the index and thumb.

In addition to the sensors and motors, the PCB contains three tactile pushbuttons. One pushbutton serves as the main power switch while the other two are used for actuation controls. One of these two is used to depressurize the pneumatic actuators to allow free movements among the finger and thumb. The last button is used to trigger an automatic

flexion and extension motion on both the finger and thumb to perform a grasp. This feature allows the exoskeleton device to serve as a standalone device for different applications such as rehabilitation. For full feature controls, the PCB can be interfaced with the Graphical User Interface (GUI) for the exoskeleton glove system that provides additional commands and functionalities. The overall architecture of the exoskeleton glove system is demonstrated in Figure 6.3.

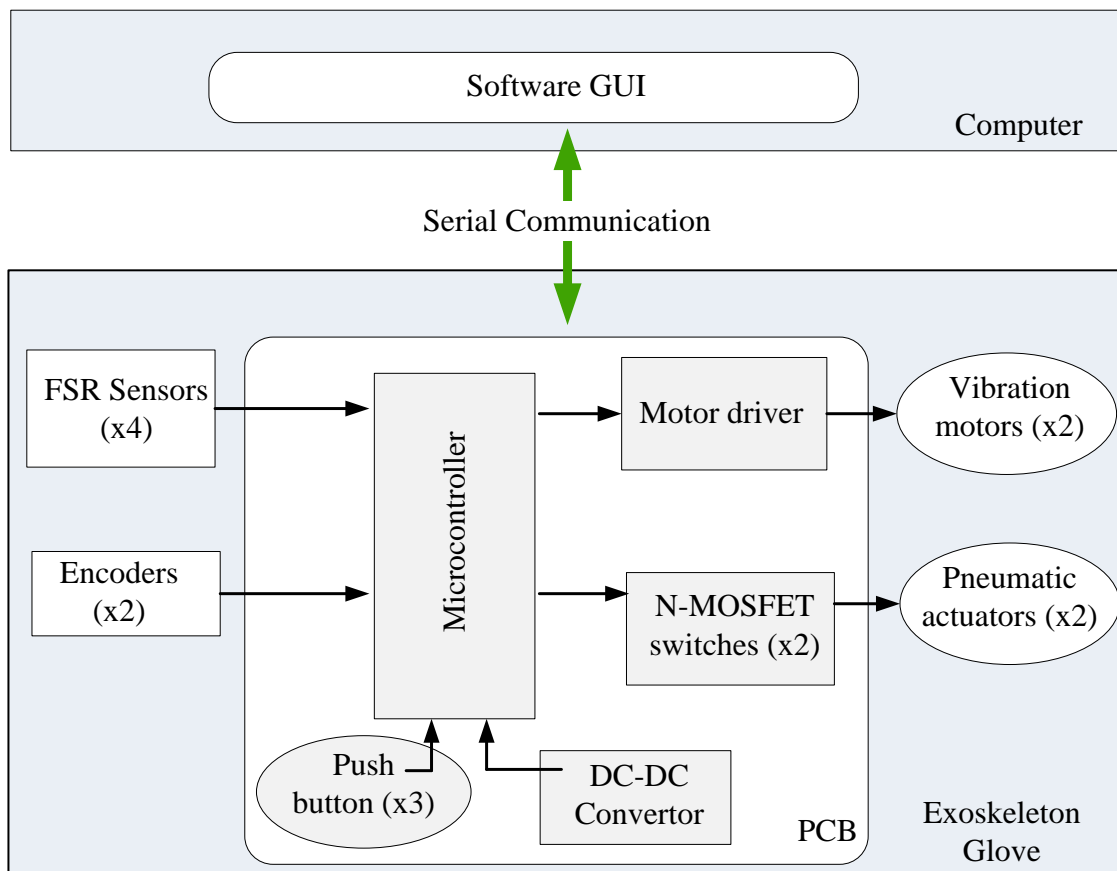


Figure 6.4: System architecture of the hand exoskeleton system

6.1.2. Experiments

An experiment was conducted to verify whether the joint angles enforced on the index finger and thumb by the glove during flexions and extensions reflect the desired trajectories for obtaining natural joint coupling.

6.1.2.1 Experimental Setup

The experiment involved mounting the exoskeleton glove on a wooden mannequin hand and tracking the motions of index finger and thumb, which were produced by the glove, as shown in Figure 6.4. The tracking was achieved using a GoPro HERO5 Session 10 MP camera with 4 K video resolution. To capture the finger and thumb at various stages during motions, the camera was set up to record videos at 30 frames per seconds (FPS). A MATLAB script was programmed to utilize basic computer vision techniques to analyze the captured images. The code first identifies red markers placed on the MCP, PIP, and DIP joints and MCP and IP joints of the inserted index finger and thumb respectively. Once these red markers were identified, the centroids of the markers were computed to determine the centers of the joints. Line segments were drawn between the joint centers such that the corresponding joint angles could be calculated (illustrated in Figure 6.4). Thus, from identifying the red markers from image to image the overall joint angles were calculated and used to analyze the joint coupling relationships enforced by the exoskeleton glove.

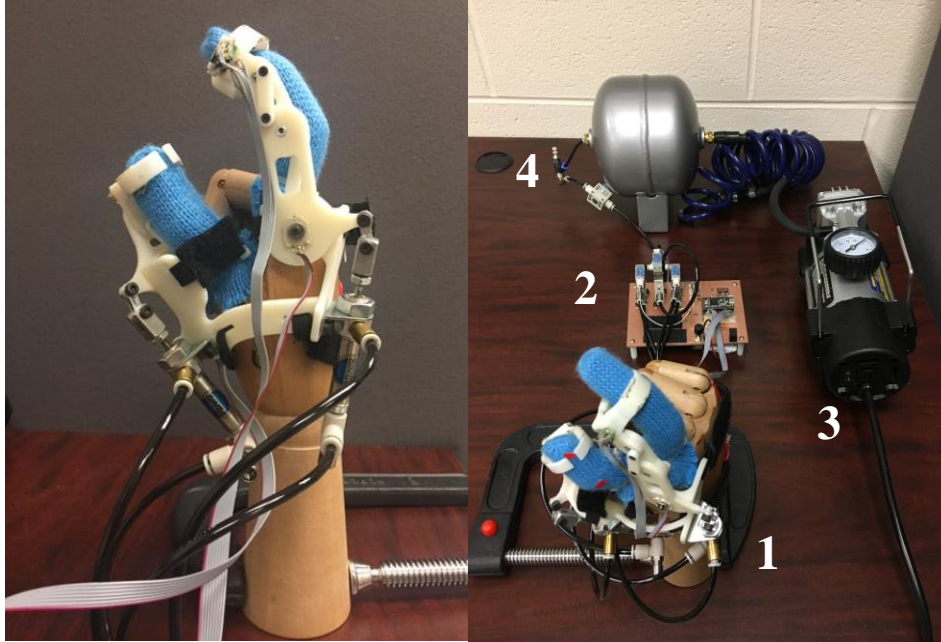


Figure 6.5: Experimental setup for the prototype: 1- Exoskeleton glove on mannequin, 2 - Embedded controller, 3 – Compressor, 4 - Air tank.

Although the GoPro camera is equipped with an ultra-wide-angle lens that has reduced distortion, it was still necessary to apply a distortion correction filter to each of the video image frames prior to the joint tracking procedure. In order to accomplish this, a camera calibration was performed using the traditional method of capturing several pictures of a standard checkerboard pattern using the subject camera [55]. The distorted images of the checkerboard were then analyzed using the MATLAB camera calibration toolbox to compute the camera intrinsic, extrinsic, and lens-distortion parameters. These parameters were used for the un-distortion filtering.

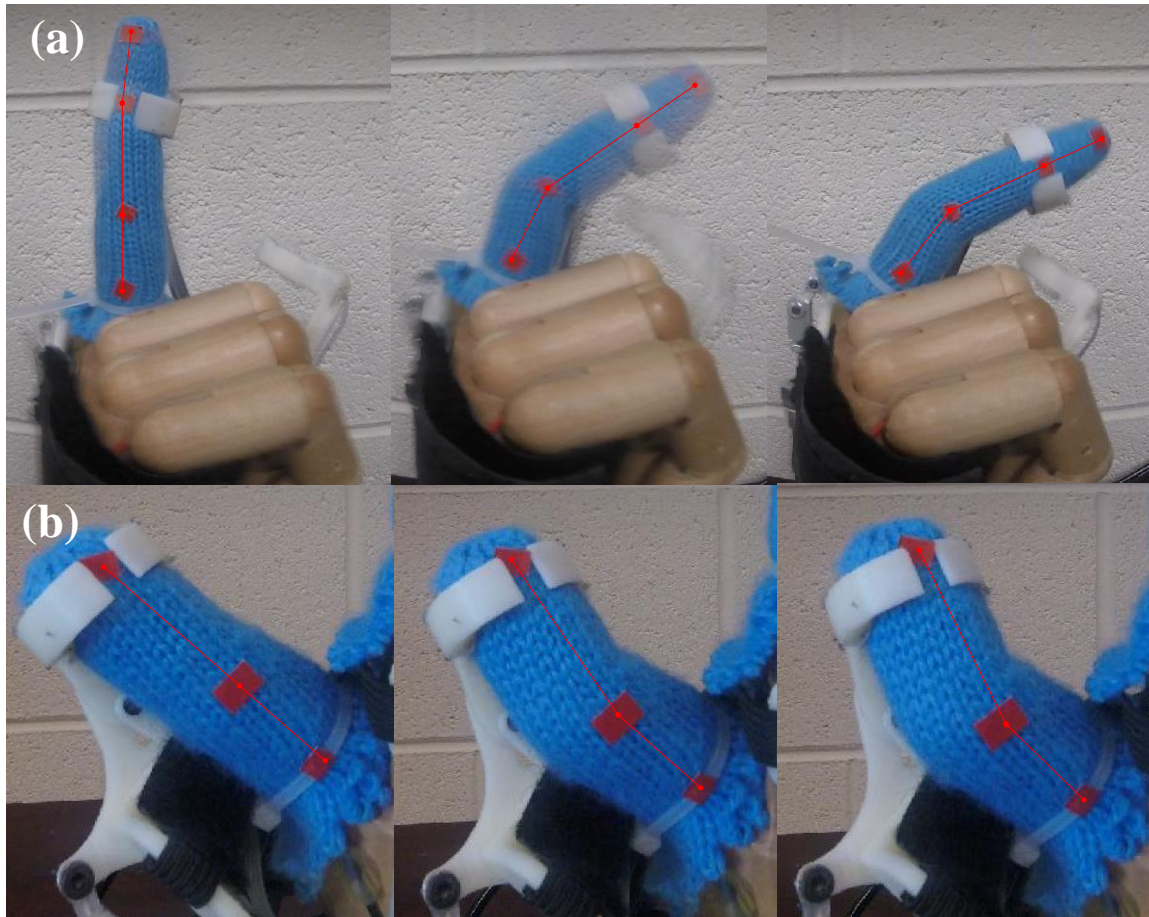


Figure 6.6: Experimental analysis at various stages of the bending motions for: (a) Index finger, (b) Thumb

To overcome the lack of inherent coupling between the respective thumb and index finger joints of the mannequin hand, the index finger and thumb were inserted into a cloth glove as shown in Figure 6.5. This allows the joints to bend in correlation, when the mechanisms for index finger and thumb apply force at the distal phalange of the corresponding finger/thumb.

6.1.2.2 Joint Angle Relationships Validation

The experimental results for the joint angle relationships for both the index finger and thumb are shown in Figure 6.6 and Figure 6.7, respectively. The calculated joint angles are displayed in respect to time. The results are explained further in detail below.

Index Finger:

During bending motions, the angular displacements for the index finger joints are presented in Table 6.1 below. These angles are verified by comparing them to the natural joint angles from [20], which were stated as the targeted reference angles in Section 4.1.

Table 6.1: Experimental results and comparison for the index finger joints

Joints	Imposed Angles	Referenced Angles	Difference
MCP	42.9°	49.1° (SD 9.5°)	0°
PIP	37.8°	41.0° (SD 10.7°)	0°
DIP	8.01°	38.5° (SD 6.8°)	23.7°

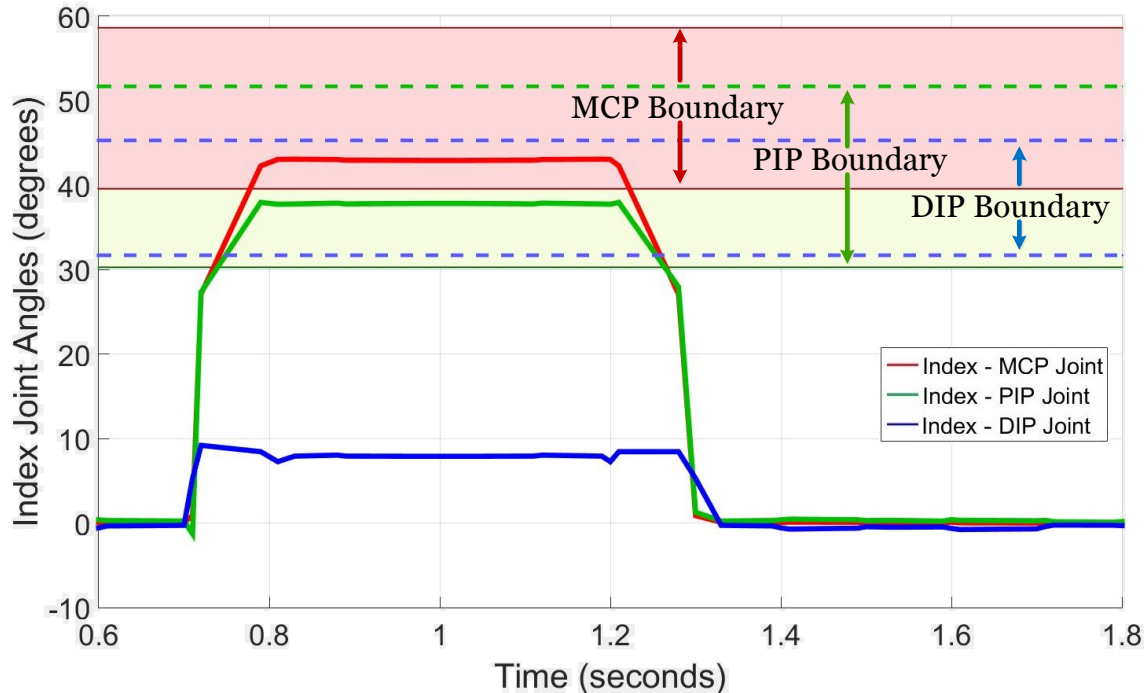


Figure 6.7: Index finger joint angles in respect to execution time

In Figure 6.6 and Figure 6.7, the resulting angles from the experiment were further plotted in respect to time in order to showcase the execution time of the hand exoskeleton to impose flexion and extension motions onto the user’s fingers and thumbs. By using the reference angles with the corresponding standard deviation values, upper and lower bounds were derived and plotted onto the figure to illustrate the range of acceptable values for the maximum angular displacement of each joint. Specifically, upper and lower bounds were computed by simply adding and subtracting the standard deviation values from and to the reference angles respectively. As shown, the angular displacements for the MCP and PIP joints of the index finger were well within their acceptable range for natural angular displacements at the end of the pinch. However, the final angular displacement for the DIP joint of the index finger fell short from reaching within its perspective boundary by 23.7°.

Thumb:

Similar to the index finger, the angular displacements for the thumb joints during bending motions are displaced in Table 6.2. These joint angles are also verified to the natural joint angles of the thumb presented in [20].

Table 6.2: Experimental results and comparison for the thumb joints

Joints	Imposed Angles	Referenced Angles	Difference
MCP	3.01°	12.8° (SD 9.4°)	0.39°
IP	22.5°	21.8° (SD 7.8°)	0°

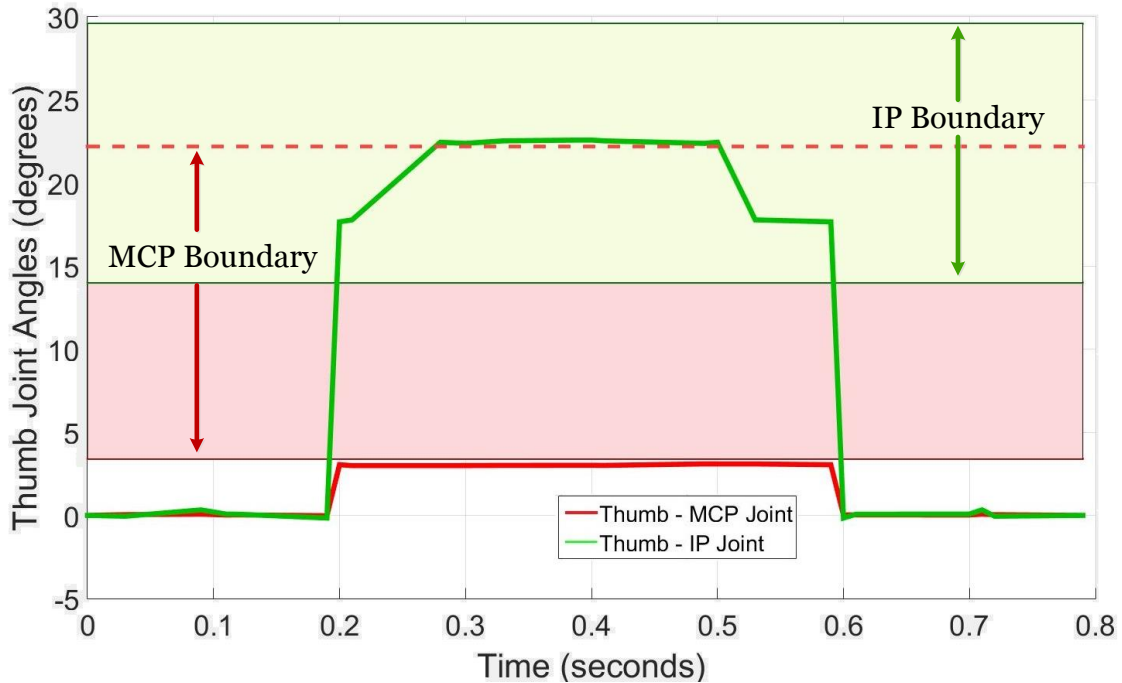


Figure 6.8: Thumb joint angles in respect to execution time

Much like the results for the index finger, the resulting angles of the thumb are plotted in respect to time to illustrate the execution time for the hand exoskeleton. Upper and lower bounds were derived by adding and subtracting the standard deviations with the corresponding reference angles. This illustrates the range of acceptable values for the maximum angular displacement of each joint. As shown in Figure 6.7, the MCP joint angular displacement for the thumb fell well within its targeted range, while the IP joint was close to the boundary of the acceptable range, falling short by 0.39° .

6.1.3. Discussion

The shortcoming of the index finger DIP joint angle is due to the misalignment of the Velcro fingertip holder. Instead of being positioned at the distal phalange region of the mannequin hand, the holder was located near the DIP joint, which can be seen in Figure 6.5. This misalignment was due to the size difference between the mannequin hand and the

human hand, for which the holder piece was originally designed to accommodate. The mannequin fingers were longer (index finger by 3cm and thumb by 1cm) than that of an average human hand and as a result, the mechanism was able to slide down the mannequin finger during the bending movements of the experiment. The same reason applies to the IP joint angles of the thumb coming short of the acceptable range. The glove can be seen properly worn on a human hand in Figure 6.8.

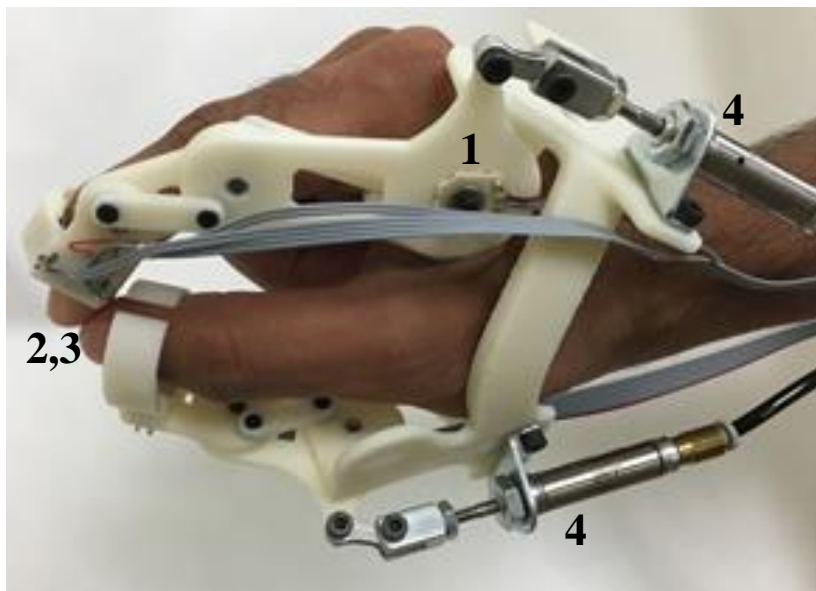


Figure 6.9: Prototype on a human hand: 1- Absolute position sensor, 2 - FSR sensor, 3 - Vibration motor, 4 - Pneumatic actuator

Overall, the pincer grasp was achieved in 0.63 seconds, with 0.1 seconds for the pinch, 0.41 seconds to hold the pinch, and another 0.12 seconds for releasing. Despite the experimental shortcoming of the DIP joint of the index finger, the results demonstrated that the joint angles produced by the exoskeleton resemble natural bending trajectories of the human hand during grasping motions, such as the pincer grasp.

6.1.4. Conclusion

This section explained the design and integration of a two-digit prototype of an exoskeleton glove that was proposed to address the commonly encountered large size, heavy weight, and unnatural coupling issues of traditional hard and soft exoskeleton gloves. The design of the exoskeleton glove allows for the finger and thumb mechanisms to be attached alongside the respective finger/thumb, decreasing the size of the exoskeleton glove as well as reducing the discomfort caused from using larger and heavier traditional gloves. The proposed concept was validated through experimental analysis, which produced results that showed the potential of the proposed design to achieve natural joint angle relationships that resemble that of a human hand.

Although the initial features of the prototype to record finger and thumb movements, measure exerted forces on the glove, and provide vibrational feedback, make it suitable for multiple applications, the pneumatic actuators present several shortcomings that affect performance. These shortcomings were analyzed in the next section, which also offers a proposed solution.

6.2 Full Hand Prototype Design

6.2.1. Motivation

Although the two-digit prototype of the proposed design (from Section 6.1) showed promising results in being a lightweight hand exoskeleton that can emulate natural joint angles, major improvements are needed to expand this proof of concept into a full hand exoskeleton. To successfully expand the two-digit prototype into a full system that can also serve as a functional haptic or assistive device suitable for ADLs, the following shortcomings must be addressed:

- **Actuation:** Even though the pneumatic actuation method offers speed and power, it lacks the ease of controllability. Specifically, pneumatic actuators naturally allow for two basic configurations: full flexion and full extension of the hand exoskeleton digits (fully open glove and fully closed). To allow for efficient grasping of the various objects that humans interact with daily, the hand exoskeleton must have the ability to conform to the shape of the object being grasped. This therefore requires the actuation system to be able to achieve any of the infinite configurations between the range of maximum flexion and maximum extension.
- **Force Feedback:** With the human hand being a complex structure with many capabilities, it can offer a variety of grasps and pinches. These grasps differ according to the joint angles, trajectories, and orientations of the fingers and thumb and the overall output grip force. To control various grasps at high precision when interacting with objects or completing tasks, the human hand incorporates sensory processing with its motor skills. This allows the human hand to receive force feedback across many nerves within the hand at high level of sensitivity and react

accordingly. Although the proposed design contains force sensors that can measure interactive forces, it lacks the ability to use this force information as feedback input for controlling the force, speed, and ending trajectories of each finger and thumb of the hand exoskeleton. Without the hand exoskeleton having this type of compliance functionality, it will not be able to adjust the strength of its grasp and finger trajectories.

- **Portability:** When designing a hand exoskeleton that can primarily serve as an assistive glove or as a haptic device portability becomes a major design parameter. The use of a pneumatic actuation system does not achieve this design goal however. As shown in Figure 6.4, pneumatic actuators require items such as an air tank and compressor to create a fully functional system, which are not ideal to carry around for an extended period of time. An impulsive solution may be to have a smaller air tank and compact compressor that could fit inside a backpack for the user to wear, thus making the pneumatic system portable. Despite this being a plausible approach, it creates the concerns of having less available air for the pneumatic actuators to use between refills and adds more weight for the user to carry, creating serious issues for the elderly and disabled. As a proof of concept for the proposed design, the pneumatic actuation was sufficient for experimental validation and as a personal in-home rehabilitation system. However, to achieve portability the actuation system should be redesigned to use compacted, lightweight DC motors powered by LiPo batteries.

6.2.2. Mechanism Design Update

In order to address the shortcomings of the two-digit hand exoskeleton prototype, the full hand exoskeleton proposes the idea to:

1. Replace the pneumatic actuation system with electrical actuators using a series elastic actuator (SEA) design.
2. Redesign the original and primary proposed mechanism from Chapter 4, to have a slimmer profile that would allow for linkages of the full hand design to fit between the fingers more comfortably, and for the height of linkages to be constrained by the finger heights of the average user.

In Figure 6.9 and Figure 6.10, the proposed design is presented with the SEA design from Chapter 5 incorporated into the hand exoskeleton.

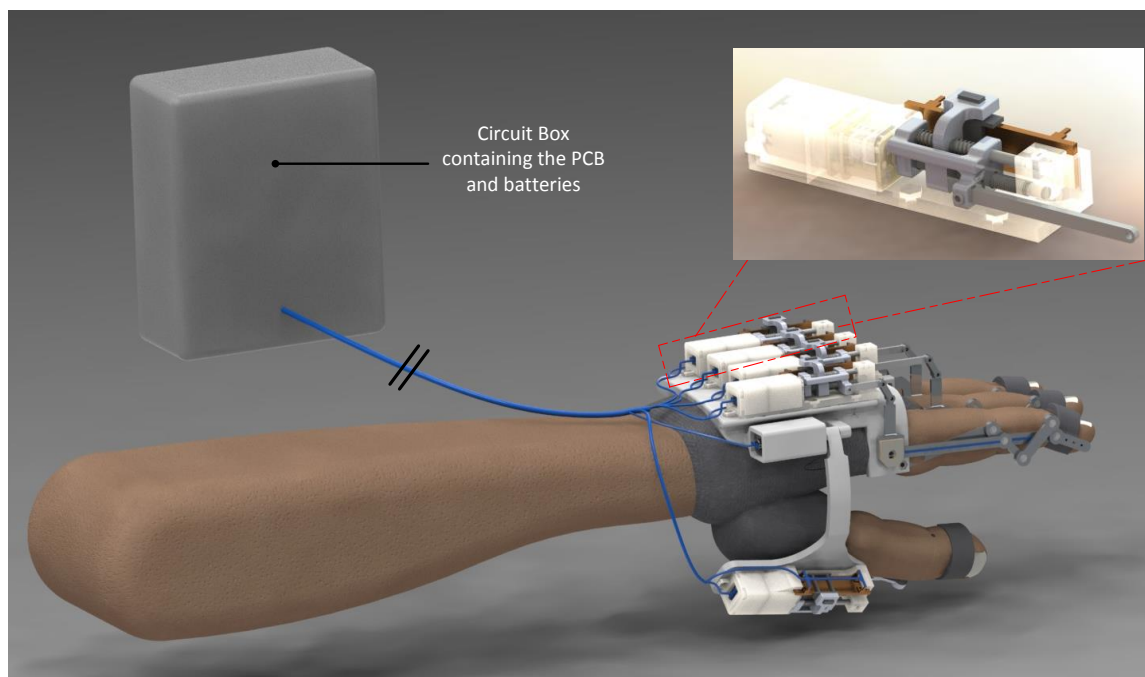


Figure 6.10: CAD model of the proposed full hand exoskeleton system with the SEA units and redesigned mechanism

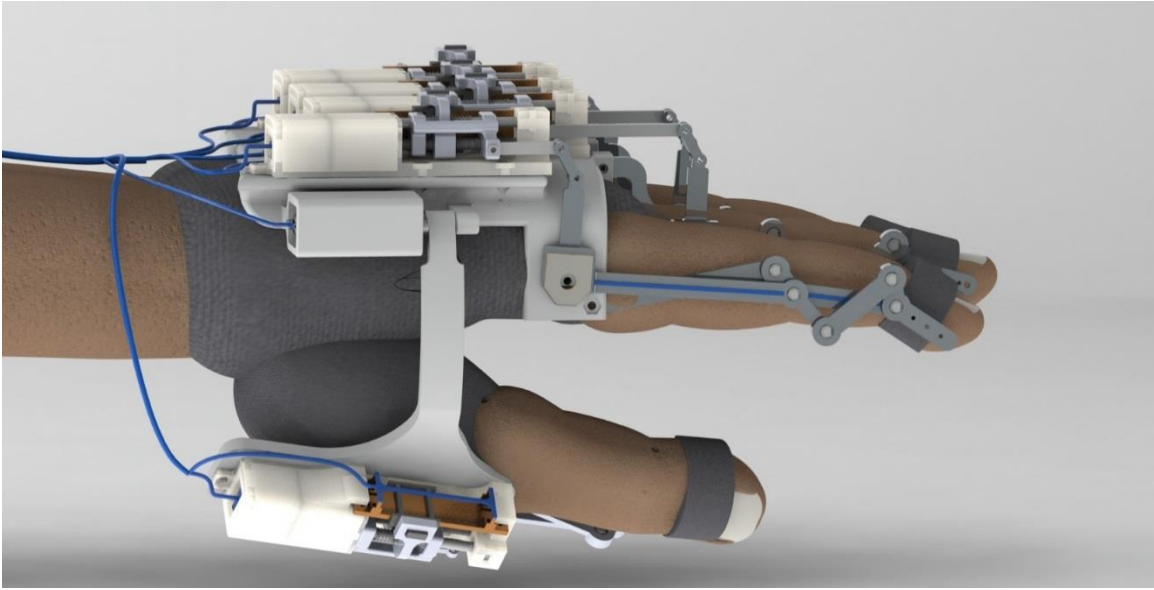


Figure 6.11: Close up view for the CAD model of the proposed full hand exoskeleton

Currently, this prototype is being manufactured and built. Once assembled, the electronic aspect will be integrated onto the design to produce a fully functional glove. A force control scheme will be implemented using the proposed SEA design and experimental validation will be performed. The application of assistive grasping will be explored by having the hand exoskeleton grasp various objects at different desired forces.

6.3 Children Two-Digit Prototype

In a collaboration effort with Dr. Nathalie Maitre of the Center of Perinatal Research and Maitre Lab at Nationwide Children's Hospital in Columbus, Ohio, a child size two-digit hand exoskeleton system was developed. The research objective was to design a hand exoskeleton system that can serve as both a rehabilitation device and a diagnostic system for high-risk infants of the age 12-36 months. This section discusses the design and prototype development of this child size hand exoskeleton system.

6.3.1. Motivation

Cerebral palsy (CP) is known as the paralysis of voluntary movement in certain body parts as a result of abnormalities to the brain's cerebrum. CP is the most common motor disorder that affects children [56]. According to population studies, an estimate of 0.3% children are diagnosed with CP [57]. Babies that are born prematurely or at a low birth weight have a greater risk of becoming diagnosed with CP [56]. As a result, many high-risk infants are closely monitored in neonatal intensive care units. The average birth weight for babies' ranges from 5.5 -10 pounds, with the low birth weight being below 5.5 pounds [58]. A report by the CDC found that among children who were born weighing less than 3.5 pounds (1,500 grams), the prevalence of CP was 59.5 out of 1,000 live births as compared to 1.1 of 1,000 live births for children born weighing more than 5.5 pounds (2,499 grams). For children born in the weight range of 3.5 pounds to 5.5 pounds (1,500 - 2,499 grams), the prevalence of CP was 6.2 out of every 1,000 live births [59].

In addition to CP, high-risk infants also suffer other neurodevelopmental morbidities and motor skills impairments. The general procedures for monitoring and performing diagnostic tests involve paternal observations and clinical assessments of the motor skills

and developmental milestones for the child. Many research groups have done studies [60], [61] that focus on neurodevelopmental and motor control disabilities in high-risk infants.

Despite the research and development on hand exoskeleton systems [26], [28], [44], [62], [63] for both rehabilitation and assistance purposes, most of these gloves are not suitable to be used as a child-sized system due to their heavy and bulky designs. In addition, most of these hand exoskeleton systems are designed for general grasp functionalities instead of a specific rehabilitation exercise like the pincer grasp. As a result, a new child-sized hand exoskeleton system was proposed.

6.3.2. Robotic Exoskeleton Design

Due to the targeted users being high-risk infants with small fingers and thumb, a new mechanism was designed. The original mechanism from Chapter 4 was unable to produce the design joint angle relationships of a natural hand when the link lengths were scaled down to be small enough for the hand of a child. Based on the above requirements, an initial mechanical design was prepared. The mechanical and electrical design approaches for this child-sized hand exoskeleton are explained in the following sections.

6.3.2.1 Kinematics

The conceptual design of the mechanism is illustrated in Figure 6.11. The concept was primarily inspired by the design of the R³ Robotic tail, a parallel project being done in the Robotics and Mechatronics Lab at Virginia Tech. The mechanism for the index finger essentially consists of three planar links that are connected by means of revolute joints. Electric motors are fixed rigidly on the base segments, actuating the first segment through

the driving gear. The rest of the segments are coupled together by gears, as discussed below:

- First segment is coupled with the motor shaft (gear ratio $G1$)
- Second segment is coupled with the stationary base segment (gear ratio $G2$)
- Third segment is coupled with the first segment (gear ratio $G3$)

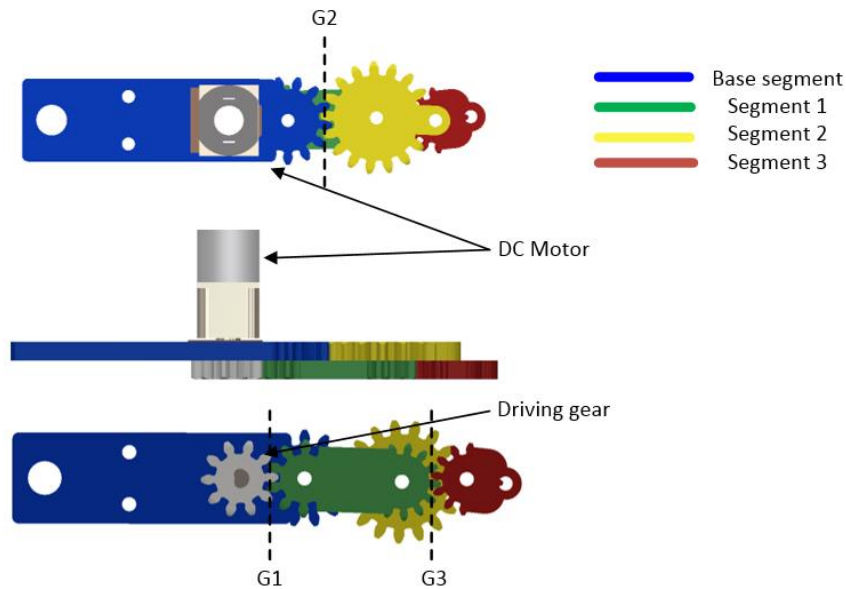


Figure 6.12: Index finger and thumb mechanisms for the proposed children hand exoskeleton

Similar to the original hand exoskeleton, these mechanisms for the fingers and thumb can be considered as a single DOF system. In order to achieve a grasping motion such as the pincer grasp, all three joints (MCP, PIP and DIP) on index finger and the IP joint of thumb are actuated to move, while keeping the MCP joint for the thumb restrained.

Like the other prototypes, the gear ratios were designed to achieve bending profiles that resemble the natural joint angles of the human hand during flexion and extension motions. Using [20], the reference angles were selected as the data from the tip-pinch force of 100g

and pulp distance of 3cm. This data point contains joint angles values of 7.1° (SD 9.1°), 35.4° (SD 16.6°), and 36.3° (SD 9.5°) for the DIP, PIP, and MCP joints of the index finger respectively. Based on the above the gear ratios were selected to be:

- $G1 = \text{DC Motor: DIP} = 1:1$
- $G2 = \text{DIP: PIP} = 1:1.037$
- $G3 = \text{PIP: MCP} = 1:1.215$

In the case of thumb, a similar but much simpler mechanism was used. Since only one joint (IP) needs to be moved, it was driven directly by the DC motor at 1:1 gear ratio.

6.3.3. Prototype Integration

In order to further develop the design into a hand exoskeleton that can be used for rehabilitation and diagnostic purposes for high risk infants, several features and design requirements had to be considered. The glove needed a haptic feature to serve as a stimulus to prompt the infant to achieve a pincer grasp. In addition, the system needed a feature to record data about the hand movement of the patient while performing pincer grasps. As mentioned in [64], [65], EEG sensors can be used to monitor the reaction time between triggering the vibration stimulus and the infant's initiation for the pinch. Using the data collected by the system and data from EEG sensors, the neurodevelopment of high-risk infants can be monitored and analyzed, as well as the child's progress in developing motor skills. For infants already impacted by hand impairments, the hand exoskeleton system can be used as a rehabilitation device to assist them in achieving the pincer grasp. The overall design requirements can be summarized as follows:

- Achieve proper joint angles for the index finger and the thumb by using only one actuator for each
- Overall size of the system must be small enough to fit a child aged 12 months to 3 years
- Mechanism should be repeatable and robust, but should not cause any fatigue to the person wearing it

6.3.3.1 Mechanical Design

The detailed design of the system was done in Solid Works, as shown in Figure 6.12. The base segments of each bending mechanism were connected onto a flat plate by means of thumbscrews. This facilitates adjusting the position and orientation of each mechanism to suit various hand sizes. The flat plate was fixed onto a 3D printed base that supports the weight of the entire system. With this design approach, the child should not experience any fatigue while operating the system. The microcontroller board, associated electronics and onboard power supply are housed in an enclosure piece on the top of the base plate, thus allowing the system to be operated as a standalone rehabilitation mechanism.

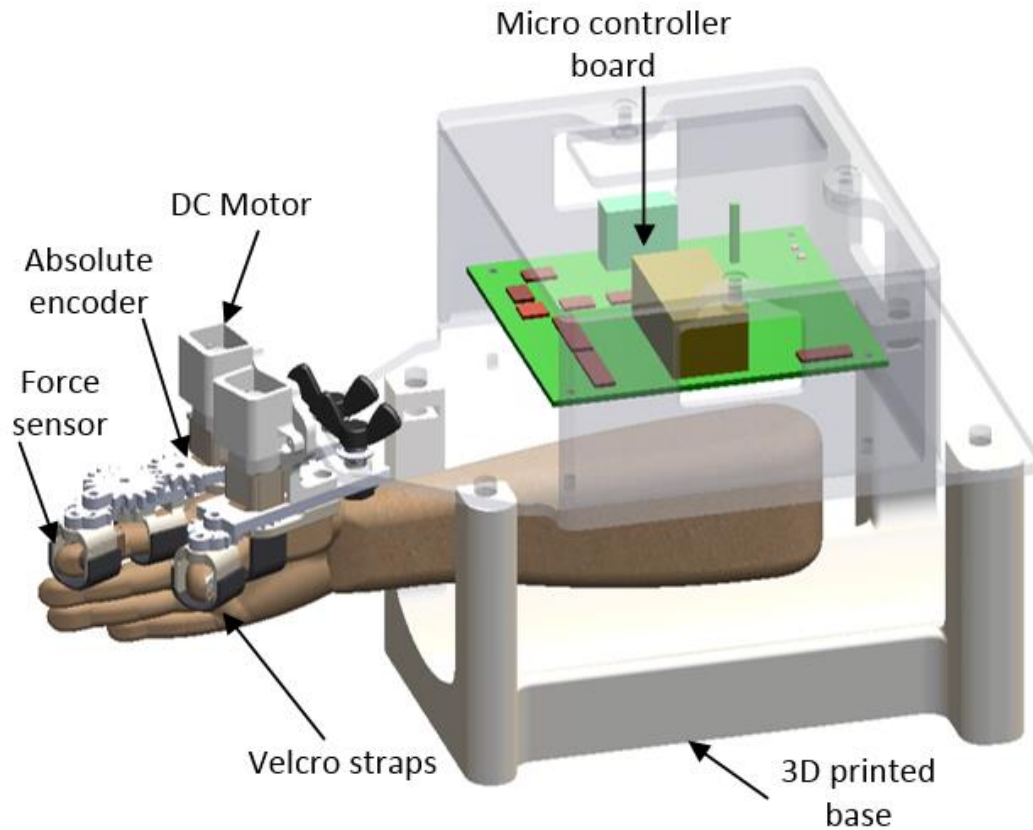


Figure 6.13: Detailed CAD design for the proposed children hand exoskeleton system

The bottom of the mechanism that makes contact with the hand is covered with 3D printed plastic pieces attached to each segment. These pieces are then covered with soft cushion to minimize discomfort for the child wearing the system. The index finger is attached to the mechanism by means of two adjustable Velcro straps that restrain the proximal and distal phalanges to move through the desired trajectory to achieve pincer grasp. Two straps also connected the thumb to its mechanism, one that connects the distal phalanx with moving link and another that connects the interphalangeal with the base to restrain the MCP joint of the thumb from moving.

6.3.3.2 Electrical Design

Actuation

Pololu micro DC gear motors, rated at 6V, 1.6A were used for both the index finger and thumb segments of the exoskeleton device. Based on the coupling mechanism for the joints of the exoskeleton, the DC motors were able to provide sufficient actuation to achieve the desired flexion and extension trajectories.

Sensors

Position Sensors:

To achieve absolute position sensing, Bourns rotary encoders were inserted at the base segment above the driving gears for each of the two base segments. These rotary position sensors can translate 0 to 360 degrees of mechanical angular positions into an electrical angle signal of 0 – 330 degrees. When the finger and thumb are inserted in the exoskeleton, the encoders in the base segments will therefore be parallel to the MCP joints. The encoder values are converted into angle measurements after proper calibration using digital protractor. The remaining PIP and DIP joints of the index and the IP joint of the thumb are estimated using the mathematical (kinematic) model of the exoskeleton.

Force Sensors:

Force Sensitive Resistor (FSR) sensors by Interlink Electronics were used to measure the amount of force the index finger and thumb are inserting on the respective exoskeleton frames. These FSR sensors have a continuous analog resolution and a force sensitivity range of 0.2N – 20N. The sensors are placed on 3D printed fingertip pieces attached to Segment 3 of both the index and thumb mechanisms. Two force sensors are used for each

of the fingertip pieces, one touching the top of finger nail and the other touching the bottom of fingertip. Since the force sensors output resistance values, the sensors had to be connected to a simple voltage divider circuit in order to convert the resistance values into output voltages. This conversion is needed in order to feed the outputs from the force sensors to the analog voltage I/O pins of a microcontroller. The final conversion step was to relate the output voltage values to meaningful force measurements, which was done by performing a calibration process with known weights.

Vibration Motors:

Vibration motors are used to provide a stimulus to prompt the user to perform a pincer grasp. The Adafruit mini vibration motors are rated for 5 V max with a current draw of 100 mA. These motors, which have a weight of 0.9 grams each, can provide a vibration output like a standard mobile phone vibration feedback.

Electric Circuit:

As illustrated in Figure 6.13, a printed circuit board (PCB) was developed to integrate the sensors and actuators with the microcontroller unit and other electrical components. The force sensors and encoders are connected to the microcontroller unit as inputs while the DC motors and vibration motors are output connections. To control the vibration motors, the microcontroller powers them on/off via N-MOSFET switches. The DC motors are directly connected to a motor driver since the current ratings of the motors exceeds the tolerance of the Teensy input/output (I/O) pins. The microcontroller connects to the motor driver with three pins: two direction pins and one PWM pin. To actuate the motors, a max PWM is given and the corresponding direction pins are set LOW/HIGH to achieve the

flexion and extension motions. To power down the DC motors, both direction pins are set LOW and the PWM pin is given a 0 V input.

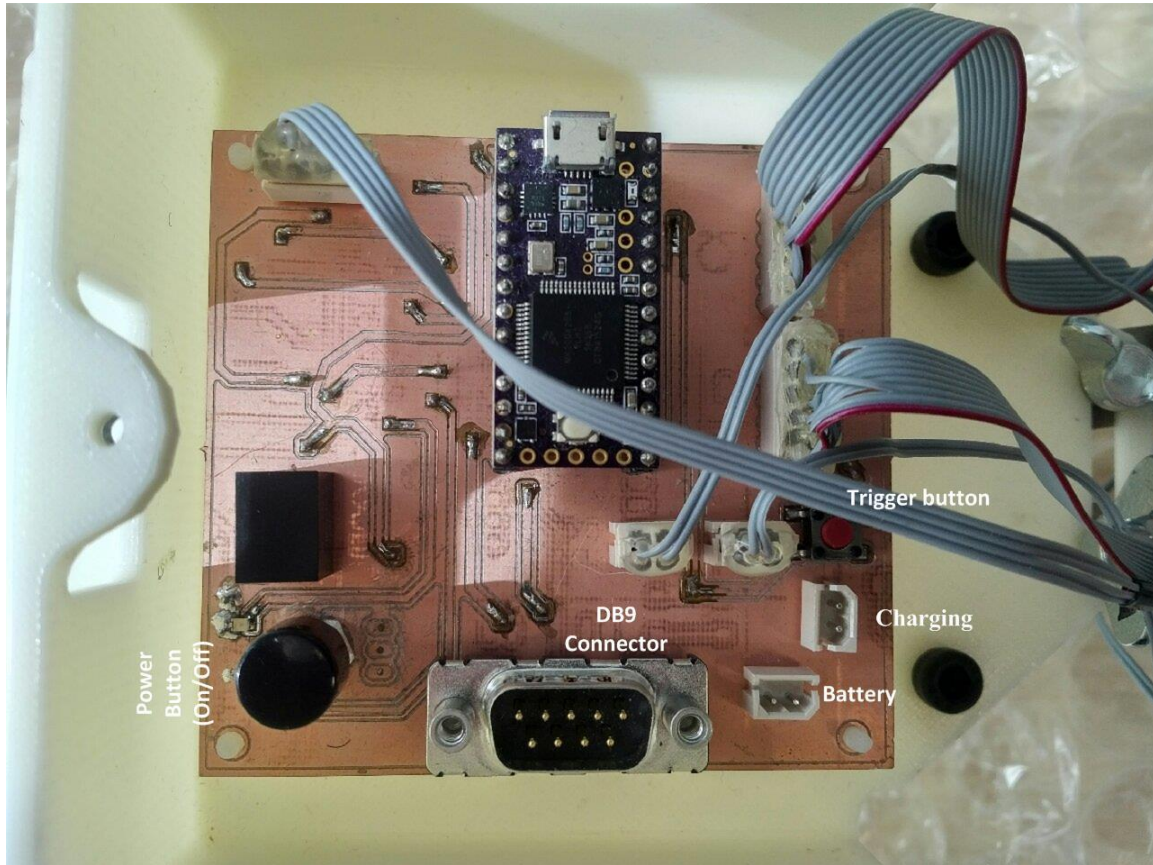


Figure 6.14: Custom printed circuit board for the children hand exoskeleton system

A Teensy 3.1 rated at a clock frequency of 72 MHz, serves as the microcontroller unit for the system. This provides sufficient speed to acquire sensor data from the encoders and force sensors while performing commands to control the vibration motors and the actuation for flexion or extension of the index and thumb. In addition to the sensors and motors, the PCB contains a DB-9 connector and a tactile pushbutton. The DB-9 connector can be used for sending signals that represents a timestamp of the triggered vibration stimulus to a computer. The pushbutton can be used to send a time automated flexion and extension

command. This allows the exoskeleton device to serve as a stand online device for rehabilitation purposes. For full feature controls, the PCB can be interfaced with the Graphical User Interface (GUI) for the Exoskeleton Glove System that provides additional commands and functionalities.

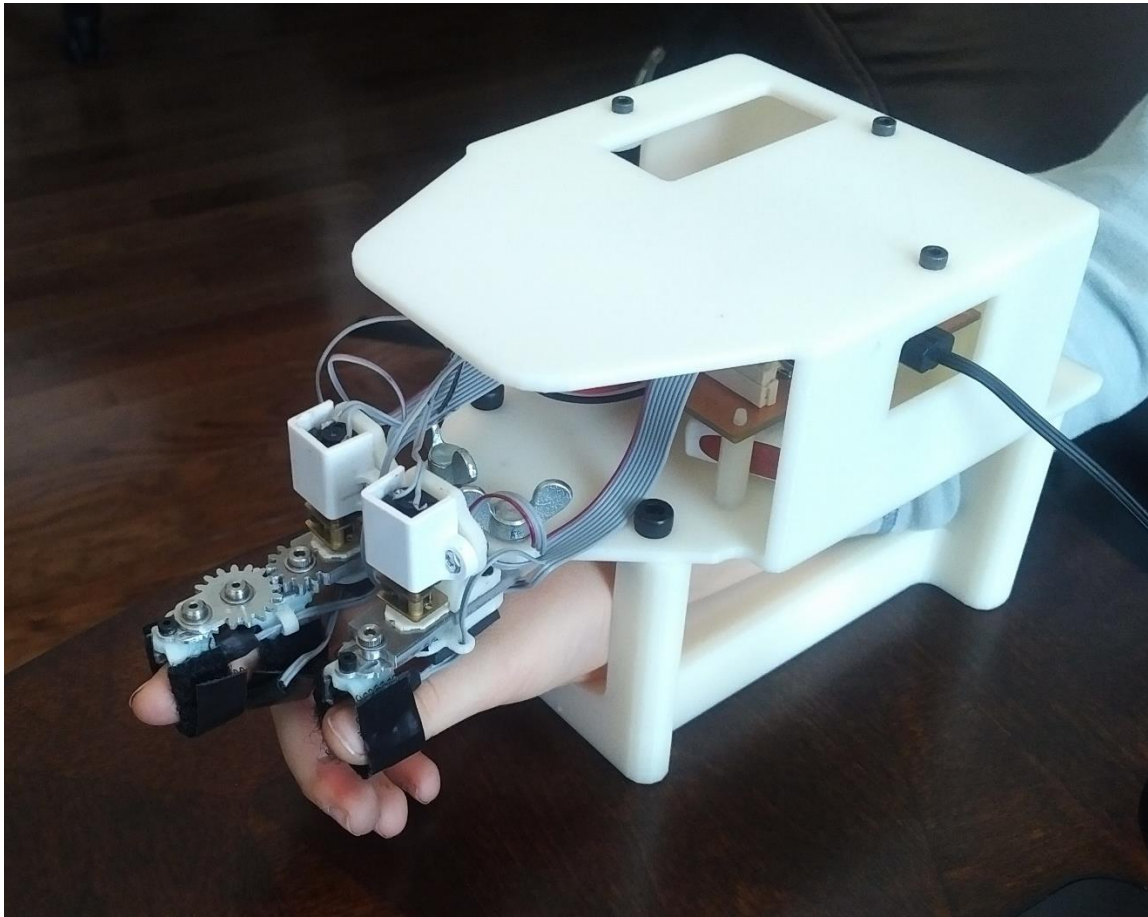


Figure 6.15: Prototype of the children hand exoskeleton system (demonstrated by a child of age 5)

6.3.4. Experiments

An experiment for verifying the actual mechanism of the device was conducted for the validation process of the exoskeleton device. The purpose of the experiment was to check that the joint angles enforced by the mechanism resemble the natural joint angles of a

human hand while performing a pincer grasp. This was accomplished by fixing the prototype onto a table and tracking the motion of the mechanism links as the device was commanded to do pinching and release pinch motions. For the duration of the experiment, no human hand was strapped into the system so that it can be actuated freely. The decision to do this was based on the assumption that when the system is being used for rehabilitation purposes, the child's hand would not affect the joint angles produced by the device in a significant manner. Therefore, the system would execute the same motion of joint angles regardless of having a child hand strapped in or not.

The tracking aspect was done using a Point Grey Chameleon 1.3 MP camera. The camera was setup to capture images at 15 frames per second (FPS), allowing for pictures at various stages of the pincer grasp to be taken. To analyze the captured images of the mechanism experiment, a MATLAB script using computer vision techniques was used. The concept of the computer vision code was to identify blue markers that was placed on each of mechanism links, specifically at the index finger joints (MCP, PIP, and DIP) and the thumb joints (MCP and IP).



Figure 6.16: Experimental analysis for children hand exoskeleton prototype

After identifying these blue markers, their centroids were computed to reflect the center of each joint angle, as shown in Figure 6.15. From using the joint angle centers, the corresponding angles between the joints were calculated accordingly. Thus, from identifying these blue markers from image to image, the positions of the index finger and thumb joints were tracked over time while recording their joint angles. The collected data is plotted below in Figure 6.14 to show the variation of each of the joint angles with respect to time. The MIP, PIP and DIP joints of the index finger each bends through angles of 37° , 36° , and 20° respectively. The IP joint of thumb bends through an angle of 70° .

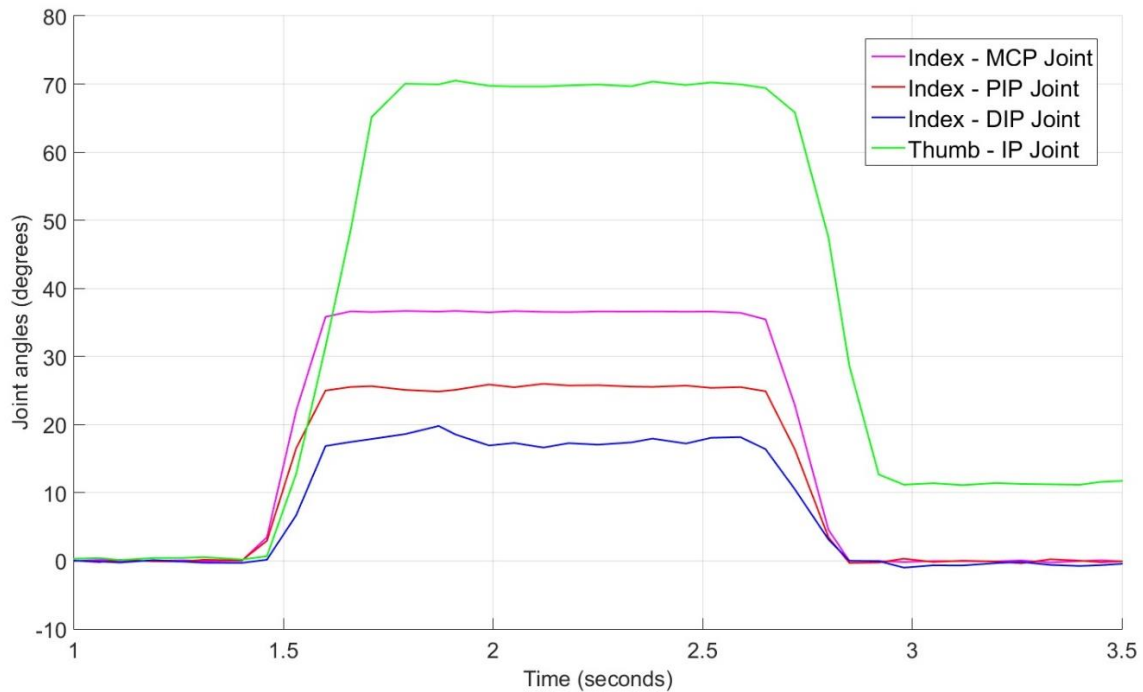


Figure 6.17: Experimental results of the joint angle relationships for the index finger and thumb in respect to execution time for pincer grasp

As seen from Figure 6.16, the thumb IP joint does not return to its starting angle. This is due to backlash present in the system between the motor and the driving gear of the

thumb link. The larger bending angle of the thumb was expected due to the design of the system suppressing the thumb MCP joint rotation. This was done by fixing the proximal phalanges of the thumb to the device using Velcro straps. The pincer grasp was achieved in 1.60 seconds; with 0.40 seconds for the pinch, 0.80 seconds to hold the pinch, and another 0.40 seconds for releasing. From Figure 6.16, the results show that the joint angles produced by the system matches with the normal joint angles of a human hand during pincer grasp as mentioned in [20].

6.3.5. Conclusion

This section presented the design and integration of a child-sized hand exoskeleton system that has the potential to serve as a rehabilitation and diagnostic device for high-risk infants. The mechanism was designed to assist the child in achieving natural joint angle relationships while performing the pincer grasp using both the index finger and thumb. The actual joint angles dictated by the system were compared with natural human hand motion and was found to be within acceptable limits.

CHAPTER 7

APPLICATIONS OF THE PROPOSED HAND EXOSKELETON PROTOTYPES

7.1 Rehabilitation Application

This section presents the application of performing a rehabilitation exercise using the proposed child-sized hand exoskeleton system. The implementation of the rehabilitation software is explained and a demonstration is given.

7.1.1. Overview

As mentioned in Chapter 6, the motivation for developing the child-sized version of the proposed hand exoskeleton was to provide a rehabilitation device for high-risk infants that have the potential to be used as a diagnostic system for the early detection of brain diseases and impairments. The system was designed to invoke the user to achieve a pincer grasp using their index finger and thumb.

The pincer grasp is known as an essential development milestone for children to accomplish during their infancy. This development typically occurs between the ages of 9 to 12 months of age. Learning the pincer grasp allows for infants to pick up small objects on their own. More importantly, infants can start to gain the ability to feed themselves by picking up small bits of food using the pincer grasp. Through further development of this grasp, children can begin to master certain tasks such as holding a pencil, or fastening a button. Thus for children at a higher risk of experiencing some brain impairments and/or

slow development of hand motor skills, having this rehabilitation device to teach infants on how to perform a pincer grasp can be of great benefits.

7.1.2. Rehabilitation Software

To assist the child-sized hand exoskeleton system in performing rehabilitation exercises, a software was developed to provide a graphical user interface (GUI). The GUI for the exoskeleton system was developed as an executable application in MATLAB. The software provides additional commands to control the glove and functionalities for data analysis. Figure 7.1 presents the layout of the GUI. As shown in Figure 7.1(a), the first screen of the GUI prompts the user to enter in the serial COM port in which the hand exoskeleton system is connected to the computer via USB. Figure 7.1 (b) presents the main screen layout for the GUI. On this screen, the user is presented with several command buttons that control the glove actuations and display buttons for reading position and force data. In addition, commands buttons to record the sensing data and even a feature button for enabling a passive mode are also implemented on the GUI.

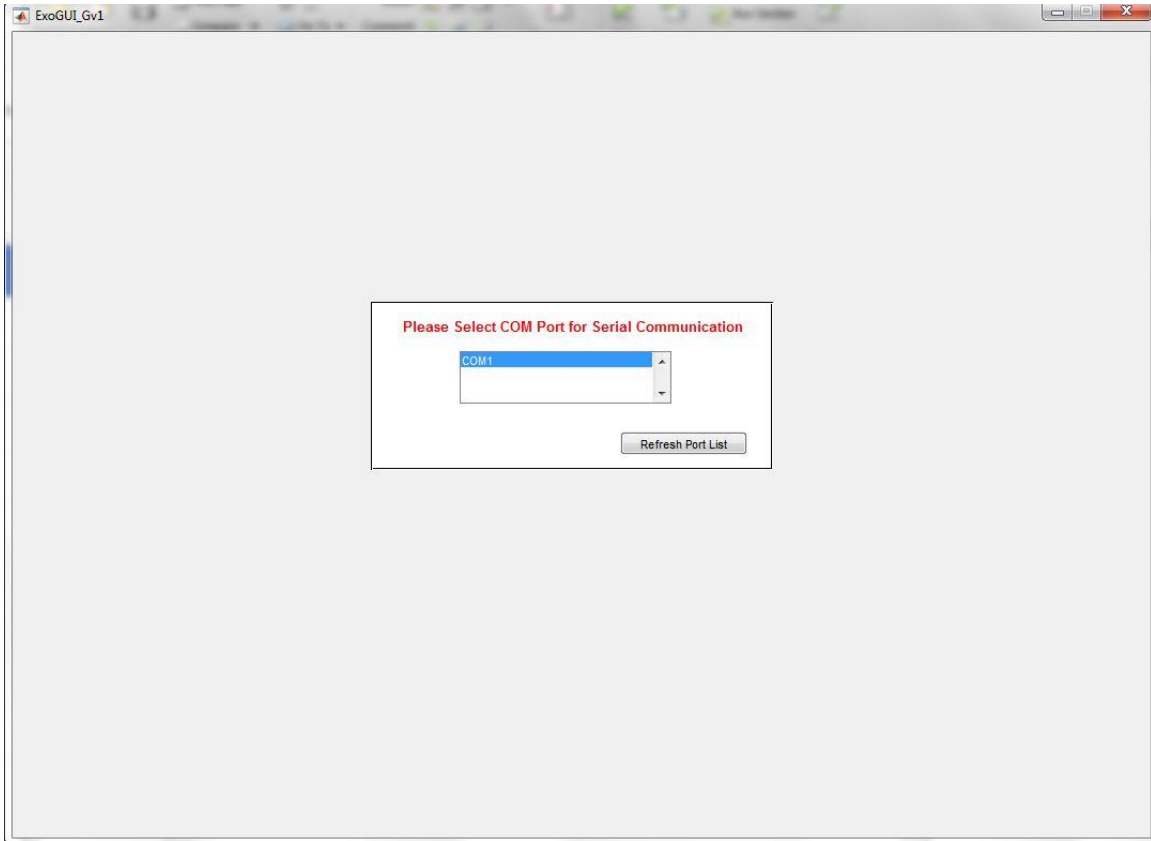


Figure 7.1: (a) Software GUI initial screen layout

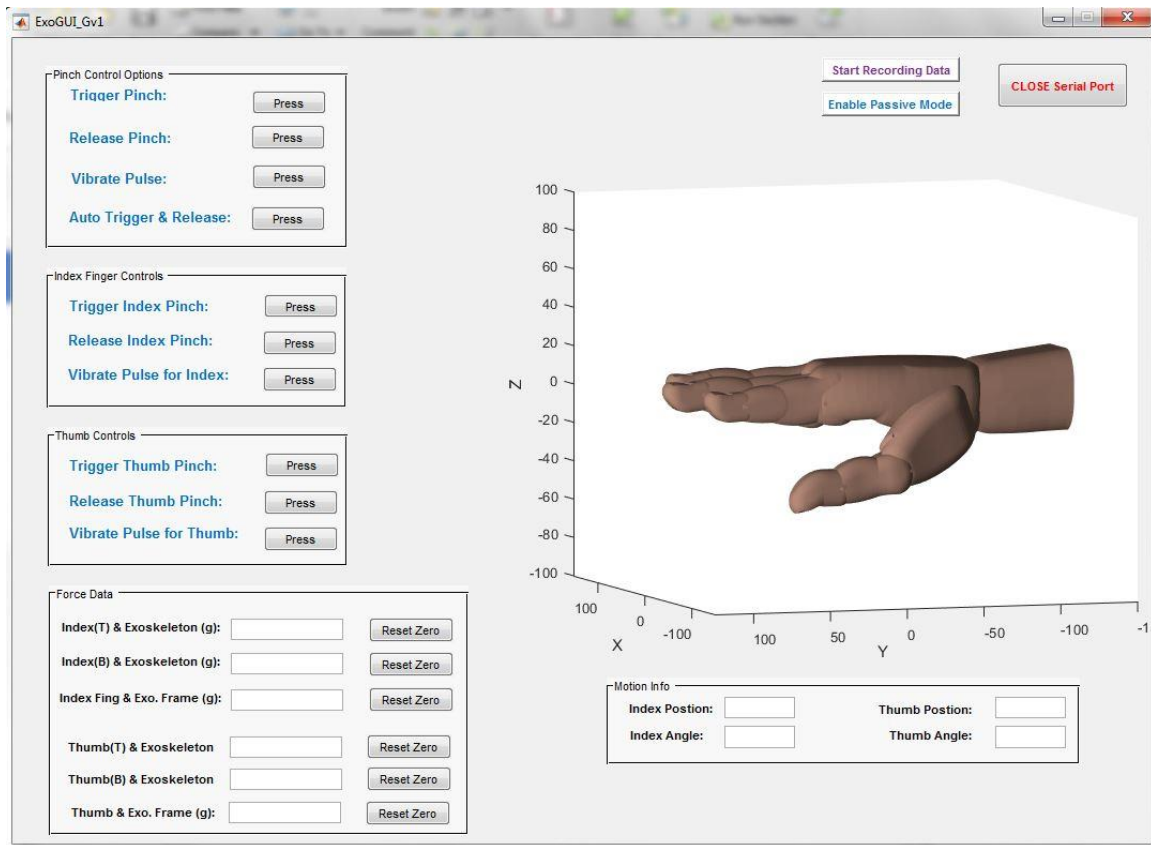


Figure 7.1: (b) Software GUI main screen layout

The passive mode allows the user to perform the pincer grasp on their own, without the full actuation by the motors. To achieve this, the passive mode relies on a simple force sensing scheme that reads the forces being exerted by user's finger and thumb. These forces are compared to specified threshold values to interpret whether or not the user is attempting to move their finger/thumb to perform the pincer grasp. This will in return, prompt the system to actuate the motors accordingly, but only when the forces are present. This is control scheme is needed since the geared DC motors are non-back drivable to allow for the finger and thumb mechanisms to move freely.

To control the glove actuation functionalities, the control command buttons are divided into groups: index finger controls, thumb controls, and both the index finger and thumb

pair controls. Each of these control groups consists of the following commands to control only its specified finger/thumb: Trigger Motion, Release, and Vibrate Pulse. The Index and Thumb combined control group contains these same commands as well as additional commands such as the Auto Trigger and Release Pinch command. This command actuates the index finger and thumb to perform a pincer grasp and then releases the pinch after a time delay of 1.50s. For all three control groups, the Vibrate Pulse commands were programmed to turn on the corresponding vibrate motors for 0.5s.

While reading in the sensor data, the GUI displays the FSR sensor data in terms of Newtons (N) and encoder values in degrees for both the index finger and thumb. For analysis purposes, the GUI has a record feature that will capture sensor data at a rate of 20Hz and store the data into a Microsoft Excel file. An additional feature of the GUI includes an imported SolidWorks CAD model of a human hand. The CAD model was incorporated to serve as a real-time animation that shows the movements of the user's hand while using the glove for the user to track their performance.

7.1.3. Demonstration

The rehabilitation software was performed using a volunteer. Each feature of the software was tested, including actuating the hand exoskeleton system to perform the pincer grasp, actuating the index finger and thumb separately, enabling the passive mode, and recording position and interactive forces during motions. Figure 7.2 presents a picture of how a user would use the exoskeleton system.

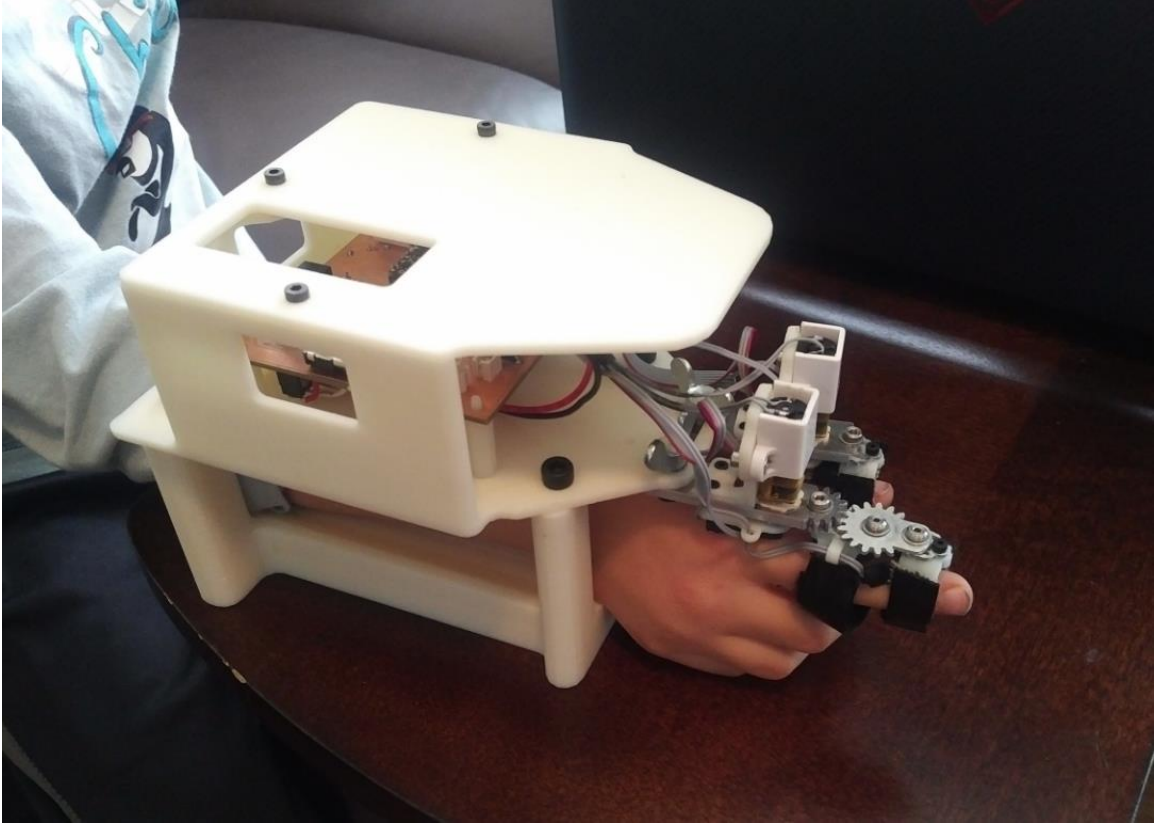


Figure 7.2: Volunteer demonstrating how to use the system

CHAPTER 8

CONCLUSION & FUTURE WORK

This chapter concludes the thesis with a summary of the current work as well as potential work in the near future.

8.1 Summary

The work of this thesis covered the design, analyses, prototype integrations, and experimental validation of the proposed hand exoskeleton mechanism. The proposed design is small sized, lightweight, portable, and possesses the abilities to produce natural joint angle relationships during flexion and extension motions to resemble that of a normal human hand. The system is capable of processing sensory information for position and interactive forces and can provide haptic feedback for needed applications. To create a robotic system that can perform intelligent grasping that imitate the basic behavior of the human hand, a force feedback controller was presented with a proposed design for a compacted SEA unit. Together, these features will allow the full hand exoskeleton to serve as a multipurpose device, whether for rehabilitation, assistive, or interactive haptic purposes.

A comprehensive literature review on hand exoskeletons and the anatomy of the human hand and its functionalities was given. This review highlighted some of the common challenges faced within the field. These challenges were evaluated and used as inspiration for the proposed hand exoskeleton system.

A discussion was provided for the preliminary analysis of the proposed hand exoskeleton mechanism for the fingers and thumb. The kinematics and dynamic behavior of the system were both analyzed with simulation modeling for initial validation process. An optimization procedure was performed to obtain the best values for the mechanism design parameters that would provide naturally enforced joint angles among the fingers and thumb during grasping, while maintaining a size profile for the mechanism linkages to remain within the height of the fingers and thumb.

In addition to the developing a prototype for the primary hand exoskeleton system, a child-sized version was designed to serve as a rehabilitation device that could monitor hand motor skills and cognitive development of high-risk infants. These prototypes are fully integrated and validated through experimental testing.

The main contributions produced by this thesis work can be summarized as follows:

1. **Size** – the proposed mechanism for the hand exoskeleton allows for the linkages to be placed alongside the fingers and thumb, which decreases the overall size of the system. In addition, an optimization process was performed to reduce the size profile and height of each digit mechanism, without sacrificing the performance of providing natural grasping motions. With these results, a slimmer design of the mechanism was presented for the full hand exoskeleton design.
2. **Weight** – the proposed hand exoskeleton results in a lightweight device from its slim mechanism design, reduction of actuators needed, and the compact size of the actuators and sensors used. The two-digit prototype weighed 24 g on the human hand, excluding the additional components of the pneumatic system.

3. **Portability** – although the two-digit hand exoskeleton prototype used pneumatic actuators, the proposed design for the full hand exoskeleton uses compacted lightweight DC motors. This design adjustment will allow the system to be portable since it will no longer require the additional equipment of pneumatic units.
4. **Safety** – the hand exoskeleton design ensures the enforced joint angles are natural to that of a normal human hand. In addition, the design limits the RoM for each finger and thumb to natural ranges to prevent unsafe bending. Safety precautions are included in the design to prevent any component from injuring users.
5. **User friendly** – the prototypes are simple in design and easy to use, especially with the assistance of a user-friendly rehabilitation GUI that can also control the system.
6. **Sensory functionality** – the prototypes contain several sensors that can produce position, force, and haptic feedbacks. For the implementation of an intelligent grasping scheme for the full hand exoskeleton, a force controller with SEA units was designed and validated with preliminary testing.

8.2 Future Work

As mentioned in Section 6.3, the full hand exoskeleton is currently being developed to overcome the limitations of the two-digit hand exoskeleton prototype. The biggest limitation of the two-digit prototype was the system's inability to produce grasping and hand configurations other than fully open or closed grips, due to use of pneumatic actuators. These actuators also limited the hand exoskeleton performance in providing essential force control during grasping motions. The constraints of being stationary due to the complex setup of the pneumatic system also presented a concern in terms of portability.

With the proposed design and added features for the full hand exoskeleton, many of these limitations will be addressed.

However, there still exist potential concerns that the full hand exoskeleton system would have to address. These challenges include having an adaptive force control that would allow the hand exoskeleton to grasp objects that are not pre-programmed in its learning database, as well as having greater features for human/brain-computer interactions to sense the users' intentions to move their hand and perform a grasp. Along with these challenges, incorporating an adjustability factor that would allow the glove to be suitable for users of various hand sizes and shapes should also be addressed. These features would allow for a highly intelligent and effective hand exoskeleton system.

REFERENCES

- [1] P. J. Kiger, “How GE’s Early Innovations Provided a Glimpse of the Future,” *National Geographic Channel*. [Online]. Available: <http://channel.nationalgeographic.com/breakthrough-series/articles/how-ges-early-innovations-provided-a-glimpse-of-the-future/>.
- [2] R. A. R. C. Gopura, D. S. V. Bandara, K. Kiguchi, and G. K. I. Mann, “Developments in hardware systems of active upper-limb exoskeleton robots: A review,” *Rob. Auton. Syst.*, vol. 75, pp. 203–220, 2016.
- [3] Y. Sankai, “Leading edge of cybernics: Robot suit HAL,” *SICE-ICASE Int. Jt. Conf.*, vol. 10, pp. 1–2, 2006.
- [4] J. C. Perry, J. Rosen, and S. Burns, “Upper-limb powered exoskeleton design,” *IEEE/ASME Trans. Mechatronics*, vol. 12, no. 4, pp. 408–417, 2007.
- [5] S. Balasubramanian *et al.*, “Rupert: An exoskeleton robot for assisting rehabilitation of arm functions,” in *Virtual Rehabilitation (IEEE)*, 2008, pp. 163–167.
- [6] A. M. Dollar and H. Herr, “Lower Extremity Exoskeletons and Active Orthoses : Challenges and State-of-the-Art,” *IEEE Trans. Robot.*, vol. 24, no. 1, pp. 144–158, 2008.
- [7] H. Herr, “Exoskeletons and orthoses : classification , design challenges and future directions,” *J. Neuroeng. Rehabil.*, vol. 9, pp. 1–9, 2009.
- [8] A. Chu, H. Kazerooni, A. Zozz, A. B. Zoss, H. Kazerooni, and A. Chu, “On the biomimetic design of the berkeley lower extremity exoskeleton (BLEEX),” in *International Conference on Intelligent Robots and Systems*, 2006, vol. 11, pp.

3132–3139.

- [9] United States Census, “Americans with Disabilities: 2010,” *U.S. Department of Commerce*, 2010. [Online]. Available: <https://www.census.gov/people/disability/publications/sipp2010.html>.
- [10] R. H. Henry Gray, H.V. Carter, T. Pickering Pick, “Gray’s Anatomy.” Barnes & Noble, 2010.
- [11] “The Wrist and Hand Complex,” in *Joint Structure and Function: A Comprehensive Analysis*, 5th ed., New York: McGraw-Hill.
- [12] J. L. Yi-Liang, “Hand Reference (Part 4_ Motion Terminology) -ASSH,” *ASSH*. [Online]. Available: <http://www.handsurgery.com.sg/wordpress/?p=152>.
- [13] C. Hume, H. Brumfield, H. Gellman, and H. Mckellop, “Functional range of motion of the joints of the hand,” *J. Hand Surg. Am.*, vol. 15A, no. 2, pp. 240–243, 1990.
- [14] S. Cobos *et al.*, “Constraints for realistic hand manipulation,” *Presence*, no. September 2017, 2007.
- [15] J. N. A. L. Leijnse, P. M. Quesada, and C. W. Spoor, “Kinematic evaluation of the finger ’ s interphalangeal joints coupling mechanism — variability , flexion – extension differences , triggers , locking swanneck deformities , anthropometric correlations,” *J. Biomech.*, vol. 43, no. 12, pp. 2381–2393, 2010.
- [16] J. D. M.-P. Sandra J. Edwards, Donna J. Buckland, *Developmental and Functional Hand Grasps*, 1st ed. Slack Incorporated, 2002.
- [17] T. I. C.L. MacKenzie, *The Grasping Hand*. Elsevier, 1994.
- [18] T. Feix, J. Romero, H. Schmiedmayer, A. M. Dollar, and D. Kragic, “The GRASP

- Taxonomy of Human Grasp Types,” *IEEE Trans. Human-Machine Syst.*, vol. 46, no. 1, pp. 66–77, 2015.
- [19] K. Lee and M. Jung, “Three-dimensional finger joint angles by hand posture and object properties,” *Ergonomics*, vol. 139, no. September 2017, pp. 1–11, 2016.
- [20] A. Hara, Y. Y. Amauchi, and K. Kusunose, “Analysis of Thumb and Index Finger Joints During Pinching Motion and Writing a Cross , as Measured by Electrogoniometers,” *Clin. Biomech. Relat. Res.*, pp. 282–293, 1994.
- [21] S. Parkway and N. P. O. Box, “JAMAR Hydrolic Hand Dynamometer User Instructions.” pp. 1–8, 2004.
- [22] M. F. Swiontkowski, “Grip test; the use of a dynamometer with adjustable handle spacing,” *J. Bone Jt. Surg.*, vol. 99, no. 17, 2017.
- [23] H. Shin *et al.*, “Reliability of the Pinch Strength with Digitalized Pinch Dynamometer,” *Ann. Rehabil. Med.*, pp. 394–399, 2012.
- [24] V. Mathiowetz, N. Kashman, G. Volland, K. Weber, and M. Dowe, “Grip and Pinch Strength : Normative Data for Adults,” *Arch. Phys. Med. Rehabil.*, pp. 69–74, 1984.
- [25] B. D. Lowe, Y. Kong, and J. Han, “Development and application of a hand force measurement system.”
- [26] Z. Ma and P. Ben-Tzvi, “Tendon transmission efficiency of a two-finger haptic glove,” *ROSE 2013 - 2013 IEEE Int. Symp. Robot. Sensors Environ. Proc.*, no. October, pp. 13–18, 2013.
- [27] N. S. K. Ho *et al.*, “An EMG-driven exoskeleton hand robotic training device on chronic stroke subjects: Task training system for stroke rehabilitation,” *IEEE Int.*

- Conf. Rehabil. Robot.*, 2011.
- [28] J. Iqbal, H. Khan, N. G. Tsagarakis, and D. G. Caldwell, “A novel exoskeleton robotic system for hand rehabilitation - Conceptualization to prototyping,” *Biocybern. Biomed. Eng.*, vol. 34, no. 2, pp. 79–89, 2014.
- [29] J. Arata, K. Ohmoto, R. Gassert, O. Lamercy, H. Fujimoto, and I. Wada, “A new hand exoskeleton device for rehabilitation using a three-layered sliding spring mechanism,” *Proc. - IEEE Int. Conf. Robot. Autom.*, pp. 3902–3907, 2013.
- [30] T. T. Worsnopp, M. A. Peshkin, J. E. Colgate, and D. G. Kamper, “An actuated finger exoskeleton for hand rehabilitation following stroke,” *2007 IEEE 10th Int. Conf. Rehabil. Robot. ICORR’07*, vol. 0, no. c, pp. 896–901, 2007.
- [31] M. Takagi, K. Iwata, Y. Takahashi, S. I. Yamamoto, H. Koyama, and T. Komeda, “Development of a grip aid system using air cylinders,” *Proc. - IEEE Int. Conf. Robot. Autom.*, pp. 2312–2317, 2009.
- [32] I. H. Ertas, E. Hocaoglu, D. E. Barkana, and V. Patoglu, “Finger exoskeleton for treatment of tendon injuries,” *Proc. 11th IEEE Int. Conf. Rehabil. Robot. ICORR*, pp. 194–201, 2009.
- [33] Y. Hasegawa, Y. Mikami, K. Watanabe, and Y. Sankai, “Five-fingered assistive hand with mechanical compliance of human finger,” *Proc. - IEEE Int. Conf. Robot. Autom.*, pp. 718–724, 2008.
- [34] M. A. Zhou, P. Ben-Tzvi, and J. Danoff, “Hand rehabilitation learning system with an exoskeleton robotic glove,” *IEEE Trans. Neural Syst. Rehabil. Eng.*, vol. PP, no. 99, pp. 1323–1332, 2015.
- [35] P. Ben-Tzvi, J. Danoff, and Z. Ma, “The Design Evolution of a Sensing and Force-

- Feedback Exoskeleton Robotic Glove for Hand Rehabilitation Application,” *J. Mech. Robot.*, vol. 8, no. 5, p. 51019, 2016.
- [36] CyberGlove Systems LLC, “CyberGrasp,” 2009. [Online]. Available: <http://www.cyberglovesystems.com/cybergrasp/>.
- [37] P. Ben-Tzvi and Z. Ma, “Sensing and Force-Feedback Exoskeleton (SAFE) Robotic Glove,” *IEEE Trans. Neural Syst. Rehabil. Eng.*, vol. 23, no. 6, pp. 992–1002, 2015.
- [38] H. In and K. Cho, “Exo-Glove : Soft wearable robot for the hand using soft tendon routing system,” *IEEE Robot. Autom.*, vol. 22, no. March 2015, pp. 97–105, 2015.
- [39] S. W. Lee, K. A. Landers, and H. S. Park, “Development of a biomimetic hand extendon device (BiomHED) for restoration of functional hand movement post-stroke,” *IEEE Trans. Neural Syst. Rehabil. Eng.*, vol. 22, no. 4, pp. 886–898, 2014.
- [40] C. J. Nycz, M. A. Delph, and G. S. Fischer, “Modeling and design of a tendon actuated soft robotic exoskeleton for hemiparetic upper limb rehabilitation,” *Proc. Annu. Int. Conf. IEEE Eng. Med. Biol. Soc. EMBS*, vol. 2015–Novem, pp. 3889–3892, 2015.
- [41] Y. Hasegawa, J. Tokita, K. Kamibayashi, and Y. Sankai, “Evaluation of fingertip force accuracy in different support conditions of exoskeleton,” *Proc. - IEEE Int. Conf. Robot. Autom.*, pp. 680–685, 2011.
- [42] I. Koo, B. Byunghyun Kang, and K.-J. Cho, “Development of Hand Exoskeleton using Pneumatic Artificial Muscle Combined with Linkage,” *J. Korean Soc. Precis. Eng.*, vol. 11, no. 11, pp. 1217–1224, 2013.
- [43] P. Polygerinos, Z. Wang, K. C. Galloway, R. J. Wood, and C. J. Walsh, “Soft

- robotic glove for combined assistance and at-home rehabilitation,” *Rob. Auton. Syst.*, vol. 73, pp. 135–143, 2015.
- [44] P. Polygerinos *et al.*, “Towards a soft pneumatic glove for hand rehabilitation,” *IEEE Int. Conf. Intell. Robot. Syst.*, pp. 1512–1517, 2013.
- [45] H. K. Yap, J. H. Lim, F. Nasrallah, J. C. H. Goh, and R. C. H. Yeow, “A Soft Exoskeleton for Hand Assistive and Rehabilitation Application using Pneumatic Actuators with Variable Stiffness,” in *IEEE International Conference on Robotics and Automation (ICRA)*, 2015, pp. 4967–4972.
- [46] M. O. Krucoff, S. Rahimpour, M. W. Slutzky, and V. R. Edgerton, “Enhancing Nervous System Recovery through Neurobiologics , Neural Interface Training , and Neurorehabilitation,” *Front. Neurosci.*, vol. 10, no. December, 2016.
- [47] M. Liu and C. Xiong, “Synergistic characteristic of human hand during grasping tasks in daily life,” *Lect. Notes Comput. Sci. (including Subser. Lect. Notes Artif. Intell. Lect. Notes Bioinformatics)*, vol. 8917, pp. 67–76, 2014.
- [48] W. E. Hook and J. K. Stanley, “Assessment of thumb to index pulp to pulp pinch grip strengths,” *J. Hand Surg. Am.*, vol. 11, no. 1, pp. 91–92, 1986.
- [49] K. Hemmi, K. and Inoue, “A Proposal of Three Dimensional Movement Model for Index Finger and Thumb,” *Proc. 4th Asia-Pacific Conf. Control Meas.*, 2000.
- [50] G. A. Bekey, R. Tomovic, and I. Zeljkovic, “Control architecture for the Belgrade/USC Hand,” *Dexterous Robot. Hands*, p. 345, 1990.
- [51] J. Pratt, B. Krupp, C. Morse, J. Pratt, and B. Krupp, “Feature Series elastic actuators for high fidelity force control,” *Ind. Robot An Int. J.*, vol. 29, no. 3, pp. 234–241, 2002.

- [52] M. Pratt, Gill; Williamson, "Series Elastic Actuators," *Proc. IEEE/RSJ Int. Conf. Intell. Robot. Syst.*, pp. 399–406, 1995.
- [53] Z. Ma and P. Ben-Tzvi, "RML glove-an exoskeleton glove mechanism with haptics feedback," *IEEE/ASME Trans. Mechatronics*, vol. 20, no. 2, pp. 641–652, 2015.
- [54] H. Tatsumi, Y. Murai, I. Sekita, S. Tokumasu, and M. Miyakawa, "Cane Walk in the Virtual Reality Space Using Virtual Haptic Sensing: Toward Developing Haptic VR Technologies for the Visually Impaired," *Proc. - 2015 IEEE Int. Conf. Syst. Man, Cybern. SMC 2015*, pp. 2360–2365, 2016.
- [55] C. Yu and Q. Peng, "Robust recognition of checkerboard pattern for camera calibration," *Opt. Eng.*, vol. 45, no. 9, p. 93201, 2006.
- [56] E. S. Gersh, "What is Cerebral Palsy?," in *Children with Cerebral Palsy: A Parent's Guide*, Second., E. Gerialis, Ed. Woodbine House, Inc. Bethesda, 1998.
- [57] D. Christensen *et al.*, "Prevalence of cerebral palsy, co-occurring autism spectrum disorders, and motor functioning – Autism and Developmental Disabilities Monitoring Network, USA, 2008," *HHS Public Access*, vol. 56, no. 1, pp. 59–65, 2015.
- [58] P. A. Janssen, P. Thiessen, M. C. Klein, M. F. Whitfield, Y. C. Macnab, and S. C. Cullis-Kuhl, "Standards for the measurement of birth weight, length and head circumference at term in neonates of European, Chinese and South Asian ancestry.," *Open Med.*, vol. 1, no. 2, pp. e74-88, 2007.
- [59] S. Winter, A. Autry, C. Boyle, and M. Yeargin-Allsopp, "Trends in the prevalence of cerebral palsy in a population-based study.," *Pediatrics*, vol. 110, no. 6, pp.

1220–1225, 2002.

- [60] O. Chorna *et al.*, “Early childhood constraint therapy for sensory/motor impairment in cerebral palsy: a randomised clinical trial protocol,” *BMJ Open*, vol. 5, no. 12, p. e010212, 2015.
- [61] N. L. Maitre, J. C. Slaughter, and J. L. Aschner, “Early prediction of cerebral palsy after neonatal intensive care using motor development trajectories in infancy,” *Early Hum. Dev.*, vol. 89, no. 10, pp. 781–786, 2013.
- [62] S. Ito, H. Kawasaki, Y. Ishigure, M. Natsume, T. Mouri, and Y. Nishimoto, “A design of fine motion assist equipment for disabled hand in robotic rehabilitation system,” *J. Franklin Inst.*, vol. 348, no. 1, pp. 79–89, 2011.
- [63] H. In, B. B. Kang, M. Sin, and K.-J. Cho, “Exo-Glove Exo-Glove A Wearable Robot for the Hand with a Soft Tendon Routing System,” no. March 2015, pp. 97–105, 2014.
- [64] M. J. Kurz, E. Heinrichs-Graham, D. J. Arpin, K. M. Becker, and T. W. Wilson, “Aberrant synchrony in the somatosensory cortices predicts motor performance errors in children with cerebral palsy,” *J. Neurophysiol. April*, vol. 5, no. November, 2015.
- [65] N. L. Maitre, Z. P. Barnett, and A. P. F. Key, “Novel assessment of cortical response to somatosensory stimuli in children with hemiparetic cerebral palsy,” *J. Child Neurol.*, vol. 27, no. 10, pp. 1276–83, 2012.